THE IMPACT OF TIMBER SINGLE HOUSING MORPHOLOGY ON ENERGY EFFICIENCY AND EMBODIED CARBON

A THESIS SUBMITTED TO
THE FACULTY OF ARCHITECTURE AND ENGINEERING
OF
EPOKA UNIVERSITY

BY

MARINELA PJETRI

IN PARTIAL FULFILLMENT OF THE REQUIREMENTS
FOR
THE DEGREE OF MASTER OF SCIENCE
IN
ARCHITECTURE

JUNE, 2023

Approval sheet of the Thesis

This is to certify that we have read this thesis entitled **"The impact of timber single housing morphology on energy efficiency and embodied carbon"** and that in our opinion it is fully adequate, in scope and quality, as a thesis forthe degree of Master of Science.

_____

Assoc. Prof. Dr. Edmond Manahasa
Head of Department
Date: June 19, 2023

Examining Committee Members:

Prof. Dr. Sokol Dervishi	(Architecture)	_____
Dr. Egin Zeka	(Architecture)	_____
Dr. Ina Dervishi	(Architecture)	_____

I hereby declare that all information in this document has been obtained and presented in accordance with academic rules and ethical conduct. I also declare that, as required by these rules and conduct, I have fully cited and referenced all material and results that are not original to this work.

Name Surname: Marinela Pjetri

Signature: _____

ABSTRACT

THE IMPACT OF TIMBER SINGLE HOUSING MORPHOLOGY ON ENERGY EFFICIENCY AND EMBODIED CARBON

Pjetri, Marinela
M.Sc., Department of Architecture
Supervisor: Prof. Dr. Sokol Dervishi

Contemporary society, in recent years has shifted its focus toward more sustainable solutions in the building sector, since it has become a significant component in the global energy consumption and greenhouse (GHG) emissions. The growing interest for passive housing can reduce the carbon footprint of the building, pushing the development of more efficient schemes and sustainable materials. The benefits that a sustainable material such as timber, has to offer to the environment are crucial to evaluate the energy performance of low-rise single housing from the lifespan aspect. The present research aims the assess the impact of timber single housing morphology on energy efficiency and embodied carbon. This research is carried out in three different climate contexts: Mediterranean, continental and tropical. Design variable incorporate timber construction systems, building morphology, glazing (window-to wall ratio), presence of the roof and courtyard. The generated low-rise housing models are simulated and estimated via Design Builder software. The 372 simulated results stress the efficacy of morphology in two timber construction systems and transparency have in reducing up to 13.84% and 24.95% of the annual energy consumption for both construction systems. Propositions are made on the suitability level of each house morphology for each considered climate context. A novel set of guidelines for design decision-making stages is generated through performed simulated result of each timber single housing morphology.

Keywords: *single housing, morphology, timber, WWR, simulation, energy performance, thermal comfort, climate*

ABSTRAKT

IMPAKTI I BANESAVE VETJAKE PREJ DRURI NE EFIKASITETIN E ENERGJISE DHE KARBONIN E PERMBAJTUR

Pjetri, Marinela

Master Shkencor, Departamenti i Arkitekturës

Udhëheqësi: Prof. Dr. Sokol Dervishi

Shoqëria bashkëkohore, vitet e fundit e ka zhvendosur fokusin e saj drejt zgjidhjeve më të qëndrueshme në sektorin e ndërtimit, pasi është bërë një komponent i rëndësishëm në konsumin global të energjisë dhe emetimet e serrave. Interesi në rritje për banesat pasive mund të zvogëlojë gjurmën e karbonit të ndërtesës, duke nxitur zhvillimin e skemave më efikase dhe materialeve të qëndrueshme. Përfitimet që një material i qëndrueshëm, si druri, mund t'i ofrojë mjedisit janë thelbësore për të vlerësuar performancën energjetike të banesave vetjake nga aspekti i jetëgjatësisë. Hulumtimi aktual synon të vlerësojë ndikimin e lëndës drusore në morfologjinë e banesave vetjake në efikasitetin e energjisë dhe karbonin e permbajtur. Ky hulumtim është kryer në tre kontekste të ndryshme klimatike: mesdhetare, kontinentale dhe tropikale. Variablat e projektimit përfshijne sistemet e ndërtimit të drurit, morfologjinë e ndërtesës, xhamat (raporti dritare-mur), prania e çatisë dhe kopshtit. Modelet e krijuara të banesave vetjake simulohen dhe vlerësohen nëpërmjet softuerit Design Builder. 372 rezultatet e simuluara theksojnë efikasitetin e morfologjisë ne dy sistemet e ndërtimit te drurit dhe transparencës që kanë në uljen deri në 13.84% dhe 24.95% të konsumit vjetor të energjisë per te dyja sistemet e ndertimit. Janë bërë propozime mbi nivelin e përshtatshmërisë së çdo morfologjie të shtëpisë për çdo kontekst klimatik të konsideruar. Një grup me udhëzime origjinale për fazat e vendimmarrjes së projektimit eshte krijuar nëpërmjet rezultateve të simuluara të kryera per çdo morfologji të një banese vetjake prej.

Fjalët kyçe: *banese vjetjake, morfologjia, druri, RDM, simulim, performanca e energjise, komoditeti termik, klima*

This thesis is a dedication to my family, whose unconditional love and support have been my constant source of inspiration. They have given me the drive and discipline to tackle any hardship with enthusiasm and determination. Without their love and assistance this research would have not been made possible. Thank you for believing in my dreams, I am forever grateful for your presence in my life.

To the Almighty God who is always there when I am in need. Thank you for guiding me, for giving me strength, knowledge, wisdom and good health in everything I do. All of these, I offer to you.

I would also like to express my infinite gratitude to everyone, friends and colleagues, who have supported me in this challenging yet memorable journey in Architecture. Thank you for motivating and supporting me in every step of the way in the completion of this research paper.

Lastly, I humbly dedicate this research paper to myself, as it is a statement of hard work, perseverance and never giving up on working toward my goals. To my younger self, who once dreamed of becoming an architect, your constant commitment and discipline have been a bridge between your dream and accomplishments.

ACKNOWLEDGEMENTS

I would like to acknowledge and express my sincere gratitude to my supervisor, Prof. Dr. Sokol Dervishi, who made this work possible. His guidance and advise carried me through all the stages of writing and giving my best in completing this master thesis. Sharing the knowledge and effective teachings have encouraged and helped me broaden my perspective as I went through with this study. Working under your guidance was a great honor and privilege.

TABLE OF CONTENTS

LIST OF TABLES

LIST OF FIGURES

LIST OF ABBREVIATIONS

List of Abbreviations

GHG	Greenhouse gas	CO_2	Carbon Dioxide
GWP	Global Warming Potential	LCA	Life Cycle Assessment
EU	European Union	LCPE	Life Cycle Primary Energy
EGD	European Green Deal	EOL	End of Life
CLT	Cross- Laminated-Timber	IPPC	International Plant Protection Convention
EP	European Parliament	MTC	Mass Timber Construction
RC	Reinforced Concrete	GLT	Glue Laminated Timer
LFT	Light-Frame Timber	PENRT	Primary Energy Content
DH	Detached House	U-value	Thermal transmittance
SDH	Semi-Detached House	WWR	Window-to-wall ratio
RH	Row House		
LH	L-shape House		
CH	Courtyard House		

CHAPTER 1

INTRODUCTION

1.1 Motivation

Setting out to encourage sustainability and the well-being of citizens have become crucial matters in relation to mitigate climate change. The European Union adopted in 2019 the "Green Deal" as a new growth strategy, to thus become the first climate-neutral continent by 2050 (Filipovic et al., 2022). Its target is to respond to the concerning climate crisis by achieving net zero greenhouse gas (GHG) emissions from the EU by 2050 (Haines & Scheelbeek 2020; Weitzel et al., 2023). To coerce the near-term emission track compatible with this new long-term goal, the European Commission in 2020 suggested the idea of meeting the target of emission reduction by 55% until 2030 (Filipovic et al., 2022; Weitzel et al., 2023). The legal framework promotes policies and guidelines that will help achieve a highly energy efficient and decarbonizing impact, in order to meet the EU's energy and environmental targets, raising awareness, but also improving the quality of life (Arbulu., et al 2022).

According to the International Energy Agency (IEA) and European Union (EU), the building sector has become a major component of global energy consumption and greenhouse gas (GHG) emissions, accounting to more than one-third of global final energy consumption and contributing to nearly 40% of total carbon emissions (Filipovic et al., 2022, Duan et al., 2022, Eurostat-European Union 2020, Jaysawal et al., 2022). The building industry is directly facing challenges to limit its negative footprint on the climate (Frank et al., 2022). New European Bauhaus (Maria et al., 2021) has set sustainability initiatives, rethinking the way of building, since this sector drives an extensive material consumption and environmental impact.

In the case of house building, global trends indicate an increase in demand for housing upgrades, especially with the new technologies to support it (Huo et al., 2022). Findings show that altering the conventional housing for passive housing can reduce carbon emission up to 5% (Vita et al., 2019). Motivating transition of housing methods with voluntary efficient schemes can push the development of more sustainable materials

and practices by making their impact visible (Frank et al., 2022).

In order to address the unfeasible current situation, there is a need to understand that buildings, in this case housing, must use a much higher proportion of renewable materials (Vita et al., 2019). The selection of the material it effects the lifecycle phases of the house building, from the energy efficiency and environment perspective (Asdrubali & Grazieschi, 2020). Selecting and using environmentally friendly materials at the design development phase can minimize the resource consumption and CO2 emission (Ding, 2020). Cellulose materials such as timber is a potential alternative that is renewable (Bukauskas et al., 2019). With the development of mass timber, cross laminated timber (CLT) has gradually become a sustainable alternative to conventional building materials to alleviate the increasing energy consumption and carbon emissions by the building sector (Duan et al., 2022).

Studies show that cross laminated timber is a fairly new construction material and contemporary CLT buildings are the first of their kind to have yet to reach the end of their lifecycle (Duan et al., 2022). However, recent lifecycle assessment (LCA) reviews on the overall carbon footprint of a building have shown that timber-based buildings have lower global warming potential (GWP) and life cycle primary energy (LCPE), than reinforced concrete and steel buildings (Fabrizio et al., 2022). Although timber structures have already been introduced and integrated in the housing construction, studies have either focused on mid-rise of high-rise building, comparing or reviewing the life-cycle assessments of the reinforced concrete, steel and timber structures for specific cases (Duan et al., 2022; Andersen et al., 2022). Therefore, more research is required on low-rise housing typologies made of timber, to establish more knowledge on how they perform on different global climates while having a low impact on energy and CO2 mitigation. This paper aims to contribute novel knowledge by addressing the gaps on having a representative catalogue of low-rise housing typologies made of timber with their respective impact on energy performance and thermal comfort in different climates and CO2 emission, through simulations.

1.2 Thesis Objective

This paper shows the results of a simulation-based research regarding the timber low-rise single housing typologies. The study attempts to understand the issues as follows:

1) how can timber-low rise single housing morphology provide with efficient answers to environmental challenges.
2) Assessing the impact of climatic conditions in the design-making decision stages of low-rise single housing.
3) Understating the need to change of the energy efficiency according to the climate.

Aside from the efficiency of energy, exploring the impact and benefits timber has in regard to sustainability: environment, economic and social.

The research sets out to accomplish the following objectives:

1) Comparing previous works that are mainly related to life cycle assessment of housing and its performance of the chosen materials, to find the missing gaps.
2) to gather results from the simulations of the chosen typologies, processing and evaluating the output data based on the variables of the modeling.
3) Evaluating the best-fit scenario for each studied climate.
4) recommending solutions for different scenarios of the timber low-rise single housing, for future implementation according to suitability.

1.3 Organization of this thesis

The structure of this thesis is divided into seven chapters. The following is the outline of the paper: the 1 chapter provides the problem statement, motivation with the introductory information of the energy consumption and GHG emission of the building construction sector and how sustainable materials, such as timber can minimize the negative impact in the environment and climate change and thesis objectives. It follows

with the 2 chapter of literature review of timber low-rise single housing morphology on their life cycle assessment, embodied energy & carbon and previous simulation-based studies. In chapter 3, a theoretical background on wood technology, wood classification, energy flows in building and LCA as a concept is explored furthermore. Chapter 4 presents the methodology framework of the study. In chapter 5 the generated results from the simulations are explored for each climate. Chapter 6, discusses furthermore the generated results. Chapter 7, presents the conclusions and recommendations for future studies.

CHAPTER 2

THEORETICAL BACKGROUND

2.1 Wood harvesting and processing

In Europe, the commonly structural timber is derived by sustainable coniferous forests and their plantations (Dickson & Parker, 2014). The first stage of timber processing is round wood harvesting (*Figure 1*), carried out by customized hydraulically controlled machines (Ramage et al., 2017). Once the round wood is harvested, the timber is transported to a sawmill for further processing to softwood & hardwood, to remove surface defects or barks, but also where it is strength graded accordingly (Bukauskas et al., 2019; Ayanleye et al., 2022; Wang et al., 2015) and cut to standard lengths. In order for processed timber materials to be able to support load, it is called for to strength grade each part of dimensional timber according to BS EN 14081(BSI. BS EN 14081-1/2005+A1/2011). Being a natural material, wood is prone to fungal degradation, but a moisture of 20% is not issue, moreover the European standards specify an upper limit of 20% moisture for 'dry graded' timber, so structural timber receives a defined strength grading (BSI. BS EN 338/2009). Dry timber also has more benefits in terms of gluing and it is lighter to transport (Pratt, 2010).

Timber is a widely used structural material due to its desirable characteristics such as high strength to weight ratio, low energy consumption, and reliability in structural applications and is used most efficiently in structures where it is carrying a lot of its own self-weigh (Ayanleye et al., 2022). The softwood composites that are manufactured into structurally optimized building known as engineered timber are characterized by increased dimensional stability, more homogenous mechanical properties and greater durability if kept dry (Gerasimov et al., 2010). Part of this family of engineered timber as building material is Glulam, laminated veneer lumber, structural veneer lumber, cross-laminated timber and many others.

Figure 1. Wood processing and eco cycle of timber

2.2 Wood treatment

Wood treatment is a process used to enhance the properties of wood as a material and to produce a material that at the end of its life cycle will not create risk to the environment (Hill, 2006). Dimensional stability, thermal stability, fire resistance, UV resistance, biological degradation resistance, or mechanical properties are only some of the properties required to be improved as wood physical or chemical treatments (Rowell, 2006).

2.3 Classification of wood construction systems in the building process

Whether designing light frame or mass timber structural systems, it is safe to say

that buildings will benefit from the material's characteristics, fire, thermal and seismic performance (Caniato et al., 2021; Li et al., 2021). Thus, there is a variety of wood construction systems and techniques developed to support them, that usually depends on the conditions of the project, such as: size, span, load and degree of prefabrication if any (Lundgren, 2014). Some of the most commonly used construction systems are described as follows.

2.3.1 Timber frame system

Timber frame system technique using vertical timber has been around from many years since 1930s and is still in use now days and its construction can be fully manual or automated and industrial (Lundgren, 2014). This system is commonly used in story-based houses, supporting solid wood load -bearing walls that span up to seven meters for the external walls, partition walls or walls in between apartments (Barnaure et al., 2016).

2.3.2 Site-build technique

The method is ideal for single-family houses, where the basic material is ready-cut timber or timber cut on site for open timber frame walls without insulation that are horizontally nailed together on the foundation slab or upper floors as well (Lundgren, 2014). The nailed wall frames are vertically lifter and shuffled into space, whereas roof trusses and beams are fixed to the top plates to fit a new ceiling or floor. It is important to mention that this structure system is sensitive to moisture and during hot weather, if left uncovered it can experience extreme drying (De Araujo et al., 2013).

2.3.3 Cross-laminated timber (CLT) system

Cross laminated timber or CLT are timber panels made of a minimum of three layers of sawn softwood glued boards or planks layered alternately at right angles to form a thickness in the range of 60-600 mm acceptable for wall, roof and floor elements up to 3.6 m wide and 20 m long (Gustafsson, 2019). The cross laminated timber panels have the advantage of being manufactured with a high prefabrication rate and accuracy, simple joining methods, easy transport, fast construction and have a high strength in low self-

weight in comparison to concrete (Gustafsson, 2019;86). CLT has improved the competitiveness of timber compared to other construction materials, not only in the ecological aspect, but also with its structural qualities, such as its great strength of load bearing capacity and stiffness, useful to stabilizing the building against lateral loads (Li et al., 2019; Petruch et al., 2019). Another characteristic is that CLT has good thermal insulation properties, therefore thermal bridges are avoided, and this type of engineering wood can provide good fire safety with appropriate design (Caniato et al., 2021; Li et al., 2021; Gustafsson, 2019). Cross laminated timber is eco-friendly and a recyclable construction material that has yet to reach the end of its service life (Younis & Dodoo, 2022; Gustafsson, 2019). It forms a climate-smart carbon sink in structures, because it sequestrates and storages carbon dioxide (CO2), thereby reducing the impact of the building (Markström et al., 2018; Sikkema et al., 2023).

2.3.4 Post and beam system

In a post and beam system, glued laminated timber columns and beams compromise the building frame, in which external walls, floors and roofs are build (Barnaure et al., 2016). The rigidity of the timber frame is achieved by installing diagonal stiffening joints or mast column (Markström et al., 2018). The structural system offers free and flexible spatial planning and enables opening up for walls, with the possibility of a fast construction phase (Lundgren, 2014).

2.3.5 Modular system

Modular or volumetric system technology is a construction method where 20-30% of the building is assembled in factory in box units, consisting of load-bearing frame elements like floors, walls and roofs, making possible a fast construction stage (Lundgren, 2014). The typical dimensions of a modular system are 12 x 4.2 x 3.2 meters (Barnaure et al., 2016).

2.4 Energy flows in buildings and formulas

According to EN ISO 13790 energy efficiency in buildings relies on energy demand for heating (Q_H) and cooling (Q_C) (ISO, E. N. 2008). If the building is considered as a thermal system with a series of heat flows, inputs or outputs, both energy demand for heating and cooling can be determined (Szokolay, 2008). Therefore, the energy balance of the building overall is made up from the transmission heat losses (Q_T), ventilation heat losses (Q_V), internal heat gains (Q_I) and solar heat gains (Q_S) (Official Gazette RS, 52/ 2010). The formula of the equation for the energy balance in building is as follows:

$Q_T + Q_V + (Q_I + Q_S) = \Delta Q = \Delta Q_H$ in cold conditions (Equation 1)

$Q_T + Q_V + (Q_I + Q_S) = \Delta Q = \Delta Q_C$ in hot conditions (Equation 2)

2.5 Life Cycle Assessment as a concept

As a principle, the sustainability of a building is evaluated when the economic, environmental and social impacts linked with the building itself are quantified, through its entire life cycle (Younis & Dodoo, 2022). Life Cycle Assessment is a specific tool for measuring the environmental impacts in all life cycle stages of a building, as provided by International Organization for Standardization (ISO, ISO 14040, 2006). The life cycle of a building starts with extraction within the product stage (A1-A3), transport (A4) within the construction stage, replacement (B4) within the use stage, transport stage (C2), waste processing (C3) and disposal (C4) within the end-of-life stage (British Standards Institution, 2011; Anex & Rifset, 2014). *Figure 2* presents the framework of LCA stages and modules of a building as per EN 15978 (British Standards Institution, 2011).

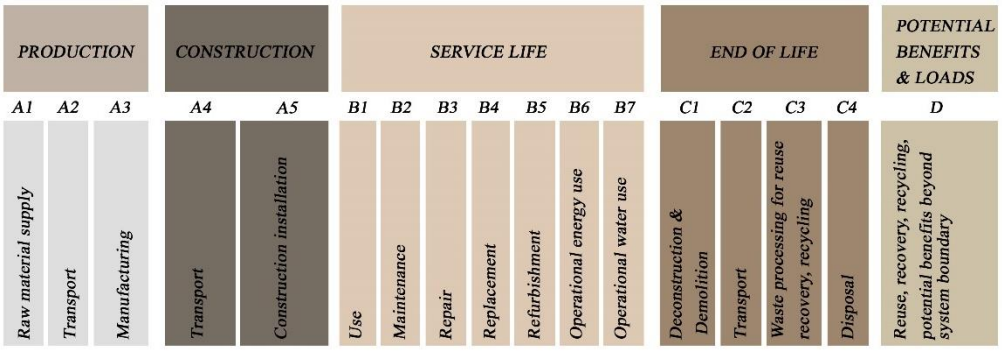

Figure 2. Life cycle assessment (LCA) stages and modules of a building as per EN 15978

CHAPTER 3

LITERATURE REVIEW

3.1 Embodied energy and carbon of timber in buildings as a material

The term embodied energy of a building is the amount of energy derived from the renewable and non-renewable resources to produce building materials and is used to produce the building itself (Jian Wen et al., 2015). In a similar way, the embodied carbon, referred also to as global warming potential is the amount of the emissions that are produced in creating the building construction materials (Mehdi et al., 2019). As a way to reduce the embodied impact of buildings, several strategies have been perceived by expert of the field in embodied GHG emissions, mitigation, thus a key policy is the implementation of low carbon materials in buildings (Pomponi & Moncaster, 2016). Referring to the embodied energy of materials, as stated by several authors, wood buildings require much lower process energy and carbon emissions than buildings of other materials such as: concrete, brick, aluminum and steel (Cabeza et al., 2013). Wood and wood related products that are harvested from sustainably managed forests are known to be as low carbon materials (Rasmussen et al., 2019). Acknowledged report of the valuable role of wood in terms of mitigating the risks of climate change is also stated in the Fourth Assessment Report of IPPC (Mackay, 2008). Moreover, the European Parliament resolution of 15 January 2020 has promoted the use of wood as a building material through European Green Deal (European Parlıament, 2021). It is known that timber captures carbon from the atmosphere as CO2, thus is considered one of the most environmentally friendly materials (Minunno et al., 2021). Several studies show that the alternative structural systems and building materials affect the design of sustainable buildings (Lukić et al., 2021). Hence, the difference between the embodied carbon and embodied energy of timber structures has been assessed that they contribute to a low amount of embodied energy, up to 43% of energy and 68% of CO2 can be saved by replacing concrete with timber (Duan et al., 2022; European Parlıament, 2021; Takano et

al., 2015). For this reason, under a typical scenario, where the sustainable forest management and remission of sequestered carbon in end of life (EOL), timber has the smallest impact (Hawkins et al., 2021; D'Amico et al., 2021).

3.2 Assessing the environmental benefits of timber in buildings

In order to assess the environmental performance of timber buildings, and timber housing in particular, tools such as life cycle analysis are frequently used (Wijnants et al., 2019; Basbagill et al., 2013; Leskovar et al., 2019). Duan et al. (2022) presents a systematic review of mass timber construction (MTC) from the perspective of LCA of previous 62 peer works, to compare it with the life cycle assessment of reinforced concrete (RC), steel and cross laminated timber, with an outcome that there is a clear trend that mass timber buildings have lower GWP. Crawford and Cadorel (2017) in their study establish a framework for assessing the environmental benefits of mass timber construction, by examining previous life cycle analysis (LCA), in order to identify the key elements that affect the environmental performance of timber. The identifying key elements that affect the performance of timber on the environment are grouped according to the life cycle stages of EN 15978, such as timber type, manufacturing processes, transport distance, construction time, quality or deconstruction (British Standards Institution, 2011). Another study analyzed the potential environmental impact reduction of timber frame constructions for rooftop extensions, focusing both on external walls and flat roofs (Wijnants et al., 2019), where the results showed that changing the material composition to timber, can lead to a total life-cycle environmental reduction of 17%. Achenbach et al. (2018) determined the environmental impact of the first two stages: production and construction of prefabricated timber houses, in which he gathered that is in the best interest to choose a house manufacturer located close site in order to limit the environmental impact. In the same note of importance, the use of LCA starting from the design process of a building can have a major influence for the reduction of environmental impact, making several changes in the performance of the building itself (Tschetwertak et al., 2017; Hollberg et al., 2020). Along the same lines, Basbagill et al. (2013), used BIM to develop an environmental assessment of buildings through a

calculative framework of the embodied impact during the design stages. Similar Verdaguer et al. (2020) demonstrated the environmental benefits of timber frame single family house versus a concrete masonry house in Uruguay, through a BIM method based LCA during design process mainly. The results showed that timber-frame houses produced lower impact (Verdaguer et al., 2020). Pajchrowski et al. (2014) showcased the environmental benefits of wood in a building life cycle, through a comparison of four single-family dwellings, two build with masonry and other two with wood timber.

3.3 Assessing the environmental impact of shape related-morphology in timber buildings

Comparing studies have focused on the shape related building typologies and how they perform. Shape related studies, in many cases are dominated by the impact of building height on the environmental performance (Foraboschi et al., 2014 & Treloar et al., 2011). In both cases it is noticed a parallel increase between embodied energy (EE) normalized per m^2 of net floor area and number of floors. Close to building height, is the relative compactness (RC) influence on the embodied energy and embodied carbon (EC) in life cycle stages for two inclusive concrete buildings by Lotteau et al. (2017), who show that both EE and EC increase linearly with the increase of the shape factor.

Serrano and Alvarez (2016) preformed a life cycle assessment to establish the carbon emissions and embodied energy for a newly residential cluster, in which they pointed out that a higher environmental impact of terraced housing compared to four-storey multi-family housing. A different comparative environmental assessment by Cuéllar-Franca and Azapagic (2012) carried out on the most common house typologies in United Kingdom (UK), shows that detached houses are more burdensome than semi-detached and terraced houses. Takano et al. (2015) analyzed the life cycle primary energy balance for a variety of residential building types concerning the climatic conditions of Finland and led to determining a link between the building geometry type and environmental performance, because of the increase of life cycle energy efficiency with the increase storeys and floor area.

Leskovar et al. (2019) focused on smaller buildings in the timber construction for their shape related typology and compared them from the environmental perspective. The research uses a reference model as a method to analyze and compare the LCA of detached (DH), semi-detached (SDH), terraced (TH), two-storey (2SH) and three-storey houses (3SH), considering three major impact categories such as global warming potential (GWP), acidification potentials (AP) and non-renewable primary energy content (PENRT) (Leskovar et al., 2019). The presented results indicated that the energy use and environmental impact decreases when having lower shape typologies such as two and three-storey models, making them more favorable. Decreasing the size and shape of the house, undoubtedly shows also benefits when choosing timber (Milwicz et al., 2015). Younis and Dodoo (2022) carried out the research focusing on the life cycle carbon footprint of cross-laminated timber building (CLT). In this paper are reviewed previous works pertaining life cycle analysis of CLT, where the findings revealed 40% savings in GWP emission and if LCA interacts with the state of practice of the structural solution of buildings in the design phase, can improve the carbon footprint of cross-laminated timber buildings. Žigart et al. (2018) highlights the environmental benefits of timber frame in wall and roof construction, especially when supported with lower impact thermal insulation. Seen from the environmental point of view, timber can be an alternative to steel and concrete in buildings, therefore becoming a more sustainable solution at a design stage and reduce impact. Markström et al., 2018 and Ismailos & Touchie. (2017) perceived a positive approach towards timber and its future application in construction. An overview of the identified contribution is summarized in *Table 1*.

Table 1. Overview of scientific literature of existing Life Cycle Assessment (LCA), concerning timber in relation with other building materials in housing

Author	**Structural system/Material**	**Typology**	**Case Study**	**Location**
Duan et al. (2022)	Mass timber (CLT), reinforced concrete & steel	Not specified	Review	Review
Crawford & Cadorel (2017)	Mass timber construction	Not specified	Review	Review
Wijnants et al. (2019)	Semi-prefabricated timber roof extension	High-rise -residential	Real building	Belgium

Achenbach et al. (2018)	Prefabricated timber	Housing	Specific LCA building model	Germany
Basbagill et al. (2013)	Concrete	High-rise	Real Building	Not specified
Verdaguer et al. (2020)	Timber frame structure & concrete masonrry	Low-rise	Building model	Uruguay
Pajchrowski et al. (2014)	Lightweight timber	Low-rise-detached	Real Buildings	Poland
Foraboschi et al. (2014)	Ridig frames (reinforced concrete & steel)	High-rise	Building model	Not specified
Lotteau et al. (2017)	Concrete	High-rise-residential	Simplified model	Not specified
Serrano & Alvarez (2016)	Concrete & brick	Mid-rise- Low rise	Real Buildings	Spain
Cuéllar-Franca & Azapagic (2012)	Concrete & brick	Low-rise	Building model	UK
Takano et al. (2015)	Lightweight timber, CLT, RC & light gauge steel	Mid-rise- Low rise	Building model	Finland
Leskovar et al. (2019)	Mass timber (CLT)	Low-rise	Building model	Slovenia
Milwicz et al. (2015)	Mass timber (CLT), brick	Low-rise	Real building	Poland
Younis & Dodoo (2022)	Mass timber (CLT), concrete & steel	High-rise	Real multistorey building	Review
Žigart et al. (2018)	Reinforced concrete, brick, CLT	Low-rise	4 Real buildings	Central Europe

3.4 Analysis and simulation of energy performance based in parameters and shape-related typology in timber housing

Several studies have focused on analyzing and making simulations for energy performance and efficiency of timber and its optimized structural building material, therefore impacting the potential carbon emission savings (Adekunle & Nikolopoulou, 2016; Milwicz et al., 2015; Setter et al., 2019). Setter et al. (2019) numerically analyzed the potential energy savings when cross lamination timber was implemented in a single-family home construction in different US climate. The noble results demonstrated the potential of storing thermal energy in cold climates and if using precooling to not increase the humidity in warm climates it will not translate into degradation of the timber performance (Setter et al., 20190). In the study of Nunes et al. (2020) it was investigated the thermos-energetic performance of cross laminated timber panes made of eucalyptus for low-income houses in Brazilian climate conditions. The results demonstrated that the

use of eucalyptus hardwood CLT panels, allowed an improvement in energy efficiency and performance of the houses compared to the masonry in different climate conditions (Nunes et al., 2020).

Moreover, identifying the building parameters that can impact the energy performance of the building can significantly enable the reduction of heating and cooling energy loads (Premrov et al., 2016, 2018). A major number of studies stress the impact that glazing size and building geometry employ on the building's energy demand located in cold climates (Persson, 2006; Ratti et al., 2005; Danielski et al., 2012; Leskovar et al., 2011; Bouden, 2007; Hassouneh et al., 2010). The strong connection between the final energy use for heating and the shape of the building in cold climates suggest that the optimum form of the building usually has a rectangular shape with minimum external surface (Premrov et al., 2016; Mingfang, 2002). Mingfang (2002) in the study of solar control in buildings, defines southern orientation of a building as the optimum solution to solar heat gains in cold weather and solar heat control in hot weather, further pointing out that a rectangular floor plan ensures solar control. On the other side, buildings located in in warm and hot climatic conditions experience a different situation, where the energy demand for cooling is the main impactful factor, because of higher solar heat transfer through the glazing (AlAnzi et al., 2009; Jaber & Ajib, 2011). Mediterranean climatic conditions were presented by Jaber and Ajib (2011) with TRNSYS simulation software, in which the outcome concluded in a 28% annual energy consumption saving by selecting the optimum window size, optimum U- value and best orientation. Depecker et al. (2001) analysed the relation between the energy requirements during winter weather and the shape of two different French climatic circumstances, where no correlation of energy consumption with a building's shape in mild climates was found.

In one study the model of a box timber-glass box model in warm and cold climates was parametrically testes through a variety of important parameter (glazing size, thermal transmittance, aspect ratio, orientation, horizontal and vertical extension on the timber-framed house (Premrov et al., 2018). It concluded that the building shape has also a major influence on the energy behavior of timber-framed houses in European climates.

Maučec et al. (2021) study focuses on utilizing the sensitivity analysis on the field of energy for the timber-framed residential buildings of six different typologies in box models. The Morris method of energy analysis concluded which design parameters

impact the energy efficiency (orientation, thermal conductivity, U-value, window to wall ratio, solar heat gain coefficient, occupant behavior), thus the most influencing parameters for energy demand are attributed for heating in cold climates and cooling in warm climates (Maučec et al., 2021). Lešnik et al. (2020) for his research, examined the optimization of energy efficient timber- glass for an upgrade module design in existing vertical buildings that are inefficient. Other results show that the optimum design for timber-glass upgrade modules is a glazing share of 25%-30% for north and east-west facades and 20%-30% for south facades (Dickson & Parker, 2014).

Seen from the energy performance aspect, timber can be an alternative on achieving energy efficiency in housing buildings, especially when introduced together with the impacting parameters in the design phase. A cumulative summary on previous simulations is presented in *Table 2*.

Although there is several of different studies presented, some numerically analyzed, others simulation based, there is still a lack of investigation on the energy behavior and environmental impact of timber housing when considering the climatic conditions and other key factors.

Table 2. Data available in previous simulations concerning energy performance of timber in housing compared to other materials.

Author	Year	Typology	Material	Software	Case study	Location/Climate
Ismailos & Touchie	2017	Low-rise	Not specified	HOT2000 energy simulation	two-story single-family house	Ontario, Canada
Adekunle & Nikolopoulou	2016	Low-rise & Mid-rise	Pre-fabricated timber	CIBSE & BSEN15251 model	2 buildings	Oxley Woods & Bridport, UK
Huang et al.	2022	High-rise	RC & CLT	Revit & Design Builder	real 11-story residential protype & 3 hybrid CLT models	China
Nunes et al.	2020	Low-rise	Cross laminated timber (CLT) eucalyptus	EnergyPlus Thermos-energetic simulation	Building model-typical dwelling	Brazil
Premrov et al.	2016	Low-rise	Timber frame	Ecotect Numerical calculation	Building model	Ljubljana, Munich, Helsinki
Premrov et al.	2018	Low-rise	Timber frame	PHPP V8.5 EnergyPlus	Building model-box model	Athens and Sevilla
Jaber and Ajib	2011	Mid-rise	Masonry brick	TRNSYS software	Building model-typical residential building	Jordan, Amman region

Maučec et al.	2021	Low-rise	Timber	OpenStudio v2.9.1 (n.d.) EnergyPlus Sensitivity analysis	Building model-box model	Ljubljana Athens Helsinki
Lešnik et al.	2020	Mid-rise	Timber-glass vertical estensions	MINLP optimization GAMS/DICOPT software	Building model-optimization model	Not specified

3.5 Aim and originality of the study

The proposed literature review shows that timber is a promising material in terms of environmental benefits and energy performance in buildings. Following the fact that light timber housing has captured a major interest in the field of building, the current innovations in engineering wood have yet to reach their end of life [45]. The research can present original contribution to the body of knowledge by addressing the potential improvements in more simulation-oriented work on the timber single low-rise housing shape typology and what impact they have in energy performance in environmental performance on three climates.

- Limited research has addressed detailed reviews on the life cycle assessment of timber, to show the environmental impact and benefits, compared to other building materials like concrete and brick (Duan et al., 2022; Crawford & Cadorel 2017; Wijnants et al., 2019; Basbagill et al., 2013; Leskovar et al., 2019; Younis & Dodoo, 2022; Žigart et al., 2018; Milwicz & Nowotarski, 2015). For instance, Crawford and Cadorel (2017), established a framework of identified key factors, to assess the environmental benefits of MTC, through an examination of previous live cycle analysis. Wijnants et al. (2019) analyzed the possible environmental impact reduction of timber frame construction in rooftop extensions, up to 17% of the total life cycle. Other reviewed literature demonstrates many studies on how life cycle assessment could have major influence if used starting from the design process of the building, realizing on a reduction of environmental impact (Achenbach et al., 2018; Hollberg et al., 2020; Hollberg et al., 2019). On account of comparative analyses, Verdaguer et al. (2020) and Pajchrowski et al. (2014) demonstrated the environmental benefits of timber in housing versus concrete, brick and steel.

- Even though some previous studies have incorporated the LCA method to demonstrate the key elements that affect the impact the environmental performance of timber from the design stage (Crawford & Cadorel, 2017; Wijnants et al., 2019), very few have considered the shape related typology factor on the topic of single low-rise housing (Foraboschi et al., 2014; Treloar et al., 2001; Lotteau et al., 2017; Serrano & Alvares, 2016). In this regard Leskovar et al. (2019) delineates the study on smaller buildings in timber construction for their shape related typology such as DH, SDH, TH, 2SH and 3SH, comparing their life cycle assessment in the terms of environmental perspective and indicated that lower shape typologies are more favorable.

- In regards of simulation studies, some have focused on thermo-energetic consumption and energy performance of wooden buildings to achieve potential carbon emission savings (Ismailos & Touchie, 2017; Adekunle & Nikolopoulou, 2016; Milwicz & Nowotarski, 2015; Setter et al., 2019). According to the reviewed literature the energy efficiency and performance of houses is highly influenced by the climate conditions and building parameters like: glazing size, orientation, aspect ratio, U-value and solar heat gain (Mingfang, 2002; Hassouneh et al., 2010; AlAnzi et al., 2009; Maučec et al., 2021). Locations that are detected concerning the climate conditions are US climate (Setter et al., 2019), Brazilian climate (Nunes et al., 2020), European climate (Depecker et al., 2001; Premrov et al., 2018], Mediterranean climate (Jaber & Ajib, 2011).

- Only two simulations by Premrov et al. (2016, 2018) develop a study on the influence of the building shape on the energy performance of timber-glass buildings in warm and different climatic conditions. In addition, more elaborated simulation-based study will contribute into solving knowledge gabs in the already presented body of literature.

- No simulation-assisted study has previously delved into developing a variety of scenarios on environmental impact and energy efficiency performance of whole timber typologies on low-rise single housing in the cold, Mediterranean, and African climatic conditions. Therefore, in this paper a framework is illustrated and generated aiming to initiate the creation of a standard manual to guide the future experts in the field of designing and constructing timber housing. The framework is supported on reviewing the current literature, regarding the timber construction and housing theoretical background and previous simulation studies, considering several factors, such as: timber wall

typologies, low rise single housing morphology, case study model, climate, program assisting the simulation with its purpose and limitations as well. The main scientific value and novelty of the paper consists on proposing and evaluating different design strategies of timber typologies in low-rise single housing with specific glazing properties. The approach is an enhancement of the other methodologies proposed by authors [5,50,51,55,56,66,67,68,69] to provide worthy contribution, compared to the introduced studies and state of the art as a whole. What accounts for the framework are the scalable results of the impact of timber application. For the purpose of providing a full evaluation of the timber typologies impact on selected house morphologies and their performance, the study is composed of several scenarios in three different climatic conditions:

- 45%, 60% and 75% window-to-wall ratio (WWR) scenarios for North-South oriented façades, to evaluate their impact on the effectiveness of the shape of the house considering two other parameters: a flat roof or a pitched roof and the timber construction systems.

CHAPTER 4

METHODOLOGY

4.1 Climate characterization

The study analyses the energy performance for three cities with different climate conditions to understand and constitute more accurate evaluations of the energy performance of timber single low-rise houses. On the central of Europe, the climate is mainly continental or temperate; on the Aegean coastline, the climate is Mediterranean; on the Atlantic Ocean coast the climate is mild humid and moderate and inland is humid tropical. Locations (*Figure 3*) are chosen based on the variance of temperatures, solar radiation, and other imputes. The climate data is retrieved from Meteonorm 7.3.

Figure 3. The selected locations

4.1.1 Athens, Greece

Athens has a hot Mediterranean/dry summer subtropical climate. This area is located in the north of the equator line, thus summer begin at the end of June and ends in September. The prevalent feature of Athens' climate is the alternation of extended hot and dry summers caused by dry and hot winds blowing from the Sahara and warm, wet winters with moderate rainfall caused by westerly winds. Under the Köppen -Geiger climate classification features a Mediterranean climate (Csa).

The average temperature for the year is 17.5°C. On the warmest month July, the average temperature is 27.7°C and on the coolest month January, the average temperature is 8.2°C. *Figure 4* illustrates the mean outdoor temperature and the amount of average solar irradiance on horizontal plane of Athens, where radiation rises from 54 W/m^2 in December to the peak of 235 W/m^2 in June.

The average annual precipitation measures up to 378 mm with annual 43 rainy days. Athens has an average of 3368.26 hours of sunshine in a year, where the duration of sunny hours in January is 171.42 h and in July is 397.42 h.

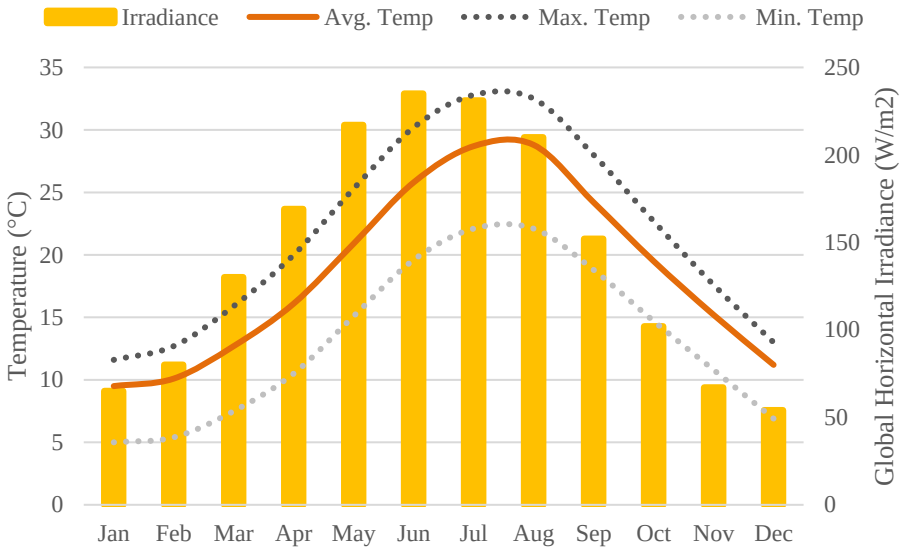

Figure 4 Annual temperatures and global horizontal irradiance for the city of Athens (Meteonorm, 2023)

4.1.2 Berlin, Germany

Berlin has a moderate continental or temperate climate offering strong winters and warm summers. This area is located poleward of the Mediterranean climate zone with predominant features of few extreme temperatures and ample precipitation in all months. Under the Köppen - Geiger climate classification features an oceanic climate (Cfb).

The average temperature for the year in Berlin is 9.9°C. On the coolest month January, the average temperature is 0.5°C. Meanwhile the on warmest month, July the average temperature is 19.8°C. *Figure 5* illustrates the annual temperatures and average solar irradiance on horizontal planes of Berlin, where radiation rises from 15 W/m^2 in December to the peak of 166 W/m^2 in June.

The average annual precipitation is measured up to 669 mm with 97 rainy days on the 1mm threshold annually. Berlin has an average of 2479.08 hours of sunshine in a year, where the duration of sunny hours in January is 79.91 h and in July is 338 h.

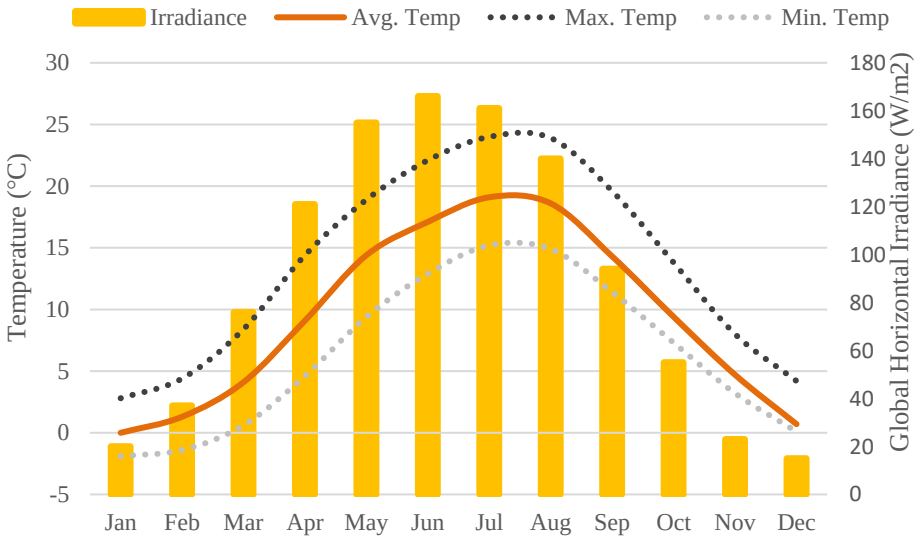

Figure 5. Annual temperatures and global horizontal irradiance for the city of Berlin (Meteonorm, 2023)

4.1.3 Garoua, Cameroon

Garoua has a tropical savanna climate, with a wet and a dry season and the temperature being hot- year long. This area is located in the northern province of Cameroon, one of the warmest regions, influenced by the local steppe climate too. Under the Köppen- Geiger climate classification features a tropical savanna climate (Aw).

The average temperature for the year is 28.9°C. On the warmest month April, the average temperature is 33.5°C and the coolest month August, the average temperature is 26.1°C. *Figure 6* illustrates the annual temperatures and average solar irradiance on horizontal plane of Garoua, where the radiation rises from 160 W/m^2 in February to the peak of 192 W/m^2 in March & April W/m^2.

The average annual precipitation measures up to 667 mm with annual 64 days of rain. Garoua has an average of 3642,2 hours of sunshine in a year, where the duration of sunny hours in January is 273 h and in May and July is 342 h.

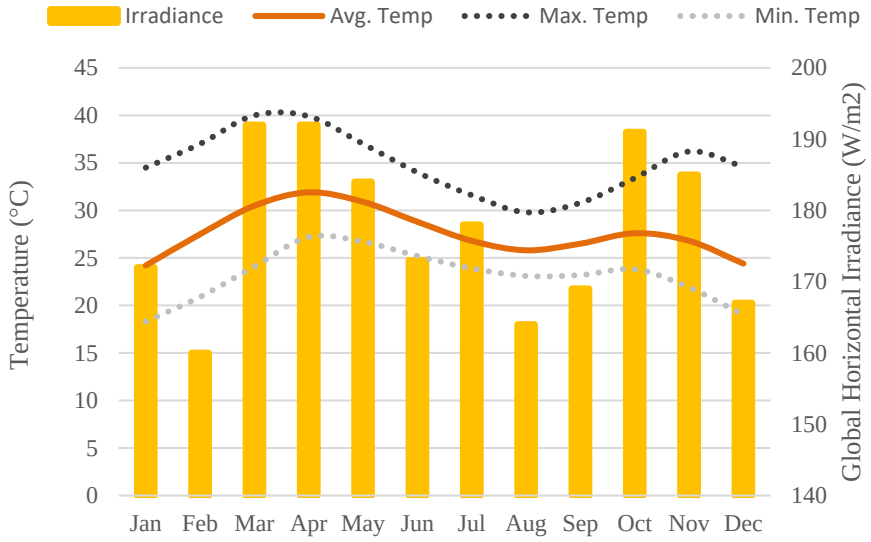

Figure 6. Annual temperatures and global horizontal irradiance for the city of Garoua (Meteonorm, 2023)

4.2 Climate comparison

As illustrated in the Mean Outdoor Temperature graphic (*Figure 7*), Garoua has the highest maximum temperature in April 31.9°C, followed by Athens 28.8°C in August and Berlin 19.1°C in July. Consistently berlin has the minimum temperature in winter January of 0°C, followed by 9.5°C in January and Garoua 24.2°C.

In this manner in Global Horizontal Irradiance graphic (*Figure 8*), Garoua has the highest maximum value of 199 W/m^2 in March and April. At the same time Berlin has the lowest maximum value of 166 W/m^2 in June. Berlin has the lowest GHI value of 15 W/m^2 in December, compared to two other locations, with Athens 54 W/m^2 and Garoua 160 W/m^2, respectively in December and February.

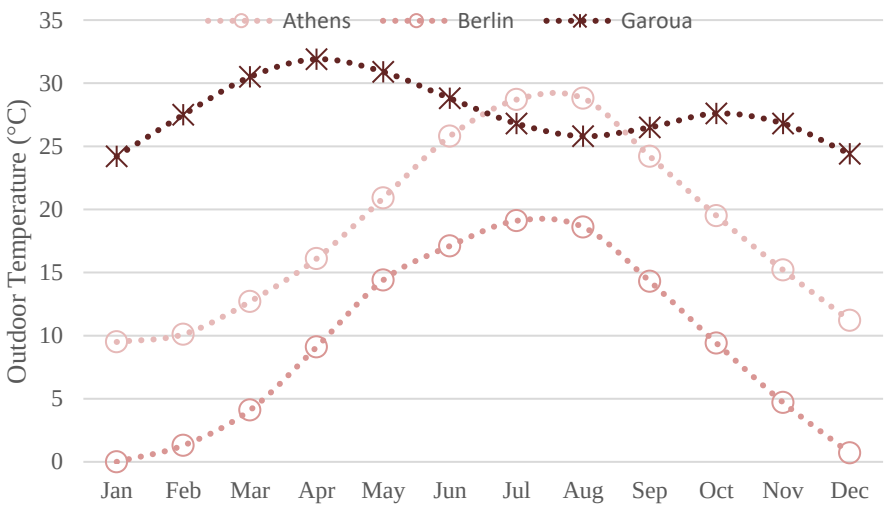

Figure 7. Mean outdoor temperatures for the selected locations (Meteonorm, 2023)

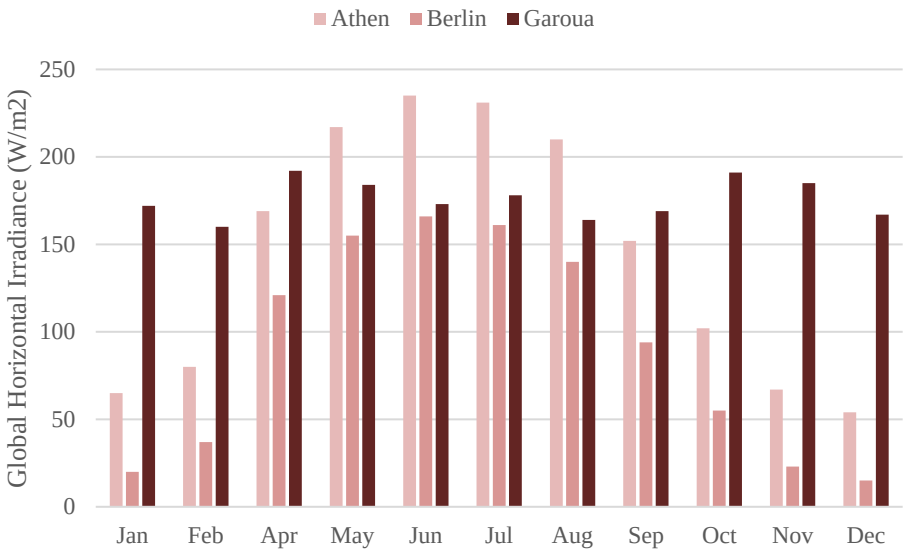

Figure 8. Global horizontal irradiance for the selected locations (Meteonorm, 2023)

4.3 Single low-rise housing morphology

The shape, number of family members, level of social interaction, the spatial organization, and climate region of the context (urban, suburban and rural), are very decisive and influencing parameters in the early stages of designing a house. The selection criteria for the developed case morphologies in this study is based on previous works of: Premrov et al. (2016 ,2018), Lešnik et al. (2020)

The architectural design of the proposed single low- rise housing morphologies are elaborated in terms of internal house layout and volumetric approach, to produce a variety in energy performance assessment. To evaluate which morphology performs better in the selected climatic conditions, total area footprint of a floor of 120 and 190meter square, WWR (20%) in West-East and height are kept constant parameters, whilst building envelope, module transparency in North and South, presence or absence of roof are the variable parameters portrayed in *Table 3*.

To represent the framework of the present study five main design types of single low-rise housing are identified: detached house, semi-detached house, row houses, courtyard house, l-shaped house. Due to the morphological variation, *figure 9* illustrates

16 possible modules for the house design. Meanwhile *Figure 10* and *Figure 11* illustrate the relative compactness of each morphology selected evaluate.

Table 3. The features of low-rise single housing morphology

Morphologies	**Envelope WWR (%)**				**Roof**		**Courtyard**
	N	**E**	**S**	**W**	×	✓	
DH_1$_f$	45,60,75	20	45,60,75	20	×		-
DH_1$_r$	45,60,75	20	45,60,75	20		✓	-
DH_2$_f$	45,60,75	20	45,60,75	20	×		
DH_2$_r$	45,60,75	20	45,60,75	20		✓	-
SDH_1$_f$	45,60,75	20	45,60,75	20	×		-
SDH_1$_r$	45,60,75	20	45,60,75	20		✓	-
SDH_2$_f$	45,60,75	20	45,60,75	20	×		-
SDH_2$_r$	45,60,75	20	45,60,75	20		✓	-
SDH_3$_f$	45,60,75	20	45,60,75	20	×		-
SDH_3$_r$	45,60,75	20	45,60,75	20		✓	-
RH_$_f$	45,60,75	20	45,60,75	20	×		-
RH_$_r$	45,60,75	20	45,60,75	20		✓	-
LH_$_f$	45,60,75	20	45,60,75	20	×		✓
LH_$_r$	45,60,75	20	45,60,75	20		✓	✓
CH_$_f$	45,60,75	20	45,60,75	20	×		✓
CH_$_r$	45,60,75	20	45,60,75	20		✓	✓

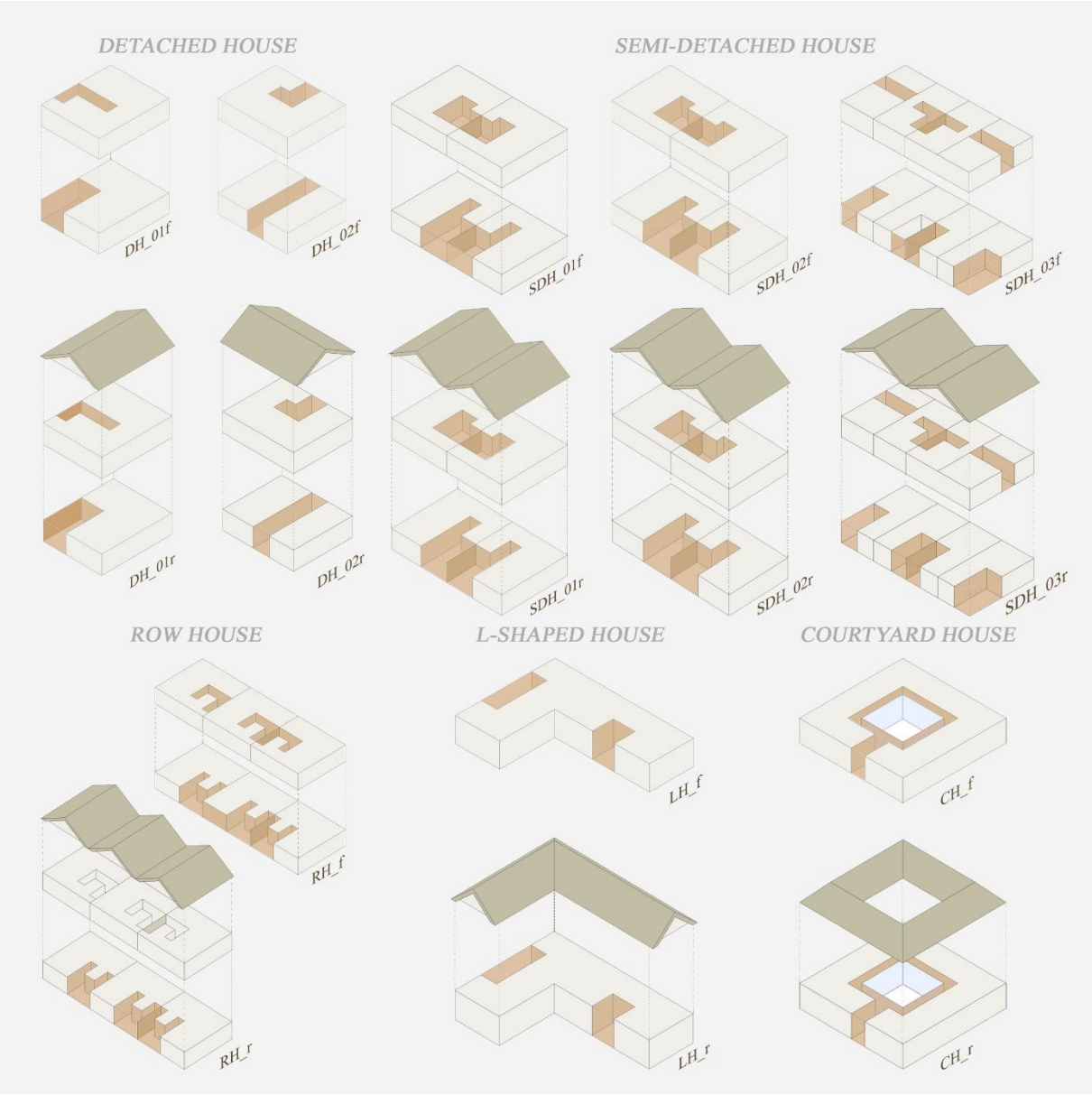

Figure 9. Low-rise single housing morphologies

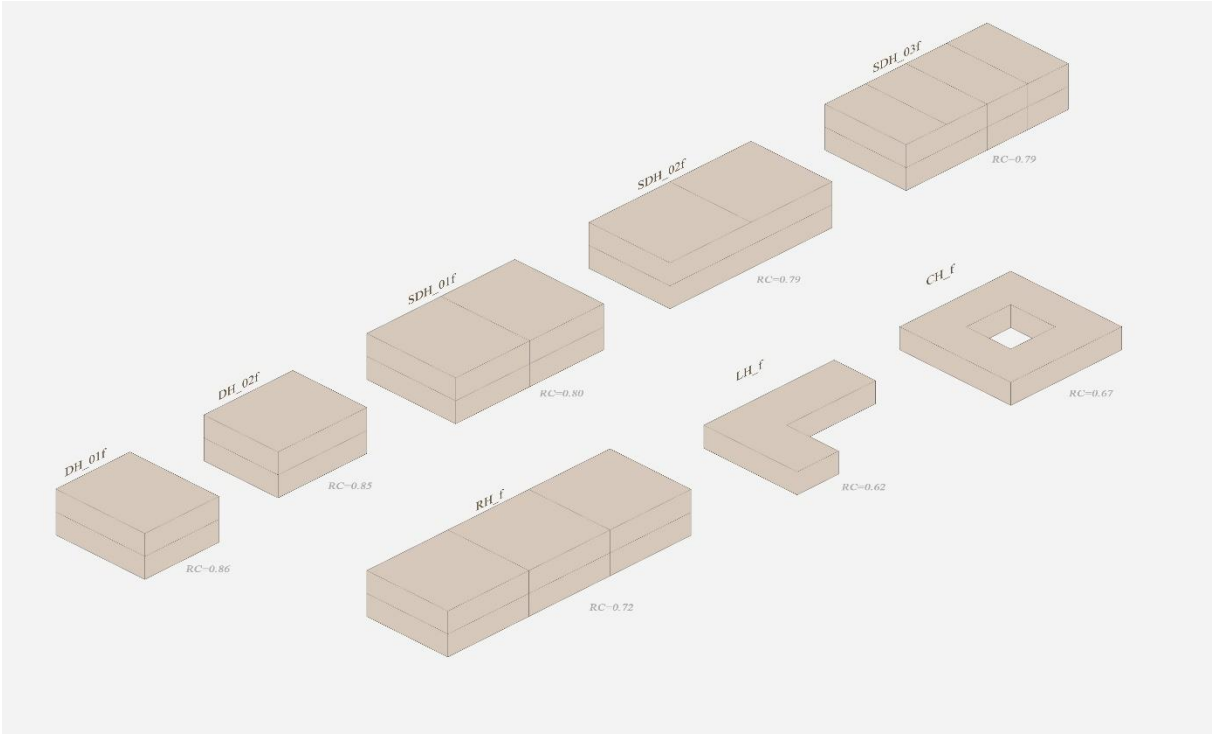

Figure 10. Relative compactness of the flat roof morphologies

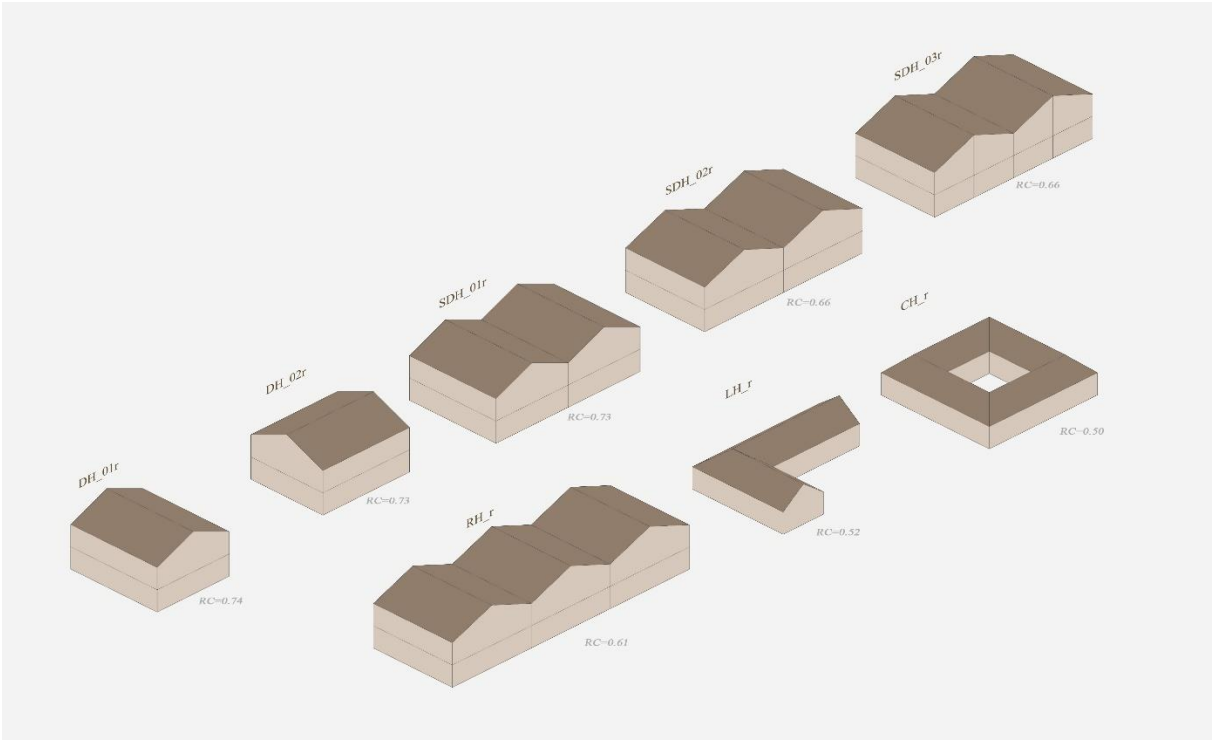

Figure 11. Relative compactness of the pitched roof morphologies

4.3.1 Detached house morphology

The first morphology is detached house, a single dwelling not attached to any other dwelling or structure and has open space on all sides that serves as garden or garage. It is characterized by simple internal layouts and compact rectangular volumes. This building type is best suited for narrow and long plots with a minimum of width of 18 meters, usually facing the main street.

The first model of this morphology is DH_1$_f$ (*Figure 12*), is formed around a simple lateral staircase with a linear vertical rise, just in the entrance hall of the house. The circulation pattern is a clear direction towards the stair and at the same time providing flexible movements for each space. The ground floor is designed to have an open-plan kitchen and dining with a designated butler or storage space and a living area, with great accessibility, transparence and ventilation to each space. The first floor has been designed so that four bedrooms for the family members are extended along the facades with great transparency to receive maximum ventilation and sunlight, and arranged toilet to meet the needs. The same philosophy follows the akin morphology DH_01$_r$ (*Figure 13*), with the presence of a pitched roof. It has the same plan as the first model.

In contrast to DH_1$_f$, DH_2$_f$ (*Figure 14*) model with a flat roof is oriented towards the longest side of the house to see if there is any difference in energy performance because of orientation. It is similar in plan, where the kitchen and dining share an open space together with an attached butler or storage, both taking advantage of the transparency of the façade. The wet space in ground floor is positioned next to the kitchen-dining wall followed by the u-shape staircase in front of the entrance. On the first floor of the house, there are four bedrooms same as the other model with arranged bathrooms, connected by a common corridor. It's akin morphology DH_2$_r$ (*Figure 14*) follows the same logic in terms of internal layout, but with the presence of a roof.

Figure 12. DH_1f morphology

Figure 13. DH_1r morphology

Figure 14. DH_2f morphology

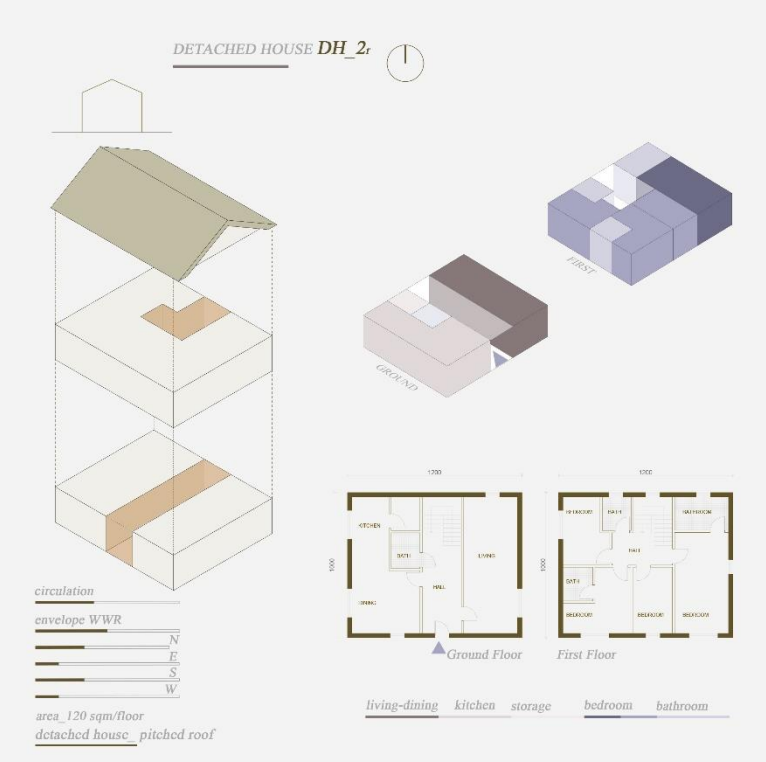

Figure 15. *DH_2r morphology*

4.3.2 Semi-detached house morphology

In comparison to the first morphology, this one consists of two dwellings attached side by side to each other in one plot, but not attached to other dwellings or structure and has open spaces on all side of the house. They are characterized by sharing a common wall, hence known as a semi-detached configuration arranged to face the front street. This house type is best suited to a lot of at least 15 meters in width. This form of low-rise density can be ideal in infill development. The model remains the same in area and volume, but in this case with a slight change in plan layout because of the shared wall.

The first model of this morphology, SDH_1_f as shown in *Figure 16,* is shaped around a linear staircase that rises vertically in levels. The circulation pattern dictated by the stair in ground floor is kept simple and open. The staircase is supported on the shared wall of the two dwellings, meanwhile on the other side of the plan, there is the living room separated with partition walls from the kitchen and dining space, where they all face the North and South façades. In the first floor, the stair takes a turn to a corridor leading to bedrooms and a common bathroom facing the shared wall of dwellings. Each space profits sunlight from the transparency of the façades and ventilation as well. SDH_1_r the semi-detached model with a roof shown in *Figure 17* follows the same layout philosophy.

In comparison to SDH_1_f, in the SDH_2_f model (*Figure 18*), the entire house volume is changed from a rectangular box into a square box, with the same area, to see a difference in the energy performance. Internal layout of the model stays the same as in the first model described above. The same approach is used for the akin morphology SDH_1_r (*Figure 19*).

Another model of this morphology is SDH_3_f as shown in *Figure 20,* where the same area of one house is divided into two houses, meaning a dual occupancy within a model. The internal layout of the dual occupancy is organized around the lateral staircase on one side whereas the living, dining, kitchen area in the ground floor and bedrooms, bathrooms on the side where the wall is shared. Meanwhile the other dual occupancy has the mirrored layout of spaces. SDH_3_r, the akin morphology shares the same attributes, only with a roof, as it is shown in *Figure 21*.

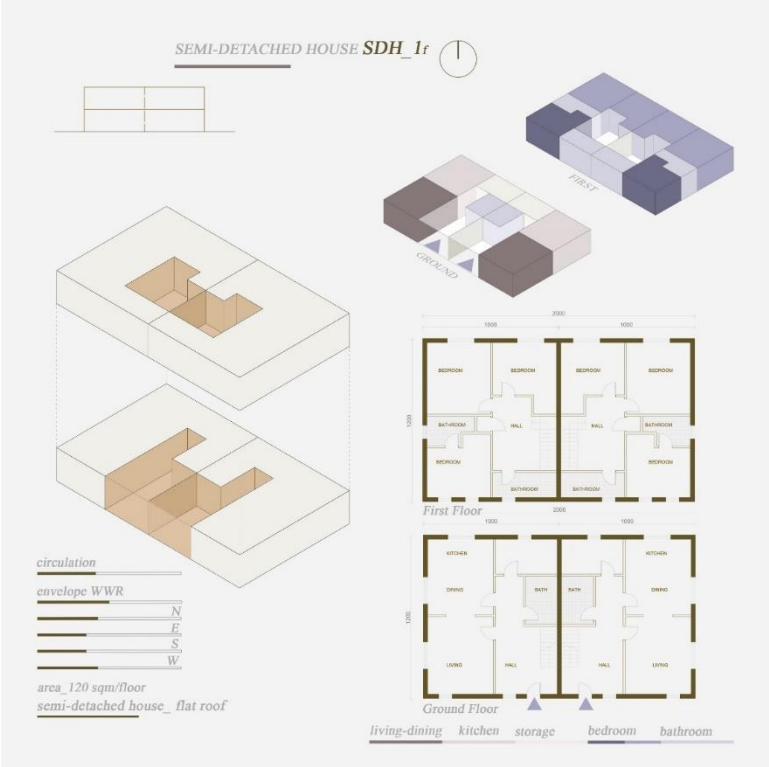

Figure 16. SDH_1f morphology

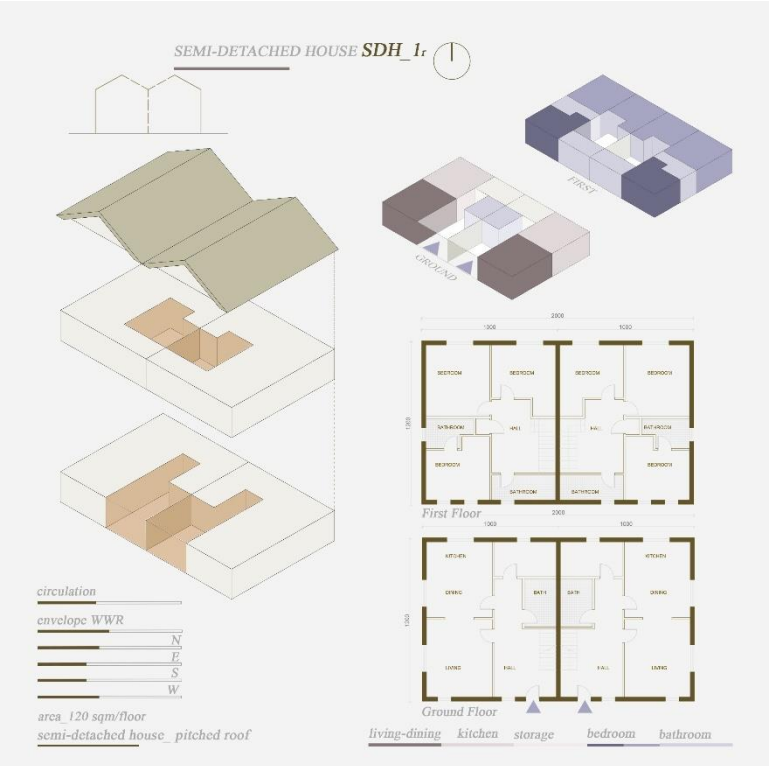

Figure 17. SDH_1r morphology

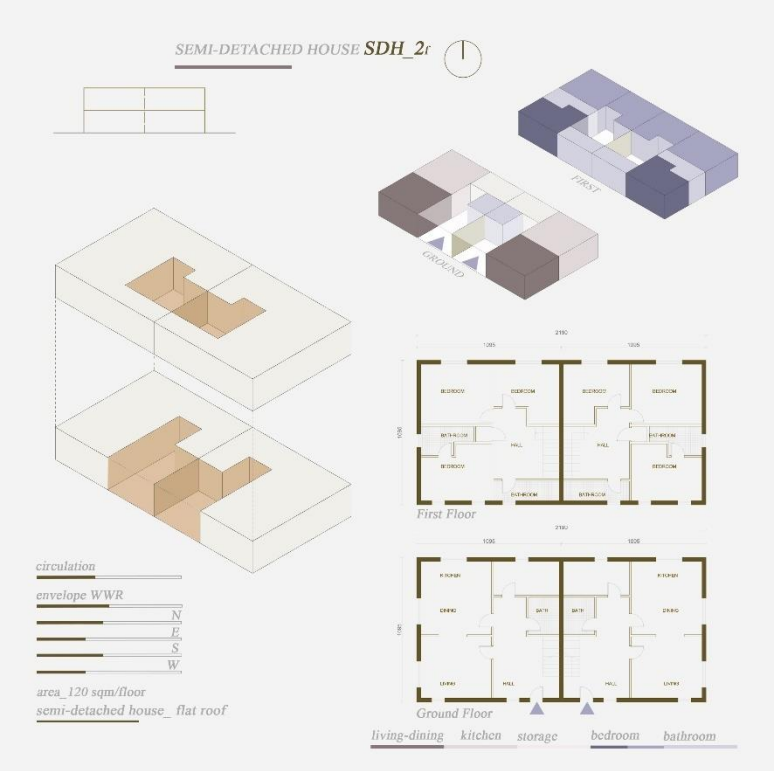

Figure 18. SDH_2f morphology

Figure 19. SDH_2f morphology

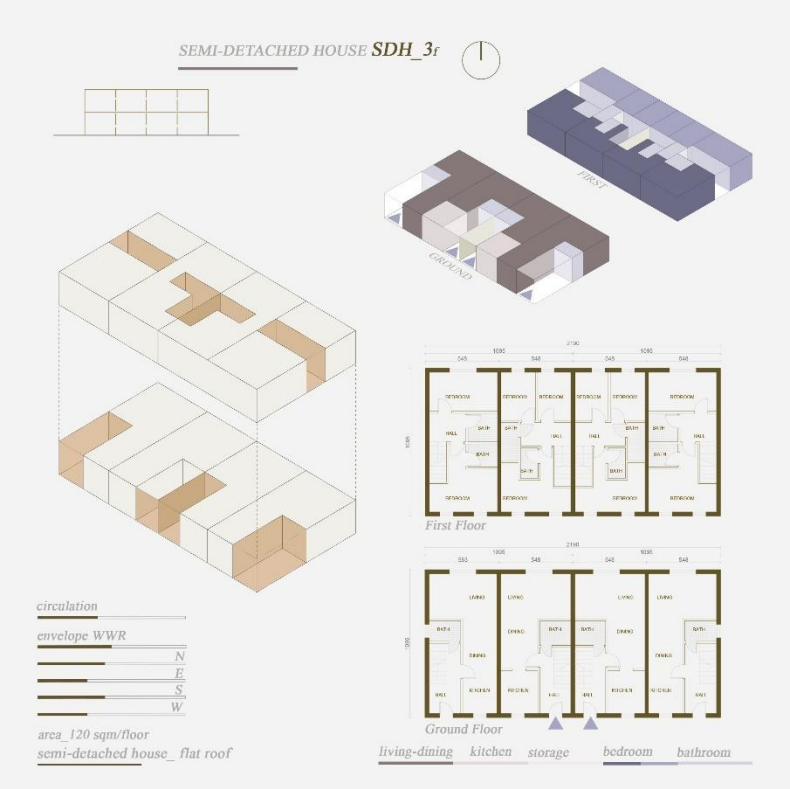

Figure 20. SDH_3f morphology

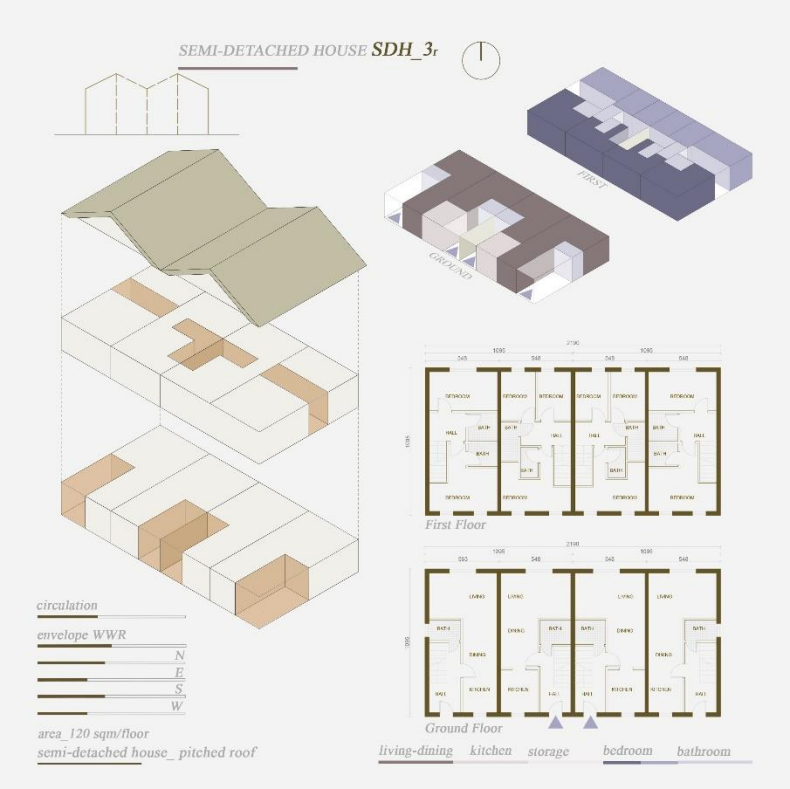

Figure 21. SDH_3r morphology

4.3.3 Row house morphology

This morphology defines three or more house attached to one another in a row, such as townhouses, or garden homes, that have no other dwelling either or above. This one of a series of houses are connected by common sidewalls and form a continuous group. Rowhouses share a roof line, similar or identical design and have a snug placement which can limit natural light through windows.

The first model of this morphology RH_f as shown in *Figure 22* is formed by three identical row dwellings. The circulation pattern in ground floor is dictated by the linear staircase leading vertically to the upper floor spaces. The kitchen space is located in the south façade together with the staircase and one bathroom, meanwhile the shared open space between the dining and living zone faces the north façade. All spaces of ground floor receive enough sunlight and ventilation. The first-floor houses three bedrooms for the family members and a common bathroom for all. The circulation is kept simple and clear in both levels of the house. A slight change in having no transparency happens in the sidewalls of the middle house, since they are shared with the other two houses of the model. The akin morphology, RH_r has the same design approach, but with a pitched roof as shown in *Figure 23*.

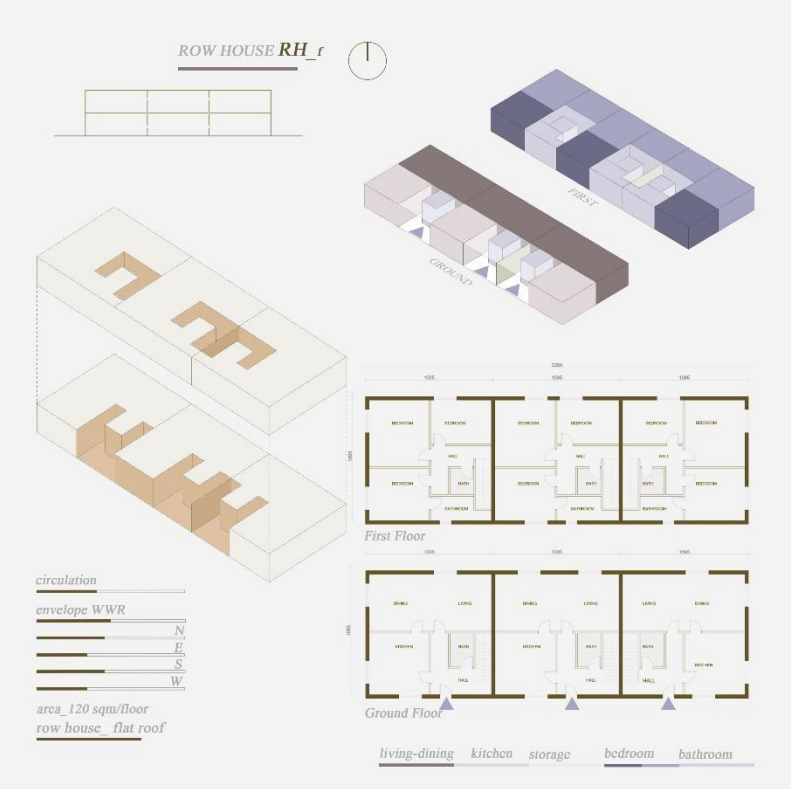

Figure 22. RH_f morphology

Figure 23. RH_r morphology

4.3.4 L-shape house morphology

This morphology consists of a L shape dwelling, featuring a flexible, semi-open plan to house all necessary spaces for the occupants. It is characterized by two wings of the house, which meet at a common courtyard, acting as a sheltered outdoor space for domestic activities or entertainment. This shape of house is adaptable on large or small plots, flat ground or not.

The model of this morphology LH_f morphology in *Figure 24*, is shaped around a front courtyard. It is a one floor model, with three-bedroom spaces and arranged bathrooms around the two wings of the house. The living space is an open concept together with the dining and kitchen space. The daytime spaces are connected with the sleeping spaces through a corridor. All spaces receive sunlight from the transparency in façades and ventilation too. Same as LH_f, the akin model LH_r has the same characteristics with the presence of the pitched roof (*Figure 25*).

Figure 24. LH_f morphology

Figure 25. LH_r morphology

4.3.5 Courtyard house morphology

This morphology consists of a square shape model that tend to bring the outdoors inside the interior of the house. A courtyard house typically has its main rooms surround and open toward the central courtyard, a significant characteristic of the house that offers recreational space. They were traditionally used in hot and humid climate regions for cross ventilation reasons. The majority of the ventilation and transparency enters the house through the open sky of the courtyard.

The first model of this morphology $CH\__f$ (*Figure 26*), is a one-story model, with a flat roof formed around a central courtyard, which has completely transparent façades and bring in sunlight and ventilation. On one side of the house, on the north façade the open plan kitchen, dining and living space is located. On the other opposite sides of the house bedrooms and bathrooms are located, with the entrance of the house on the south façade. All spaces of the house are connected through a common hall that goes around the central courtyard and looks toward it. $CH\__r$ is the akin morphology, with a roof construction (*Figure 27*).

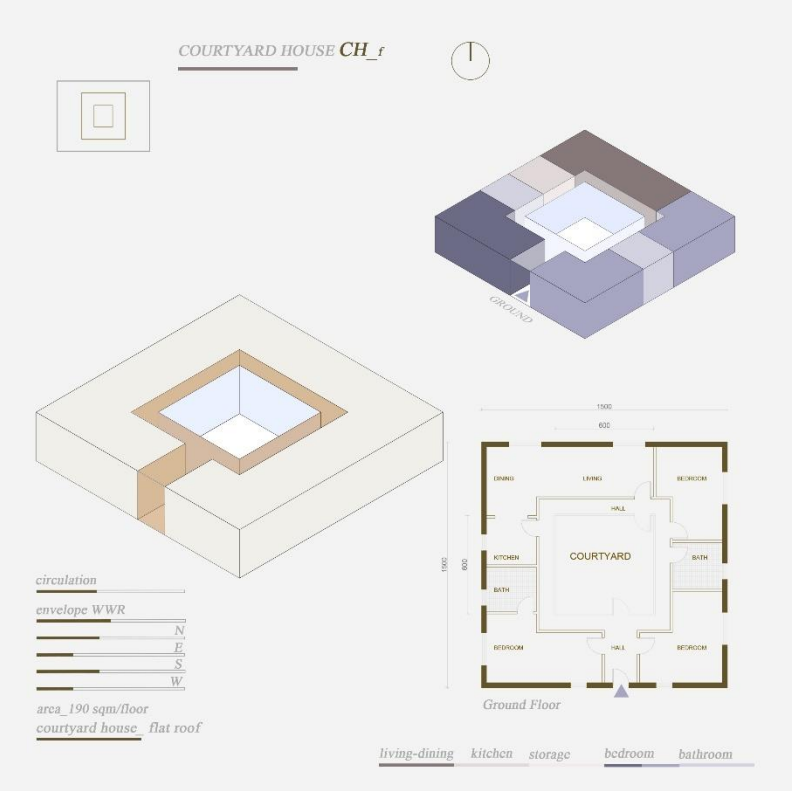

Figure 26. CH_f morphology

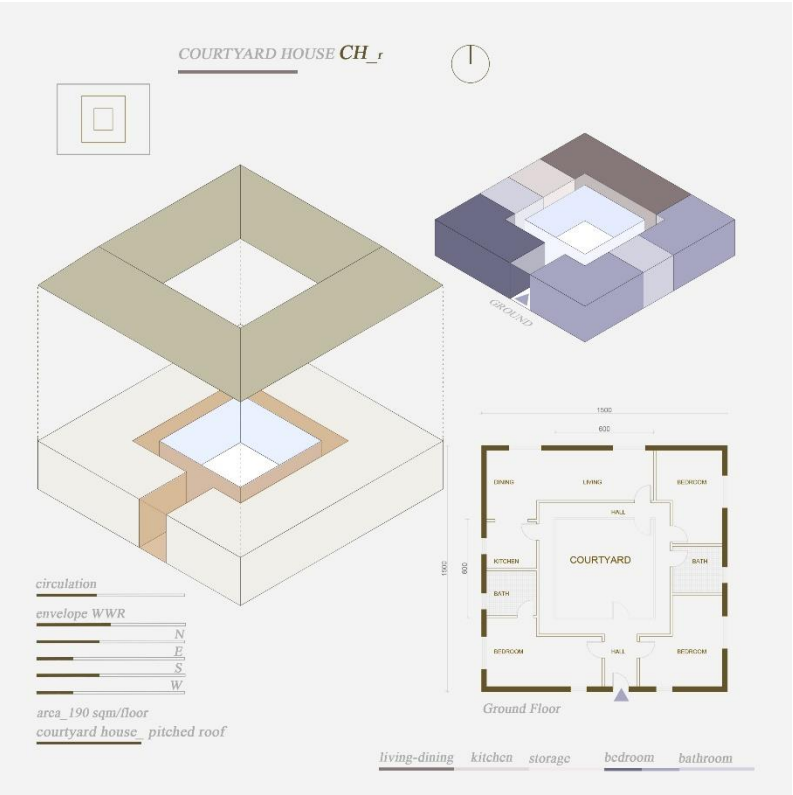

Figure 27. CH_r morphology

4.4 Modeling and simulation

Design Builder software is used to model sixteen low-rise single housing morphologies and generate virtual simulations inputs stay the same for every morphology that are shown in figures and tables below.

4.4.1 Building models

To assess the performance of various low-rise single housing morphologies under three different climate regions, prototypes of one-to-two storey single family houses of a 3.1m floor-to-floor height and a footprint of 120 m2 and 190 m^2 per floor are selected then generated. Eight flat roof housing models and eight pitched roof housing models with similar spatial composition, but different morphologies are designed and later modeled in Design Builder. The layout of the house accommodates the living and dining area, kitchen, storage or butler space and a toilet area in the ground floor, connected through circulation and stairs with bedrooms, toilet spaces in the first floor. The distribution of spatial functions is shown in *Figure 28*.

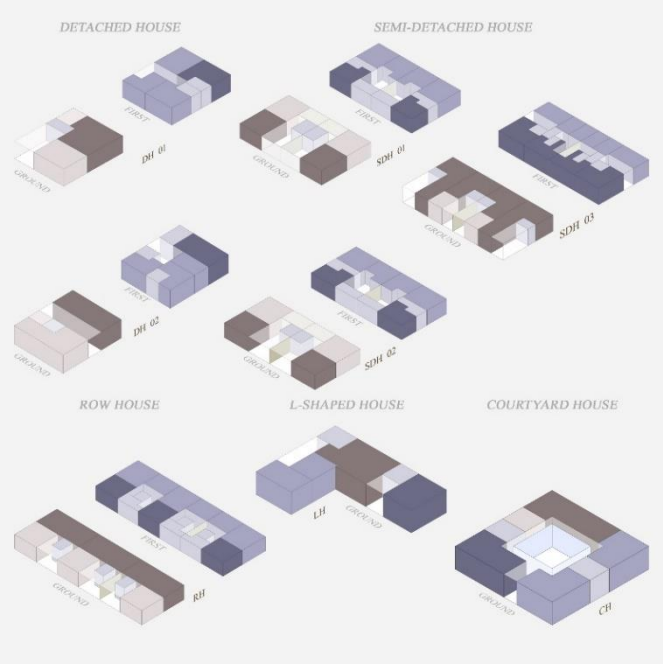

Figure 28. Distribution of spatial function

Hence the occupancy schedules respond to the demand of the family member's daily activity from January to December as shown in *Figure 29*. The input parameters of both construction templates, HVAC templates, internal loads are kept the same in all house modules for comparative reasons only, as shown in *Table 4*, *Table 5*, *Table 6*, *Table 7*. *Figure 30*, *Figure 31* and *Figure 32* showcase the 2D detailed construction properties of the two selected timber construction systems and *Figure 33* and *Figure 34* showcase the 3D detailed construction properties of both timber systems.

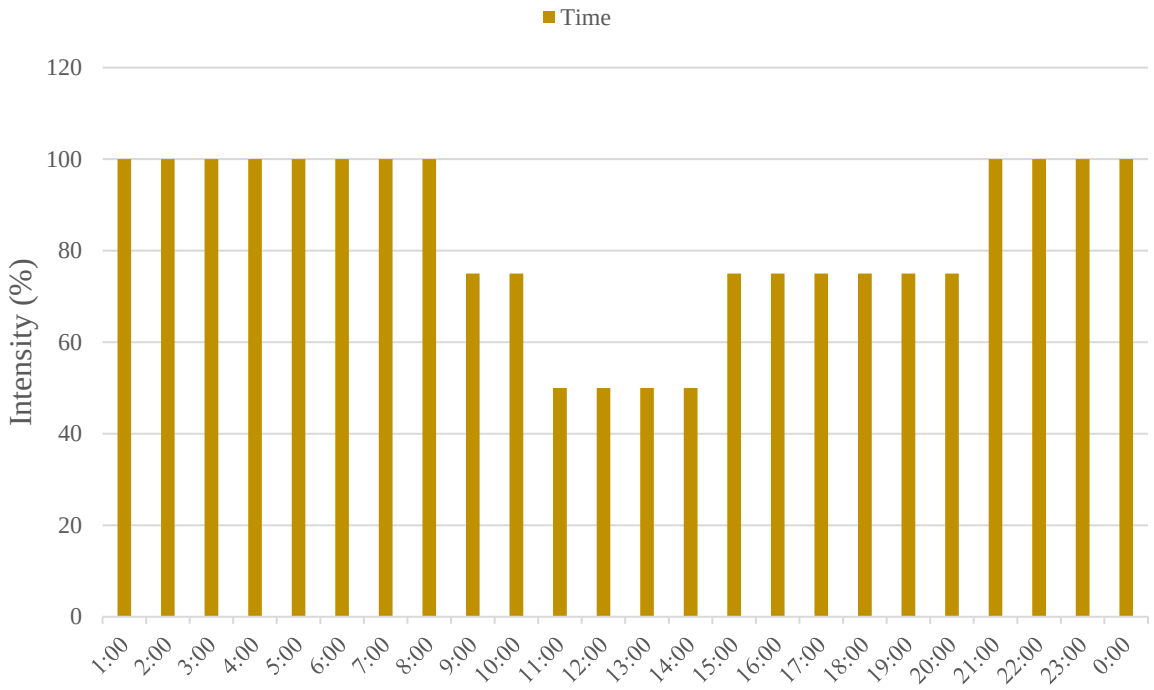

Figure 29. Occupancy schedule

Table 4. Construction properties for Mass timber construction system

Mass timber construction		**Density [kg/ m3]**	**Conductivity [W/m ◦C]**	**Specific heat [J/ kg ◦C]**	**Thickness [m]**
External wall	Solid wood	510	0.1200	1380	0.08
U-value	GLULAM	100	0.0330	710	0.06
=	Rockwool ins.	980	0.5	1800	0.001
0.321	Polyethylene high				
[W/m2 . K]	dens. sheet	-	-	-	0.05
	Ventilation gap	560	0.15	2500	0.022
	Plywood board				

Internal wall U-value = 0.534 [W/m2 . K]	Plywood panel(lightweight)	560	0.15	2500	0.042
	Mineral fiber	140	0.038	840	0.040
	Plywood panel(lightweight)	560	0.15	2500	0.042
Insulated flat roof U-value = 0.244 [W/m2 . K]	Glued laminated beam	510	0.12	1350	0.025613
	Vapor retarding layer	-	-	-	0.006
	Cross wood rafters	510	0.12	1380	0.04289
	Rockwool ins.	100	0.0330	710	0.06
	Polyethylene high dens. sheet	980	0.5	1800	0.0016
	Ventilation & drainage	-	-	-	0.04
		510	0.12	1380	0.2
	Plywood strip/plank	170	0.216	1300	0.004
	Fiber cement sheet				
Insulated pitched roof U-value = 0.244 [W/m2 . K]	Glued laminated beam	510	0.12	1350	0.025613
	Vapor retarding layer	-	-	-	0.006
	Cross wood rafters	510	0.12	1380	0.04289
	Rockwool ins.	100	0.0330	710	0.06
	Polyethylene high dens. Sheet	980	0.5	1800	0.0016
	Counter batons	-	-	-	0.04
	Ventilation & drainage	-	-	-	0.05
	Plywood strip/plank	510	0.12	1380	0.2
	Fiber cement sheet	170	0.216	1300	0.004
Ground floor +foundation U-value = 1.117 [W/m2 . K]	Gravel-soil base	2050	0.52	184	0.045
	Polyethylene high dens. Sheet	980	0.5	1800	0.001
	Floor screed	1200	0.41	840	0.007
	Foundation	1300	2.3	1000	0.1
	Floor screed	1200	0.41	840	0.007
	Timber flooring	650	0.14	1200	0.022

Table 5. Construction properties for Mass timber construction system

Light-frame timber construction		**Density [kg/ m3]**	**Conductivity [W/m ◦C]**	**Specific heat [J/ kg ◦C]**	**Thickness [m]**
External wall U-value = 0.572 [W/m2 . K]	Weatherboarding (douglas fir)	650	0.14	2000	0.0255
	Stud wall system	510	0.12	1310	0.0194
	Tyvek sheet	980	0.5	1800	0.01
	Softwood board	550	0.14	1880	0.022

	Rockwool ins.	100	0.033	710	0.03
	Polyethylene high dens. sheet	980	0.5	1800	0.01
	Plywood panel(lightweight)	560	0.15	2500	0.022
Internal wall U-value = 0.534 [W/m2 . K]	Plywood panel(lightweight)	560	0.15	2500	0.042
	Mineral fiber	140	0.038	840	0.040
	Plywood panel(lightweight)	560	0.15	2500	0.042
Insulated flat roof U-value = 1.401 [W/m2 . K]	Water-tight adhesive board (plywood)	510	0.12	1350	0.0225
	Cross wood rafters	510	0.12	1380	0.009
	Rockwool ins.	100	0.0330	710	0.03
	Polyethylene high dens. sheet	980	0.5	1800	0.0016
	Fiber cement sheet	170	0.216	1300	0.004
Insulated pitched roof U-value = 1.483 [W/m2 . K]	Cross wood rafters	510	0.12	1380	0.009
	Rockwool ins.	100	0.0330	710	0.03
	Polyethylene high dens. Sheet	980	0.5	1800	0.0016
	Softwood board	550	0.14	1880	0.06
	Fiber cement sheet	170	0.216	1300	0.004
Ground floor +foundation U-value = 1.117 [W/m2 . K]	Gravel-soil base	2050	0.52	184	0.045
	Polyethylene high dens. sheet	980	0.5	1800	0.001
	Floor screed	1200	0.41	840	0.007
	Foundation	1300	2.3	1000	0.1
	Floor screed	1200	0.41	840	0.007
	Timber flooring	650	0.14	1200	0.022

Table 6. Input parameters for HVAC operation

Input parameters	
Fan coil unit	(4 pipes) water-cooled chiller, waterside economizer
Heating/cooling system	Electricity from grid
Coefficient of Performance [CoP] (Heating)	3.8
Coefficient of Performance [CoP] (Cooling)	3.4
Heating set back [°C]	12
Cooling set back [°C]	28
Natural ventilation setpoint [°C]	15

Table 7. Brief spatial program of a morphology

Building models	Footprint area m2	Total area m2	Fresh Air (L/S-Person)	Air Exchange Rate (Ac/h)	Power density (W/m²- 100 lux)	Heating temperature set points °C	Cooling temperature set points °C	Occupancy density [P/m2]
DH_1_f	120	205.01	10	10	4	22	24	0.020
DH_1_r	120	205.01	10	10	4	22	24	0.020
DH_2_f	120	200.91	10	10	4	22	24	0.020
DH_2_r	120	200.91	10	10	4	22	24	0.020
SDH_1_f	120	419.75	10	10	4	22	24	0.016
SDH_1_r	120	419.75	10	10	4	22	24	0.016
SDH_2_f	120	418.5	10	10	4	22	24	0.016
SDH_2_r	120	418.5	10	10	4	22	24	0.016
SDH_3_f	120	405.16	10	10	4	22	24	0.016
SDH_3_r	120	405.16	10	10	4	22	24	0.016
RH_{f}	120	626.98	10	10	4	22	24	0.016
RH_{r}	120	626.98	10	10	4	22	24	0.016
LH_{f}	120	105.6	10	10	4	22	24	0.016
LH_{r}	120	105.6	10	10	4	22	24	0.016
CH_{f}	190	162.77	10	10	4	22	24	0.021
CH_{r}	190	162.77	10	10	4	22	24	0.021

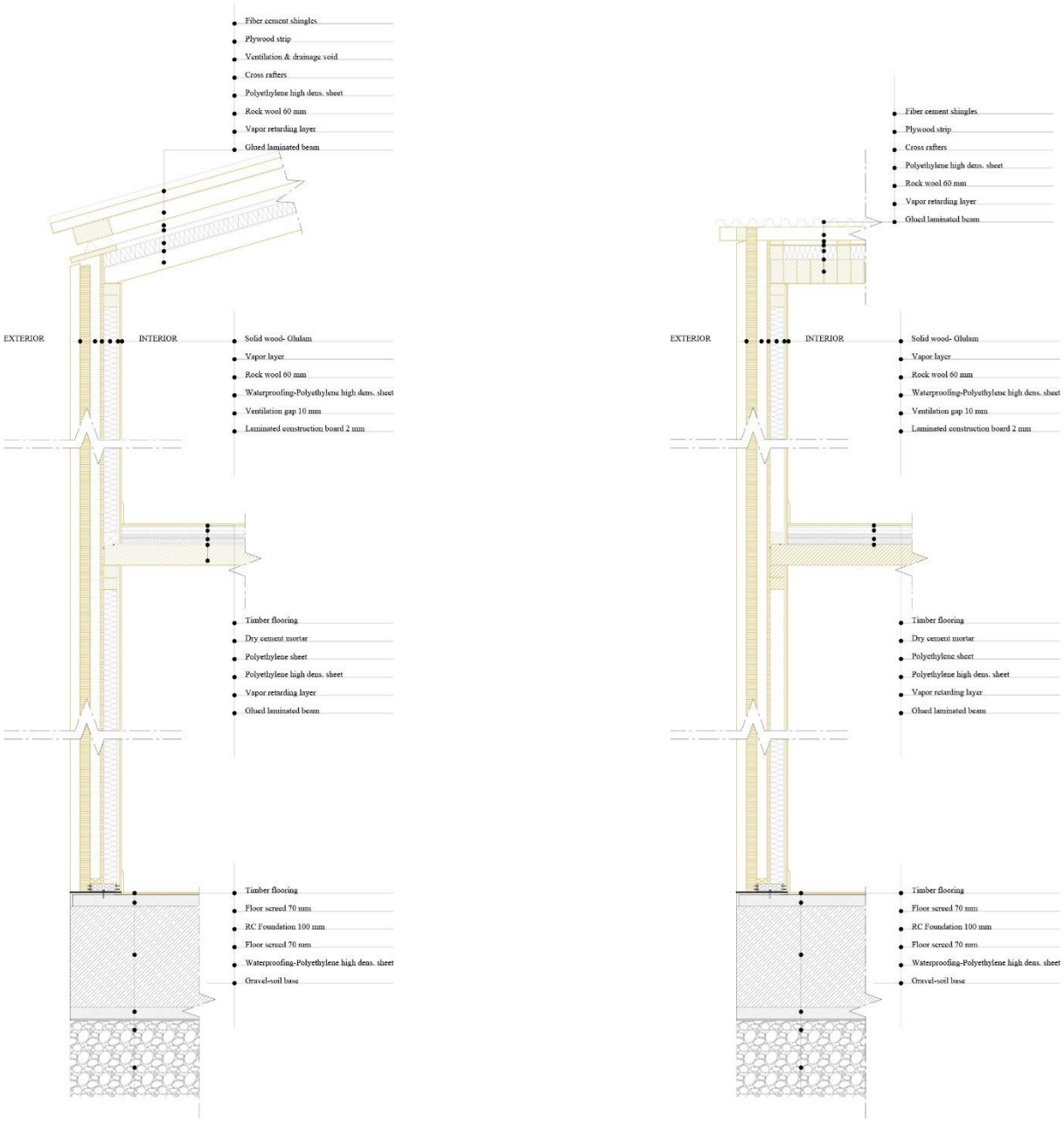

Figure 30. Mass timber construction section system

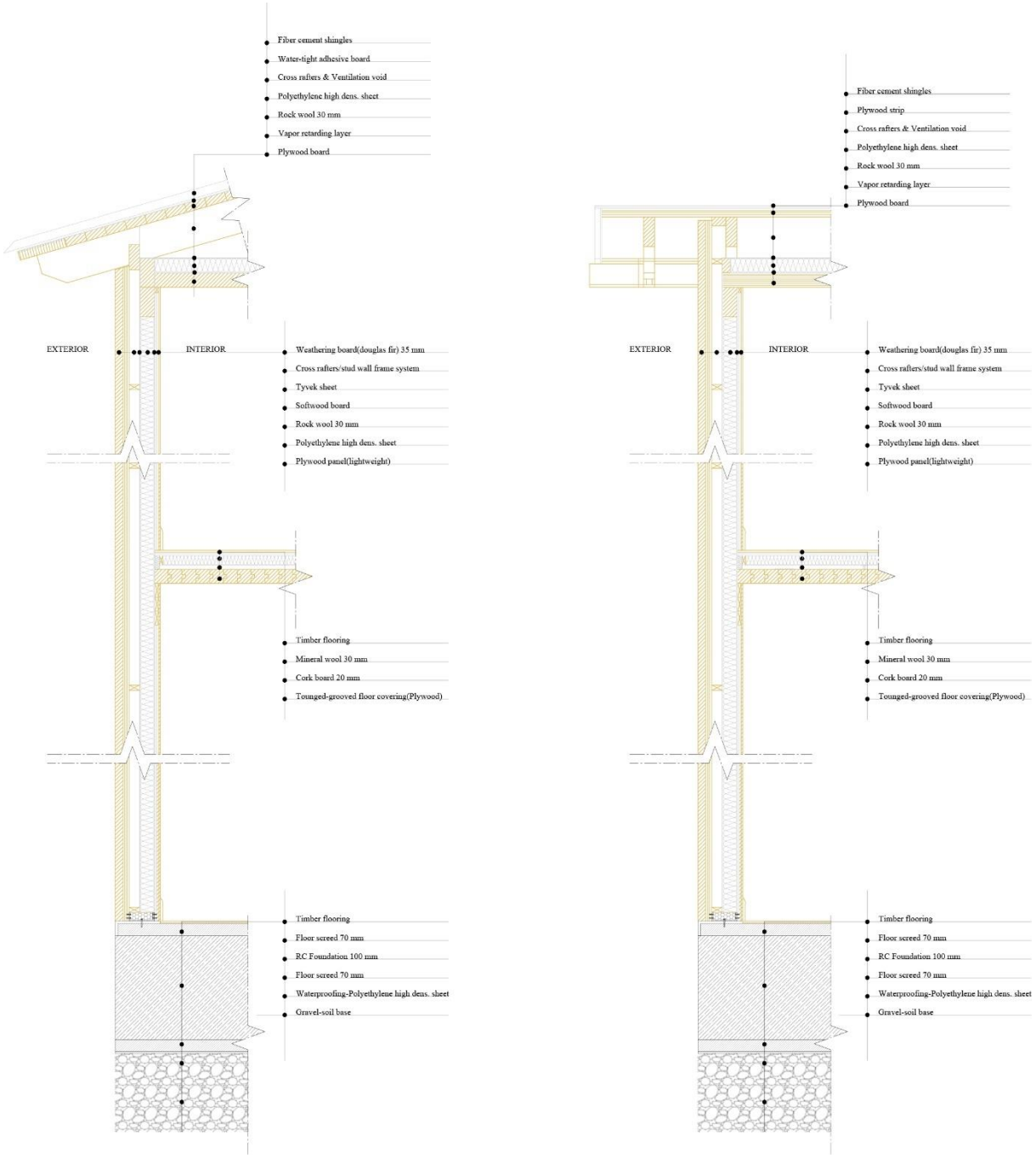

Figure 31. Light-frame timber construction section system

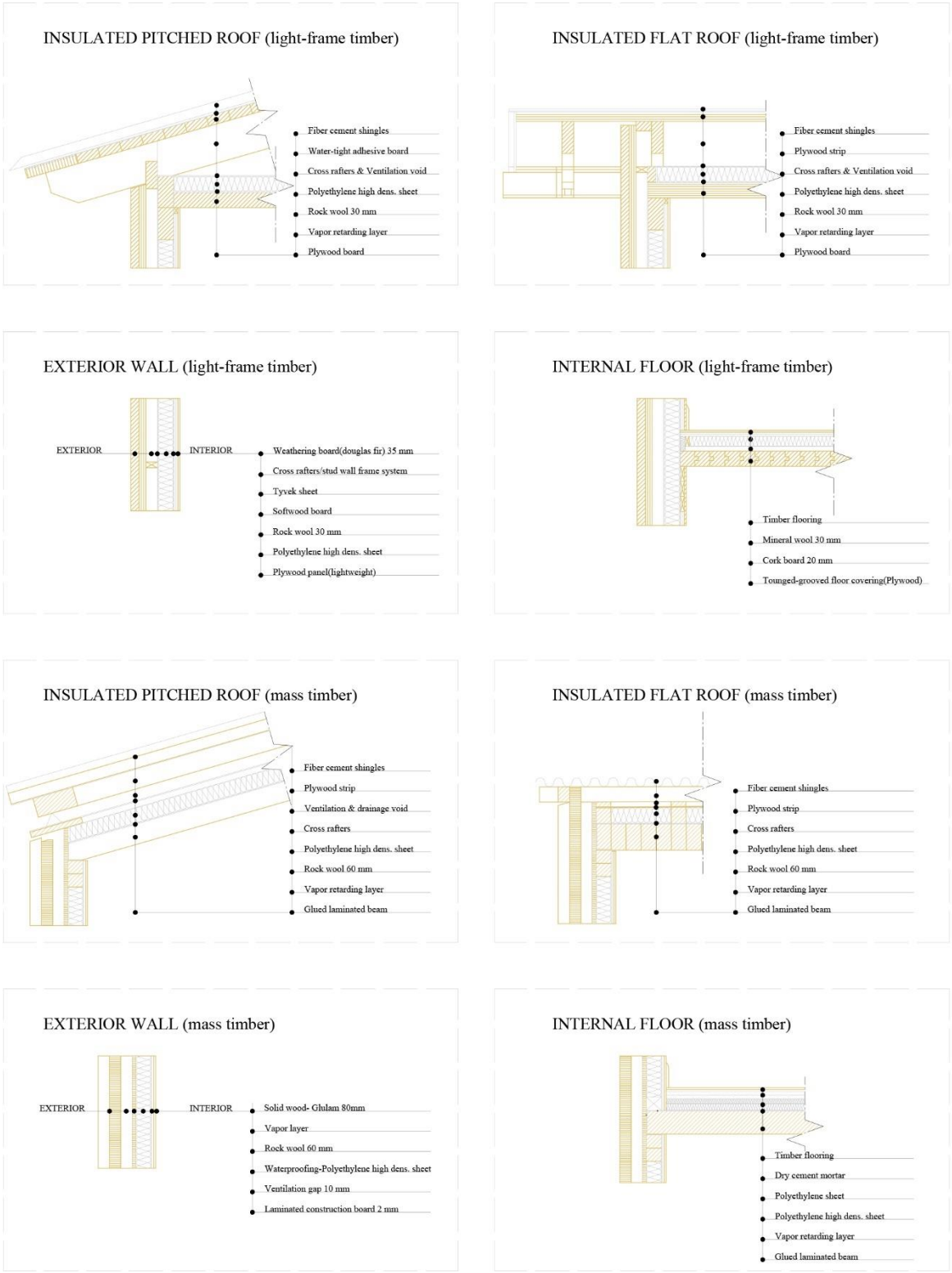

Figure 32. Sections of detailed construction for the simulation models

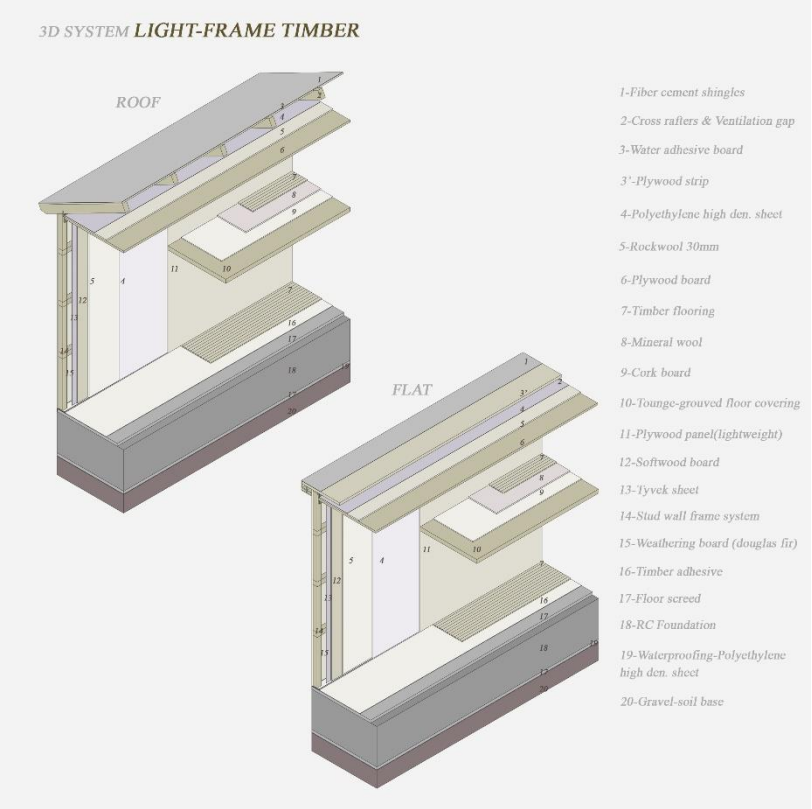

Figure 33. Mass timber construction 3D section system

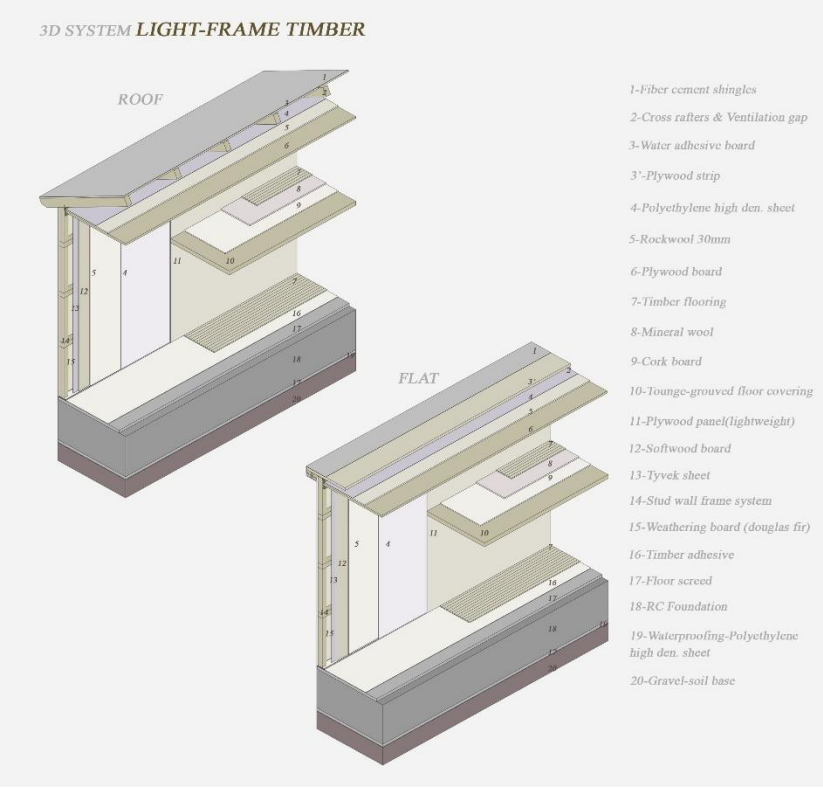

Figure 34. Light-frame timber construction 3D section system

CoP (coefficient of performance for heating and cooling) is established on the selected HVAC system for all low-rise single housing morphologies in three climatic contexts used to run the computational simulation. The simulation runs for every specific functional zoning, with their set occupancy schedules, cooling and heating set points/backs temperatures [°C], minimum fresh air flow rate per person [l/s], air exchange rates [ac/h] and occupancy density [P/m^2].

As for the energy simulation operation, all selected input parameters account as essential to the detailed model development process, based on the reviewed research studies (Nunes et al., 2020; Premrov et al., 2016; Depecker et al., 2001, Persson,2006; AlAnzi et al., 2009, Jaber & Ajib, 2011; Lešnik et al., 2020).

Window-to-wall ratio (WWR), sets the percentage of the exterior wall area covered by glazing material. In the West-East oriented façades it is a set of constant 20% glazing. This value varies on the North-South oriented façades from 45%, 60% and 75% glazing. For the purpose of achieving building energy efficiency and optimal daylight factor, said values are set according to façades glazing scenarios (Depecker et al., 2001; Maučec et al., 2021; Dickson & Parker, 2014). *Table 8* displays the glazing properties used in all house morphologies. The natural ventilation schedule (*Table 9*) is set the same for three climatic conditions for comparison purposes.

Table 8. Glazing properties for WWR 45%,60%75%

Glazing properties	
Glazing type	Double LoE (e2=1) clear 6mm/13mm Air
Frame properties	Painted wood frames
SHGC (Total solar transmission)	0.568
U-value of glass [W/m2 .K]	1.761
Opening position	middle
Glazing area opens [%]	30
Airtightness [ac/h]	0.5

Table 9. Natural ventilation schedule

Ventilation	**Warm months**	**Intensity (%)**	**Cold months**	**Intensity (%)**
	1:00-8:00	100	1:00-8:00	0
	8:00-10:00	75	8:00-10:00	100

Natural	10:00-14:00	50	10:00-14:00	0
	14:00-18:00	75	14:00-18:00	0
	18:00-20:00	75	18:00-20:00	100
	20:00-00:00	100	20:00-00:00	0

4.4.2 Simulation scenarios of the proposed design strategies

Several related design variables are obtained from the energy and thermal comfort computation of the sixteen building shapes. The impact of glazing transparency of the housing models is tested by using a base glazing of 45% as a starting point, then followed by 60% and 75% (representing the north and south oriented façades) in three different climatic conditions, furthermore investigating the effect it has on the energy performance (*Figure 35*).

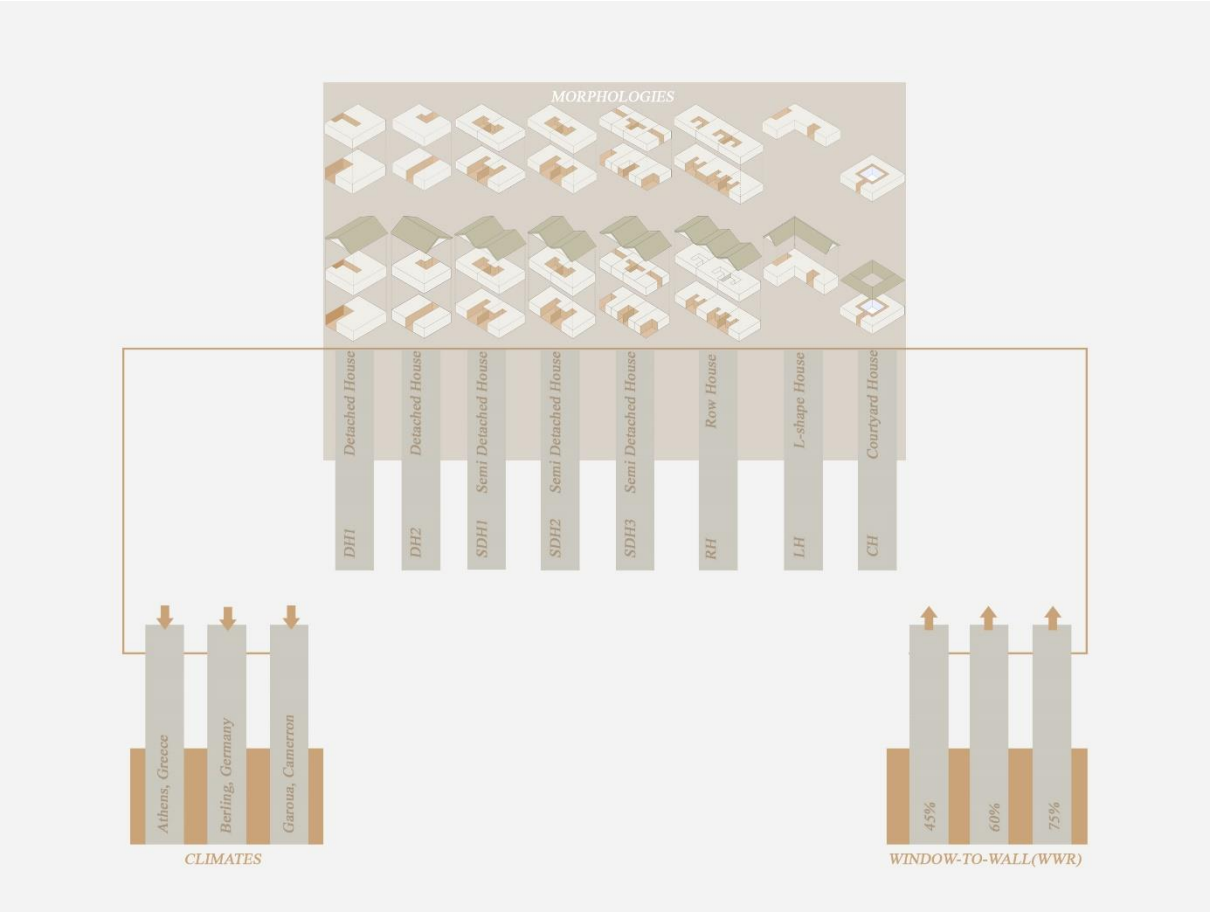

Figure 35. Simulation scenarios for 16 morphologies

Table 10 explains the simulation scenarios for each morphology. Description of each and every shape is detailed based on its formation, presence of construction elements and façade openings.

The table includes morphologies that are south-oriented as the base scenario. Indicated changes in the module range are made to adapt to the concept of each low-rise single housing morphology.

Table 10. Description of the simulation scenarios

Morphology		***Code***	***Scenario***	***Description***
Detached Housing	**D**	DH_1_f	Base case scenario, detached house, rectangular box, 2-storey high, flat-roof	Single-dwelling, a vertical block which is organized around a linear staircase and has transparency on all façades.
		DH_1_r	Base case scenario, detached house, rectangular box, 2-storey high, pitched roof	Single-dwelling, a vertical block which is organized around a linear staircase and has transparency on all façades.
		DH_2_f	Detached house, square box, 2-storey high, flat-roof	Single-dwelling, a horizontal block which is organized around a linear staircase and has transparency on all façades.
		DH_2_r	Detached house, square box, 2-storey high, pitched roof	Single-dwelling, a horizontal block which is organized around a linear staircase and has transparency on all façades.
Semi-Detached Housing	**SD**	SDH_1_f	Semi-Detached house, rectangular box, 2-storey high, flat-roof	Single-dwellings (2), attached to one another, vertical blocks which are organized around a linear staircase and have not transparency on the shared wall.
		SDH_1_r	Semi-Detached house, rectangular box, 2-storey high, pitched roof	Single-dwellings (2), attached to one another, vertical blocks which are organized around a linear staircase and have not transparency on the shared wall.
		SDH_2_f	Semi-Detached house, square box,	Single-dwellings (2), attached to one another, horizontal blocks which are

			2-storey high, flat-roof	organized around a linear staircase and have not transparency on the shared wall.
		SDH_2$_r$	Semi-Detached house, square box, 2-storey high, pitched roof	Single-dwellings (2), attached to one another, horizontal blocks which are organized around a linear staircase and have not transparency on the shared wall.
		SDH_3$_f$	Semi-Detached house, 2-storey high, flat-roof, dual occupancy	Single-dwellings (2), with dual occupancy attached to one another, vertical blocks which are organized around a staircase and have not transparency on the shared walls.
		SDH_3$_r$	Semi-Detached house, 2-storey high, pitched roof, dual occupancy	Single-dwellings (2), with dual occupancy attached to one another, vertical blocks which are organized around a staircase and have not transparency on the shared walls.
Row Housing	**R**	RH_$_f$	Row housing, 2-storey high, flat-roof	Single-dwellings (3), with dual occupancy attached to one another, vertical blocks which are organized around a staircase and have not transparency on the shared walls.
		RH_$_r$	Row housing, 2-storey high, pitched roof	Single-dwellings (3), with dual occupancy attached to one another, vertical blocks which are organized around a staircase and have not transparency on the shared walls.
L-shape Housing	**L**	LH_$_f$	L-shape housing, one or 2-storey high, flat-roof, front courtyard	Single-dwelling, consisting of two wings which are organized around a courtyard that receives transparency from.
		LH_$_r$	L-shape housing, one or 2 storey high, pitched roof, front courtyard	Single-dwelling, consisting of two wings which are organized around a courtyard that receives transparency from.
Courtyard Housing	**C**	CH_$_f$	Courtyard housing, one or 2-storey high, flat-roof	Single-dwelling, consisting of a square which is organized around an inner courtyard and a common hall that receives transparency from.
		CH_$_r$	Courtyard housing, one or 2-storey high, pitched roof	Single-dwelling, consisting of a square which is organized around an inner courtyard and a common hall that receives transparency from.

4.4.3 Output variables

To evaluate the impact of the virtual morphologies on energy performance and thermal comfort for each house model, one reference summer day (July 22) for Athens, Greece and one reference summer day (May 3) for Garoua. Same logic is used for one reference winter day (January 18) for Athens, Berlin and one reference winter day (January 4) are assessed for each worst scenario to predict the hourly indoor temperature, specifically the living-dining room area. In all developed models, the required inputs for energy simulation together with heating/cooling, take into account previous work in this field.

Following the assessed results from the chosen reference days, the hourly mean overheating (Ohm) is used to interpret the comparison between scenarios (*Equation 3*).

$$\sum_{j=1}^{n} \frac{\theta ij - \theta r}{n} m \qquad \text{(Equation 3)}$$

where θi in the formula indicates the operative mean indoor air temperature at hour j(averaged over all simulated house zones), θr denotes the reference indoor operative temperature for overheating and n for the total number of occupied hours in the house.

Generally, terms θ i, j − θ r are applicable to those hours when θ i, j > θ r. The temperature differences are considered to be all positive, otherwise, the value is zero. The reference operative indoor temperature, for the studied climates is an assumed comfort temperature of 24°C (July).

The annual heating and cooling energy use for each selected scenario is compared to estimate the impact of timber construction types in housing morphology on energy consumption. The timber low-rise single housing morphology effectiveness is determined by comparing the heating and cooling loads of the better performing morphologies to those of the worst performing morphologies.

4.4.5 Simulation Software

The Design-Builder software version 6 for EnergyPlus is selected to compute simulations in different climatic regions: Mediterranean, continental and tropical. The

selected software is based on the verified accuracy through BESTest (Building Energy Simulation TEST) process developed by International Energy Agency. Its interface is qualified to generate virtual models with geometrical properties of real-life buildings, supported on energy loads inputs, HVAC, occupancy, glazing and detailed construction. The local weather files for all climates are generated by Meteonorm 7.3 software.

CHAPTER 5

RESULTS

Morphology has a major impact in a building energy performance, hence this research paper it aims to present the influence it has on timber-low rise single housing. The framework of the research is illustrated in *Figure 36.*

The completed and detailed steps in the methodology chapter are followed by the Design-Builder generated results. Results are evaluated, interpreted and then compared using graphical charts. Calculations are obtained for all sixteen-timber low-rise single housing, with each morphology having three transparency properties, two timber construction systems and located in three specific climate conditions. It demonstrates the correlation between the timber low-rise single housing morphology and their respective energy performance.

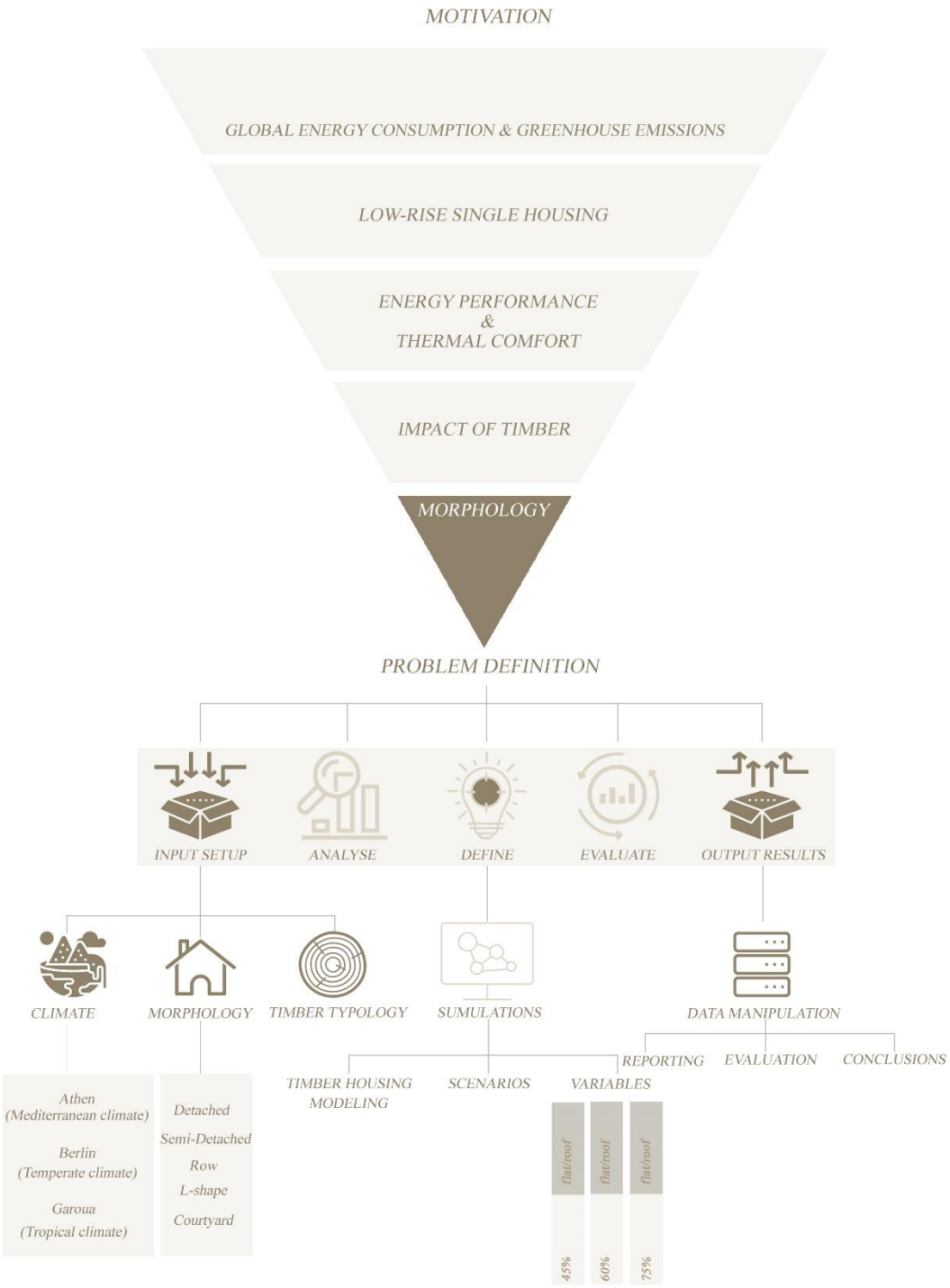

Figure 36. framework of the study

5.1 Climate of Athens

To determine the impact of the hot Mediterranean climate of Athens in the computed morphologies, a comparison between yearly active energy consumption is run and represented in the illustrations below.

5.1.1 Energy performance

The graphical charts below illustrate the relationship of annual energy consumption for heating and cooling loads of all sixteen low-rise single housing morphologies.

5.1.1.1 Energy performance of mass timber construction

The graphical charts below illustrate the relationship of annual energy consumption for heating and cooling loads of all sixteen low-rise single housing morphologies. The graph shown in *Figure 37* represents heating demand in each month for all morphologies, in the case of mass timber construction system and a percentage of WWR 45% for the North-South oriented façades scenario. Taking into account that SDH_03$_f$ is formed by two attached units and have dual occupancy within one unit, it presents a poorer performance in the climate context of Athens. It is followed by SDH_03$_r$ with slight changes, is the same shape of housing, only in this case with a roof shell. Next in terms of a poor performance is CH$_f$ & CH$_r$, due to fully transparent inner courtyard of the one-storey house, concluding that this morphology isn't the most ideal for the Athens climate. Following the former models, DH_02$_f$ and DH_02$_r$, due to the square box layout of the morphology, it displays a deficient performance.

LH$_f$ morphology, an L-shaped and flat roof house shows the best performance, due to the layout and being a one-story house. It's akin morphology LH$_r$, performs even better than LH$_f$, probably because of the insulation in the pitched roof. It is followed by RH_$_r$ and RH_$_f$, then SDH_01$_r$ and SDH_01$_f$. *Figure 38* demonstrates the monthly cooling demand for every morphology in the case of mass timber construction system and a percentage of WWR 45% N-W scenario. On account of the plan length, LH_$_f$,

shows a considerable need of conditioned-air for cooling during summer months, followed by its akin morphology LH_r, hence making them doubtful of their efficiency in the Athens climate. On the other hand, a better performance in terms of cooling demand it is noticed in SDH_01r and SDH_01r, then RH_r and RH_f, due to the fact that this morphology of three units attached to one another, have not a very high percentage of WWR (45%) in the south-oriented façades.

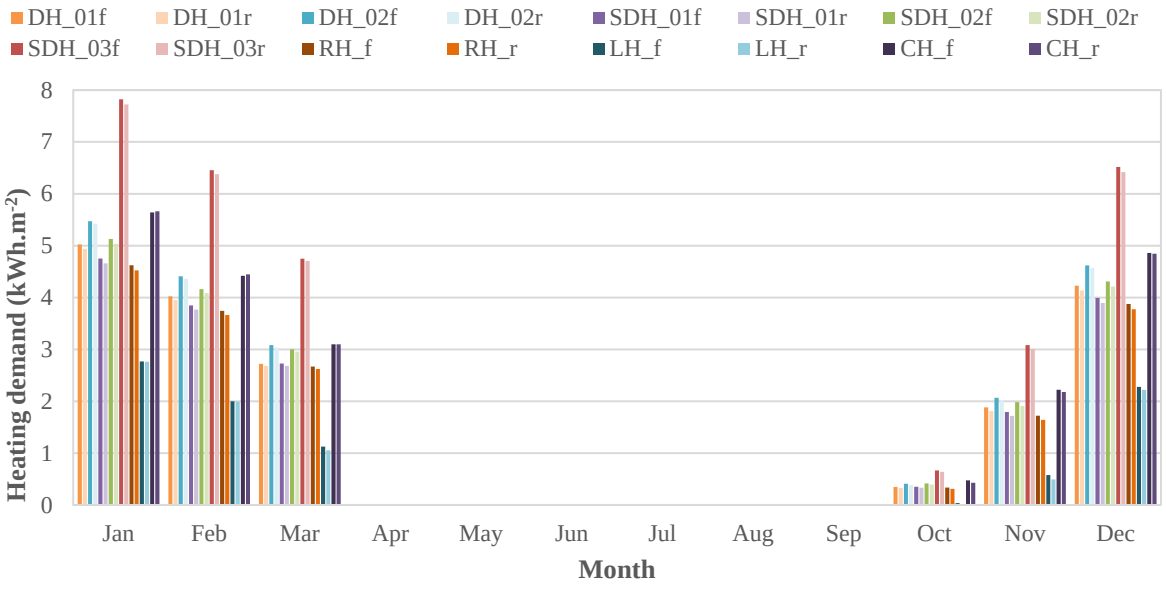

Figure 37. Comparison of simulated heating demand (kWh.m^{-2}) of WWW=45% (N-S), Athens climate, MTC system

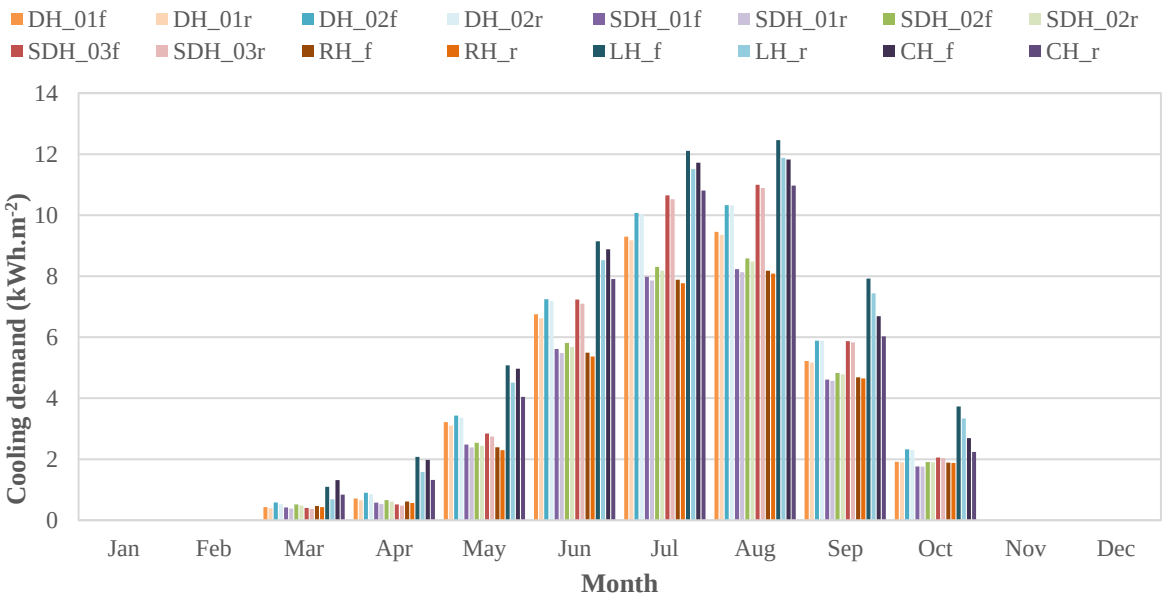

Figure 38.Comparison of simulated cooling demand (kWh.m^{-2}) of WWW=45% (N-S), Athens climate, MTC system

Figure 39 displays the monthly heating demand for all morphologies, in the case of mass timber construction system and a percentage of WWR 60% for the North-South oriented façades scenario. It is depicted an increase of the heating demand for all months in almost each model, highlighting SDH_03$_f$ and its akin SDH_03$_r$ as poorer performatives even in this scenario. RHr and RHf keep performing better. *Figure 40* represents the monthly cooling demand for all morphologies, in the case of mass timber construction system and a percentage of WWR 60% scenario. SDH_01$_r$ and SDH_01f has remained on a better performance stance for cooling demand, same with RH_$_r$ and RH_$_f$. Meanwhile LH_$_f$ and LH_$_r$ experiences slight decrease on cooling demand compared to previous scenario, but still represents a poor performance.

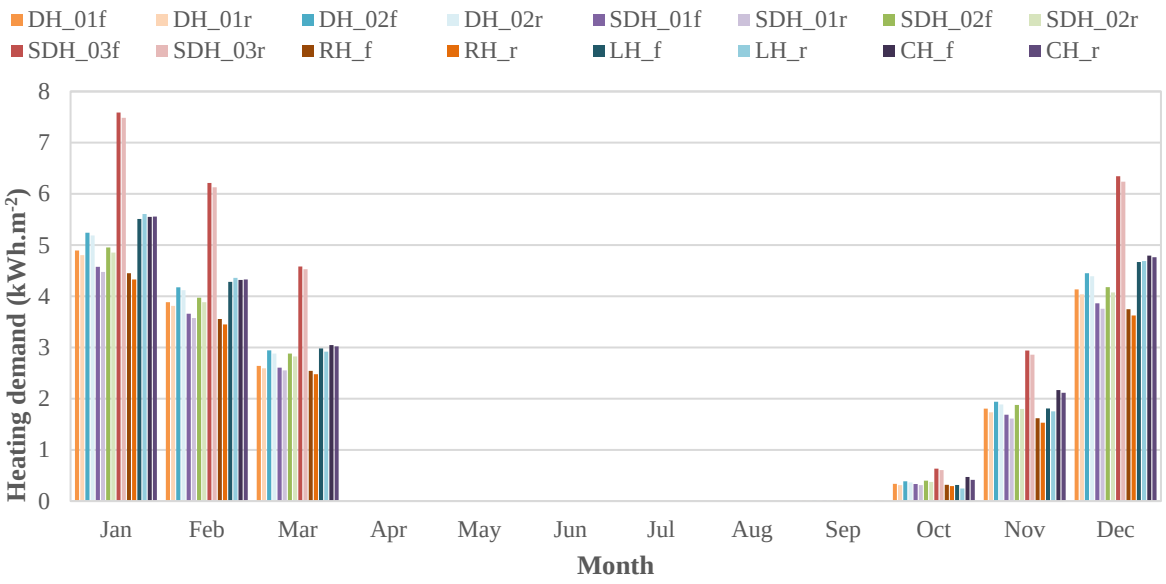

Figure 39. Comparison of simulated heating demand (kWh.m^{-2}) of WWW=60% (N-S), Athen climate, MTC system

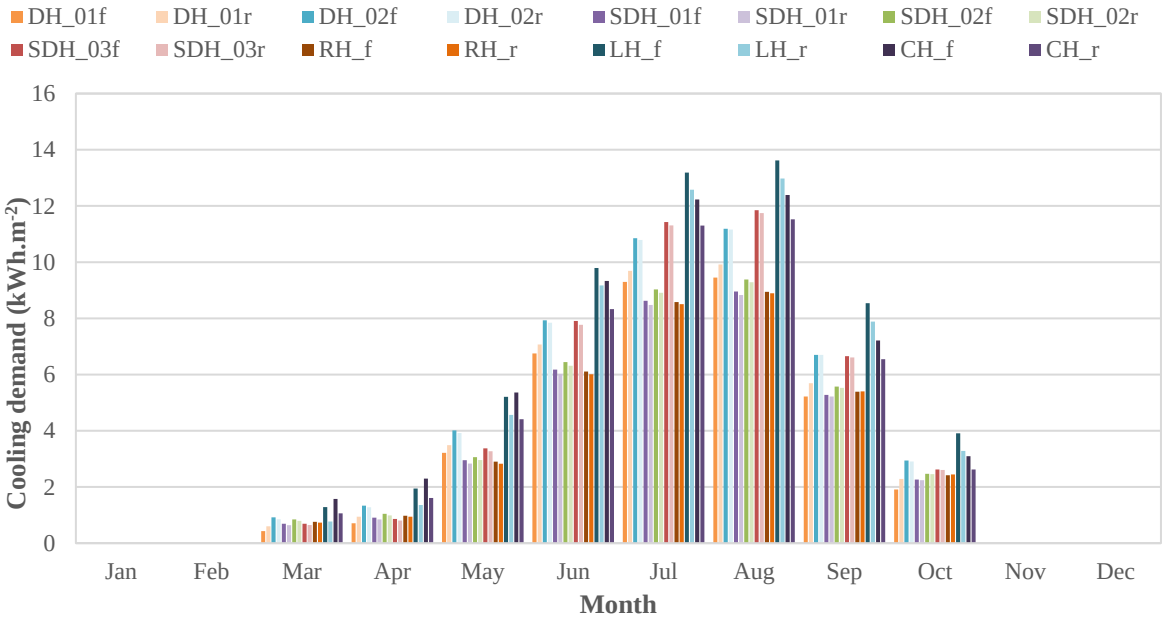

Figure 40. Comparison of simulated cooling demand (kWh.m^{-2}) of WWW=60% (N-S), Athens climate, MTC system

Figure 41 represents the monthly heating demand for all morphologies, in the case of mass timber construction system and a percentage of WWR 75% for the North-South oriented façades scenario. *Figure 42* represents the monthly cooling demand for all morphologies, in the case of mass timber construction and WWR 75% scenario.

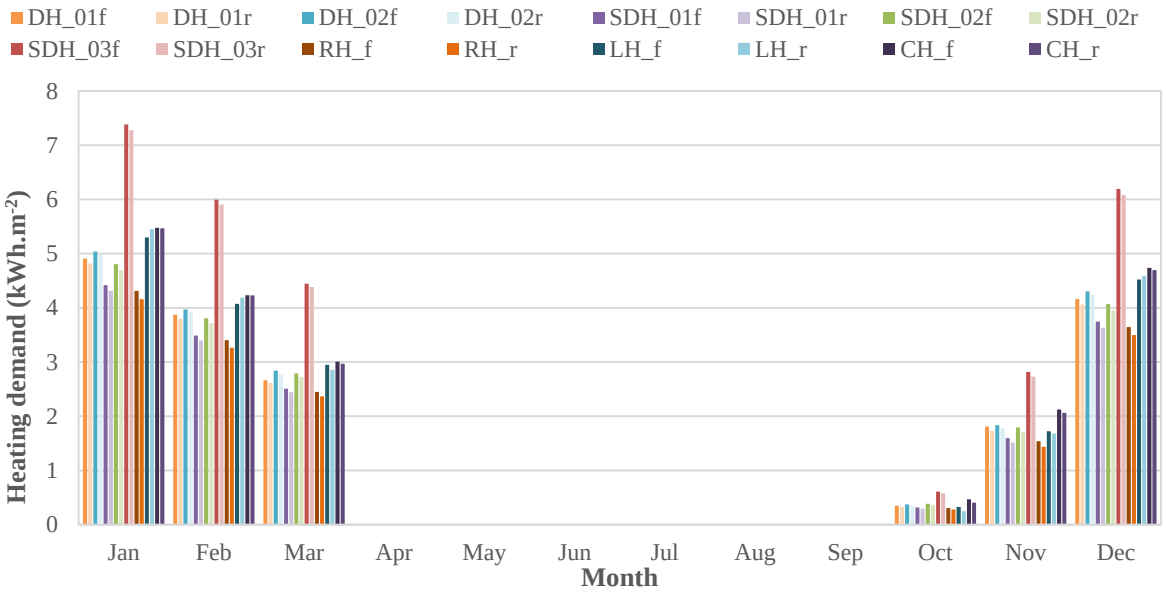

Figure 41.Comparison of simulated heating demand (kWh.m^{-2}) of WWW=75% (N-S), Athens climate, MTC system

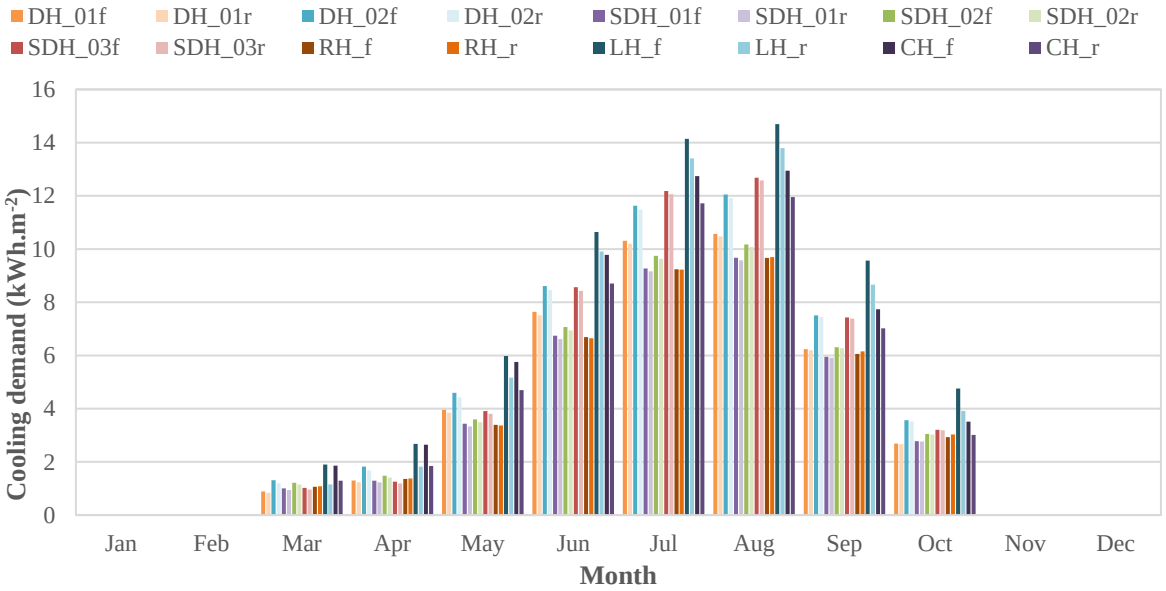

Figure 42. Comparison of simulated cooling demand (kWh.m^{-2}) of WWW=75% (N-S), Athens climate, MTC system

5.1.1.2 Energy performance of light-frame timber construction

The graphical charts below represent the relationship of annual energy consumption for heating and cooling demand of all sixteen low-rise single housing morphologies. The graph shown in *Figure 43* show heating demand in each month for all morphologies, in the case of light-frame timber construction system and a percentage of WWR 45% for the North-South oriented façades scenario. Overall, in the case of light-frame construction system, all morphologies have a poorer performance than mass timber construction system. Considering the fact SDH_03$_f$ is formed by two attached units and have dual occupancy within one unit, it still presents a poorer performance in the climate context of Athens. It's akin SDH_03$_r$ morphology, shows bigger changes, thus performing better. It is noticed that both RH_$_r$ and RH_$_f$, show a better performance in this climate with this construction system compared to the other models. *Figure 44* represents the monthly cooling demand for conditioned air for all morphologies, in the case of light-frame timber construction system and a percentage of WWR 45% scenario. LH_$_r$, shows a considerable need of conditioned-air for cooling during summer months, followed by its akin morphology LH_$_f$, meanwhile RH_$_r$ and RH_$_f$, perform better.

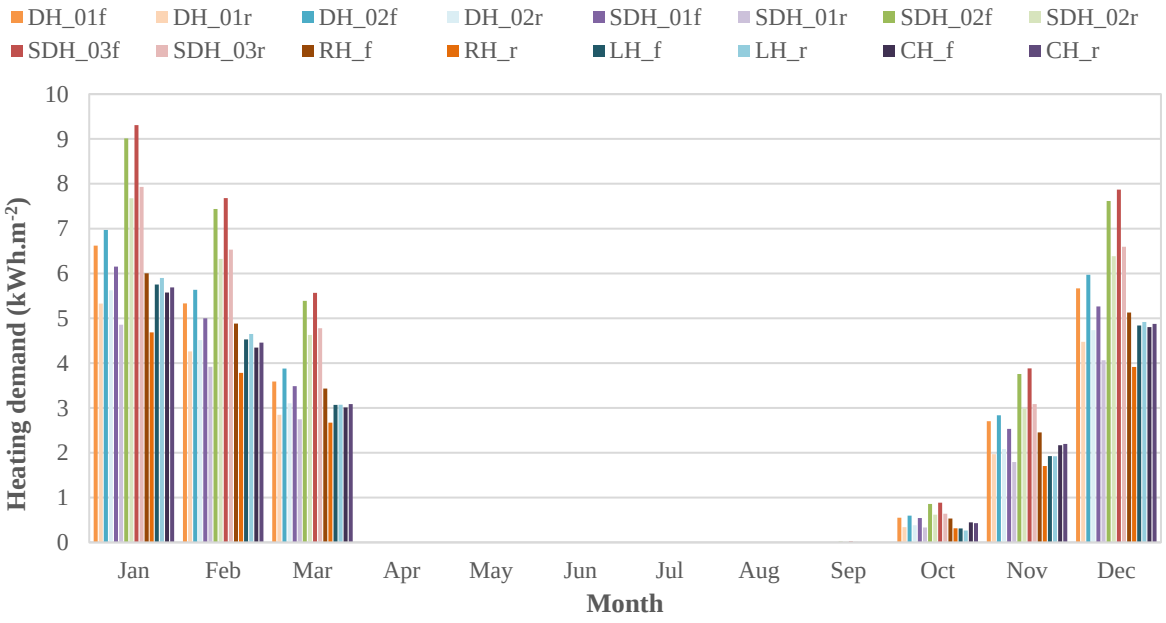

Figure 43. Comparison of simulated heating demand (kWh.m^{-2}) of WWW=45% (N-S), Athens climate, LFT construction system

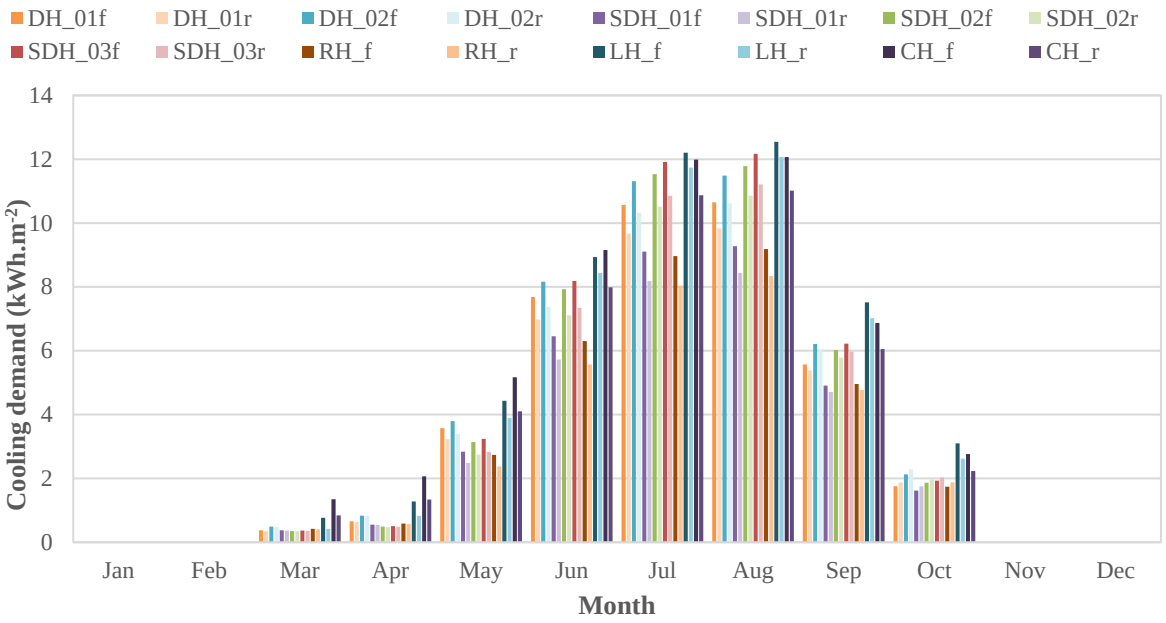

Figure 44. Comparison of simulated cooling demand (kWh.m^{-2}) of WWW=45% (N-S), Athens climate, LFT construction system

Figure 45 displays the monthly heating demand for all morphologies, in the case of light-frame timber construction system and a percentage of WWR 60% for the North-South oriented façades scenario. It is depicted a decrease of the heating demand for all months in almost each model, for this particular construction system and climatic region, compared to the previous scenario. *Figure 46* displays the monthly cooling demand for all morphologies, in the case of light-frame timber construction system and a percentage of WWR 60% scenario. It is noticed a significant increment of the heating demand in each morphology.

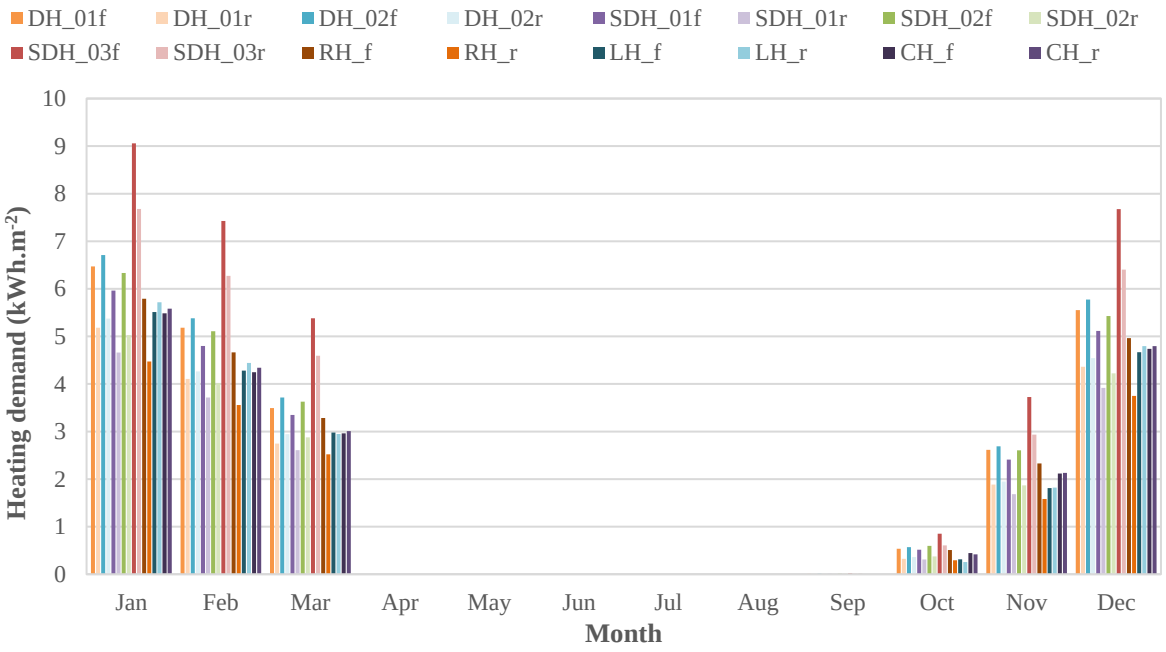

Figure 45. Comparison of simulated heating demand (kWh.m^{-2}) of WWW=60% (N-S), Athens climate, LFT construction system

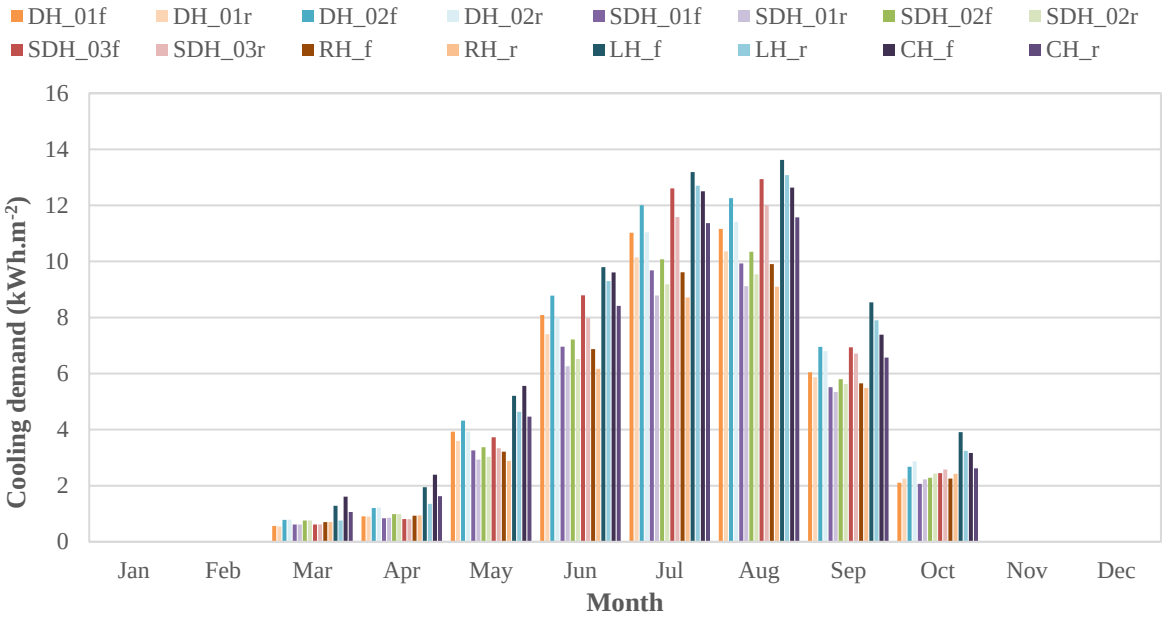

Figure 46. Comparison of simulated cooling demand (kWh.m^{-2}) of WWW=60% (N-S), Athens climate, LFT construction system

Figure 47 represents the monthly heating demand for all morphologies, in the case of light-frame timber construction system and a percentage of WWR 75% for the North-South oriented façades scenario. It is noticed a slight decrease in all morphologies for heating demand compared to the previous scenario. *Figure 48* represents the monthly cooling demand for all morphologies, in the case of light-frame timber construction system and a percentage of WWR 75% scenario. It shows an increment in all typologies for cooling demand for summer months compared to the previous scenario of transparency.

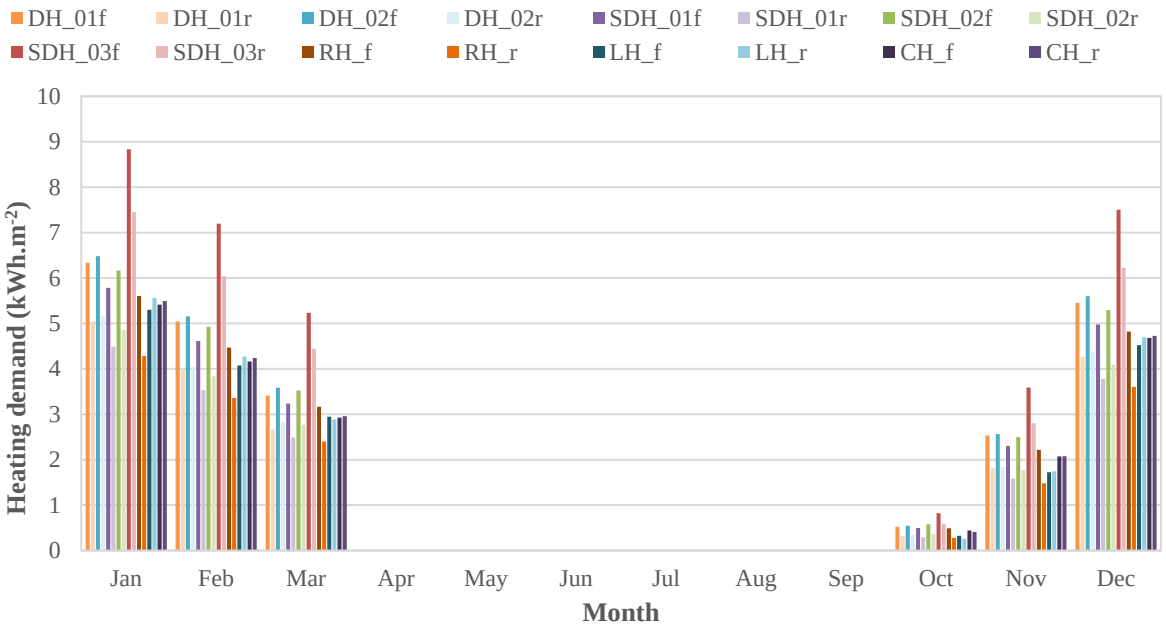

Figure 47. Comparison of simulated heating demand (kWh.m^{-2}) of WWW=75% (N-S), Athens climate, LFT construction system

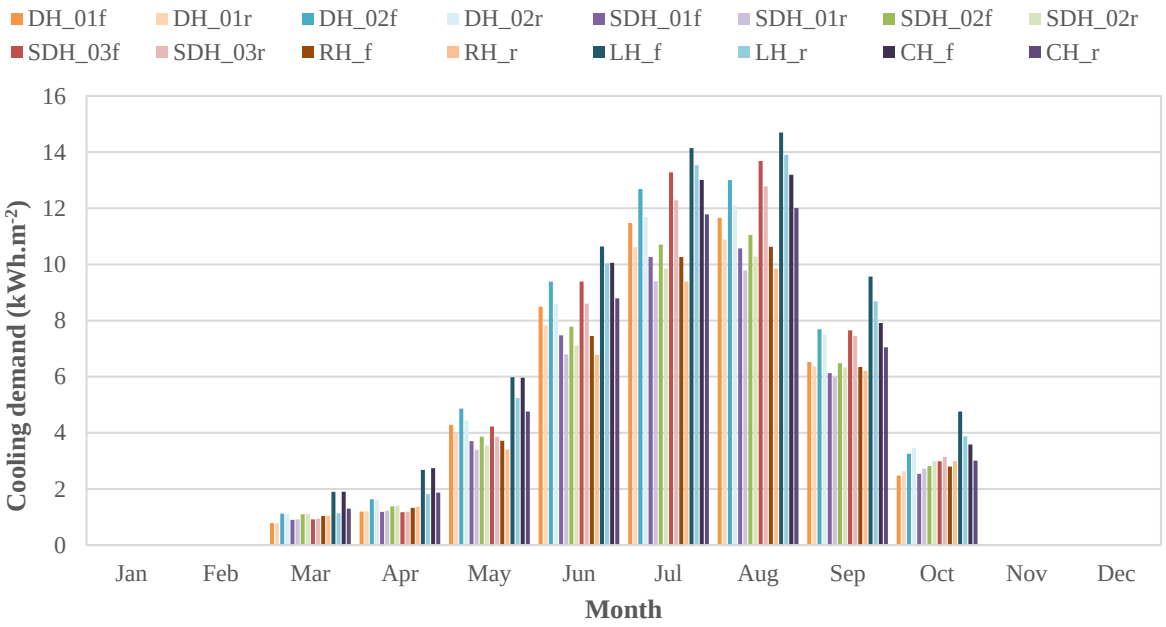

Figure 48. Comparison of simulated cooling demand (kWh.m^{-2}) of WWW=75% (N-S), Athens climate, LFT construction system

5.2 Climate of Berlin

To determine the impact of the moderate continental climate of Berlin in the computed morphologies, a comparison between yearly active energy consumption is run and represented in the illustrations below.

5.2.1 Energy performance

The graphs below illustrate the annual energy consumption for heating and cooling demand of sixteen low-rise single housing morphology.

5.2.1.1 Energy performance of mass timber construction

The graph shown in *Figure 49* displays the heating demand for each month in the case of mass timber construction system and a percentage of WWR 45% for the North-

South oriented façades scenario. SDH_03$_f$ and SDH_03$_r$ continue to display a poor performance, meanwhile LH_$_r$ and LH_$_f$ remains the better in terms of performance in this scenario. *Figure 50* represents the cooling demand for conditioned air in summer for all morphologies, in the case of mass timber construction system. It is noticed that LH_$_f$ and LH_$_r$, continue to have a poor performance even in the temperate climate of Berlin. The CH_$_f$ and CH_$_r$, don't have a great energy performance for cooling demand either, due to the fully transparent inner courtyard. It is noticeable that morphologies like SDH_01$_r$, its akin SDH_01$_f$, then RH_$_r$ and RH_$_f$, have the best energy performance during these moths in terms of cooling.

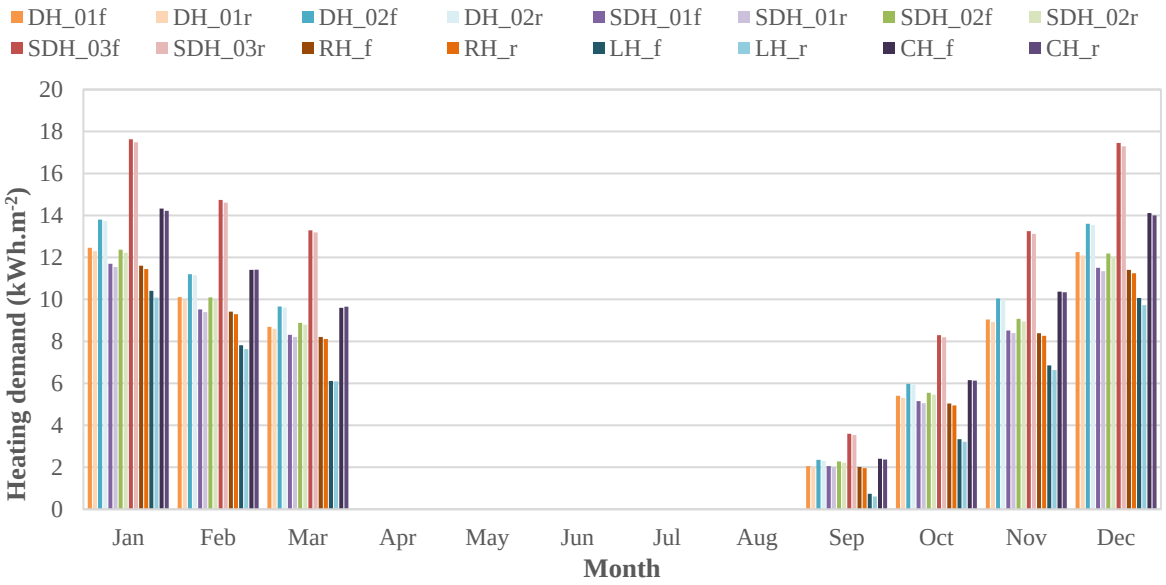

Figure 49. Comparison of simulated heating demand (kWh.m^{-2}) of WWW=45% (N-S), Berlin climate, MTC system

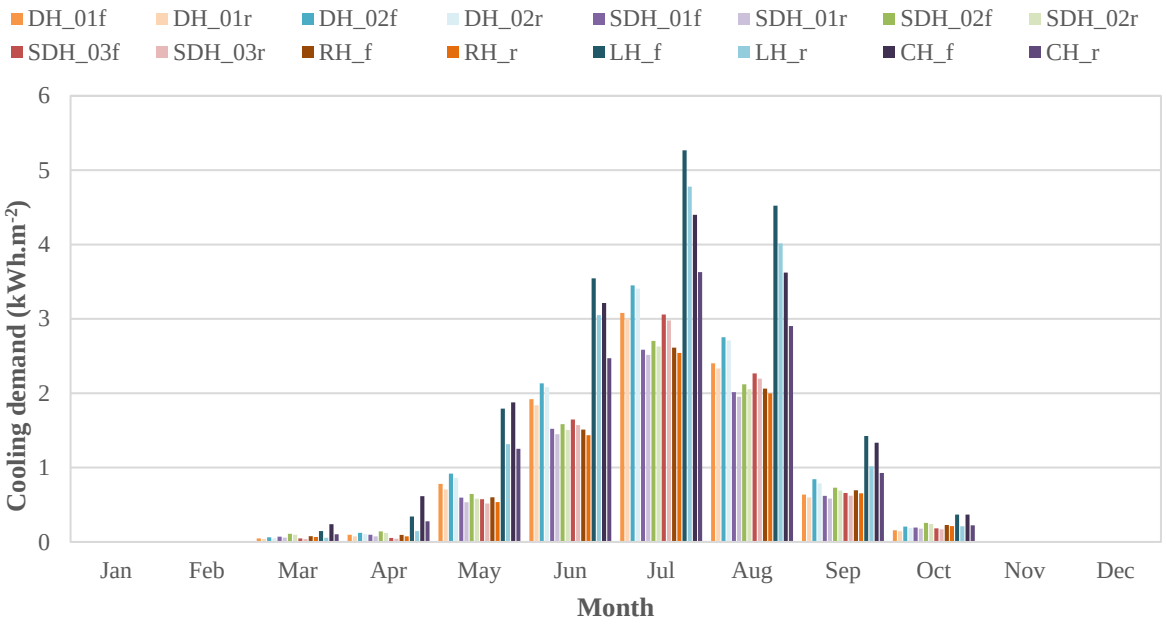

Figure 50. Comparison of simulated cooling demand (kWh.m^{-2}) of WWW=45% (N-S), Berlin climate, MTC system

Figure 51 represents the monthly heating demand for all morphologies, in the case of mass timber construction system and a percentage of WWR 60% for the North-South oriented façades scenario. The heating demand for each month shows a slight increase for each month, making SDH_03$_f$ and SDH_03$_r$ have a poor performance even with this transparency scenario, whereas LH_$_r$ and LH_$_f$ continue to perform better. *Figure 52* shows the monthly cooling demand for all morphologies, in case of mass timber construction system and WWR (60%) scenario. It is noticeable that SDH_01$_r$ and SDH_01$_f$ have a slight increase in cooling load, but it continues to perform better than other morphologies. Meanwhile LH_$_f$ and LH_$_r$, demand lower cooling loads in this scenario compared to the previous one.

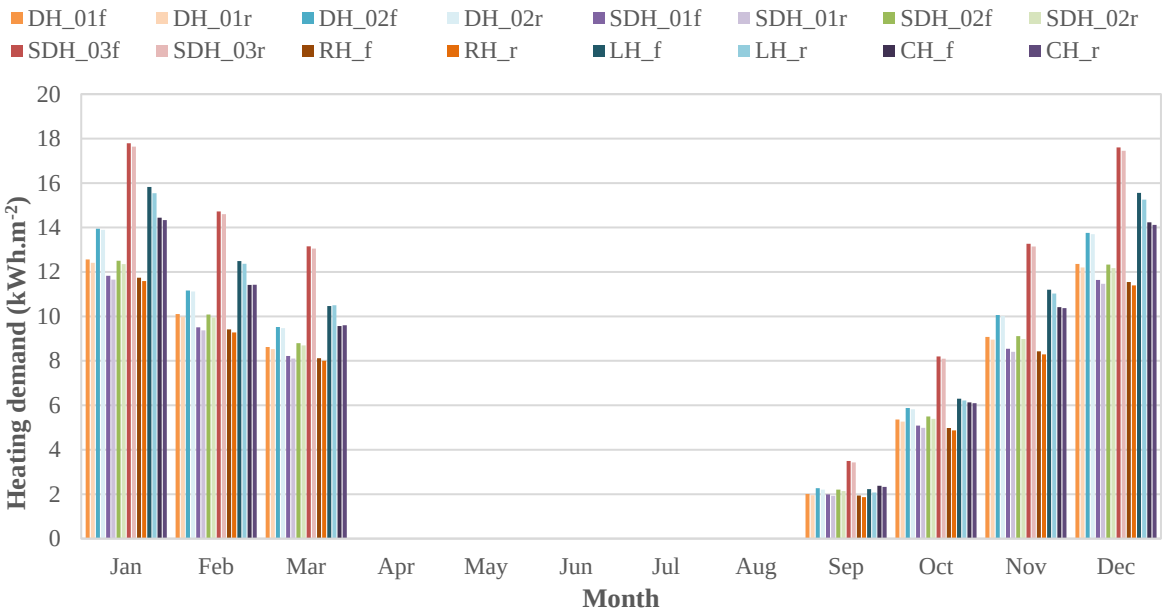

Figure 51. Comparison of simulated heating demand (kWh.m^{-2}) of WWW=60% (N-S), Berlin climate, MTC system

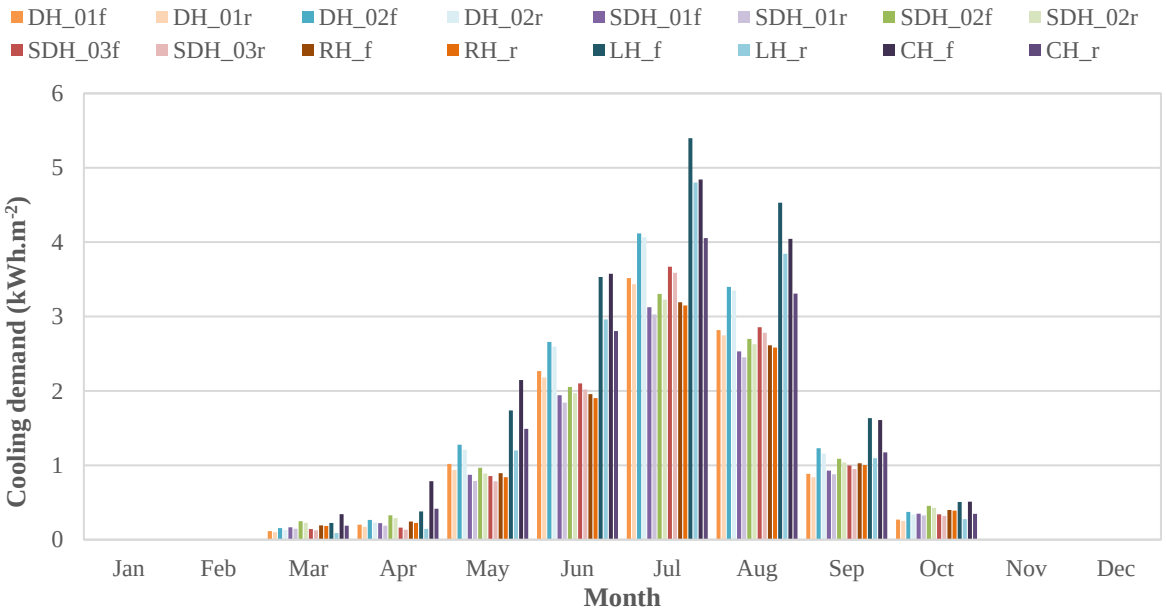

Figure 52. Comparison of simulated cooling demand (kWh.m^{-2}) of WWW=60% (N-S), Berlin climate, MTC system.

Figure 53 represents the monthly heating demand for all morphologies, in the case of mass timber construction system and a percentage of WWR 75% for the North-South

oriented façades scenario. The monthly demand for heating experiences a slight increment for all morphologies, where even in this scenario, SDH_03$_f$ and SDH_03$_r$, have a poor performance, whereas RH_$_r$ and RH_$_f$, followed by SDH_01$_r$ and SDH_01$_f$ with a slight increment for heating demand have the better performance. *Figure 54* displays the monthly cooling demand for all morphologies, in the case of mass timber construction system and WWR (75%). Even the cooling demand in this scenario experiences a slight increment for all morphologies, except LH_$_r$ and LH_$_f$.

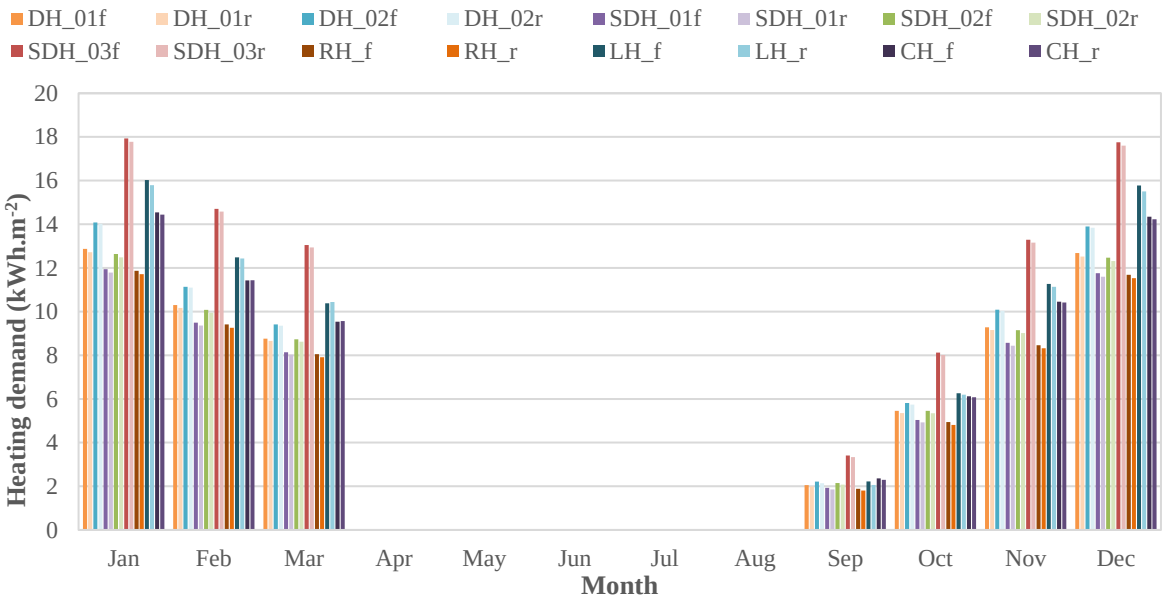

Figure 53. Comparison of simulated heating demand (kWh.m^{-2}) of WWW=75% (N-S), Berlin climate, MTC system

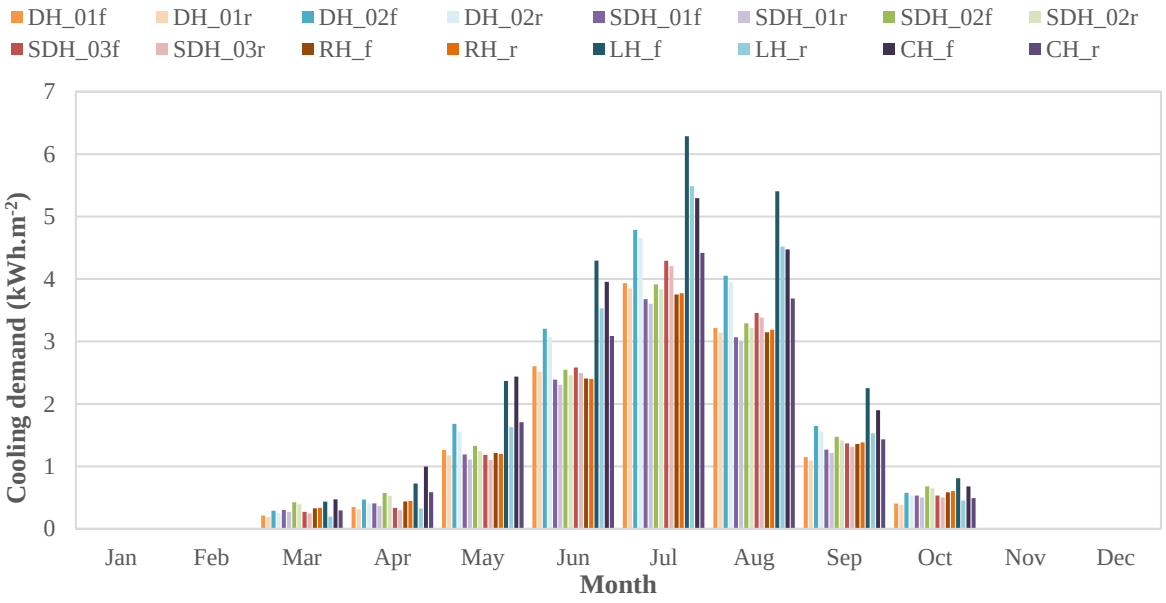

Figure 54. Comparison of simulated cooling demand (kWh.m^{-2}) of WWW=75% (N-S), Berlin climate, MTC system

5.2.1.2 Energy performance of light-frame timber construction

The graphical charts below represent the relationship of annual energy consumption for heating and cooling demand of all sixteen low-rise single housing morphologies. The graph shown in *Figure 55* show heating demand in each month for all morphologies, in the case of light-frame timber construction system and a percentage of WWR 45% for the North-South oriented façades scenario. Overall, in the case of light-frame construction system, all morphologies have a poorer performance than mass timber construction system. SDH_03$_f$ and SDH_03$_r$ experiences a high demand for heating loads. Next is DH_02$_f$ and DH_02$_r$, have a poor performance too, followed by LH_$_f$ and LH_$_r$. On the other side SDH_02$_r$ and SDH_02$_f$ show a better performance in this scenario. *Figure 56* represent the monthly cooling demand for all morphologies, in the case of light-frame timber construction system and WWR 45% scenario. Even in the case of cooling loads, with a light-frame construction system, all morphologies have an overall poorer experience. It is noticed that CH_$_f$, LH_$_f$ and their akin CH_$_r$, LH_$_r$, have a poorer performance in terms of cooling loads. Meanwhile RH_$_r$ and Rh_$_f$, display a better performance.

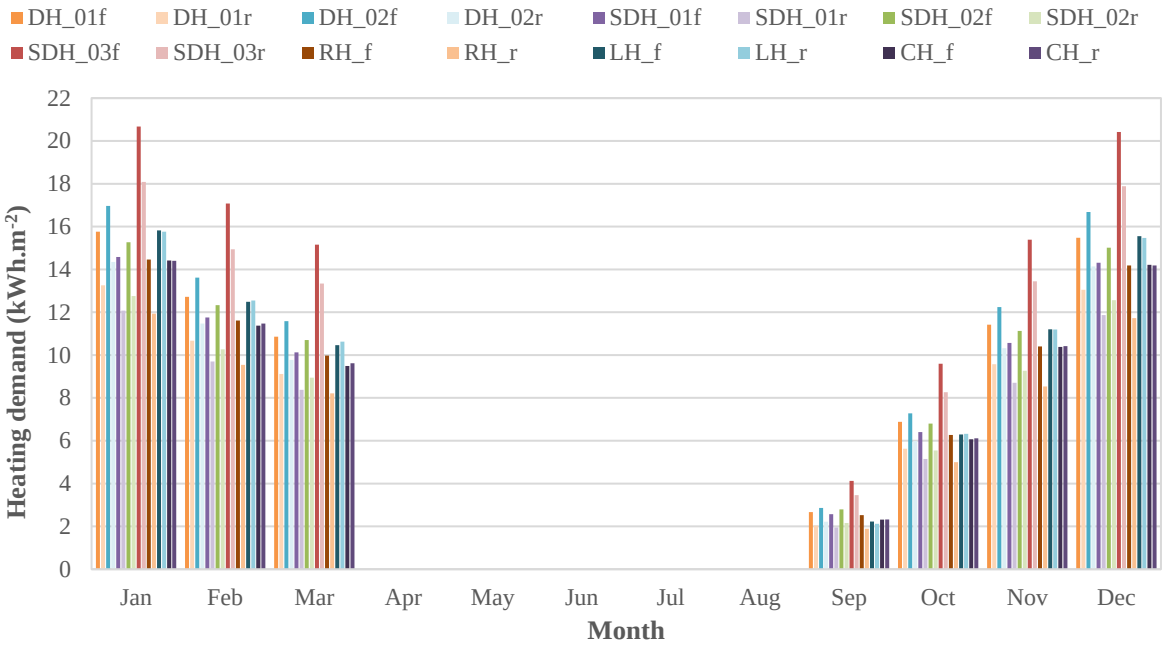

Figure 55. Comparison of simulated heating demand (kWh.m^{-2}) of WWW=45% (N-S), Berlin climate, LFT construction system

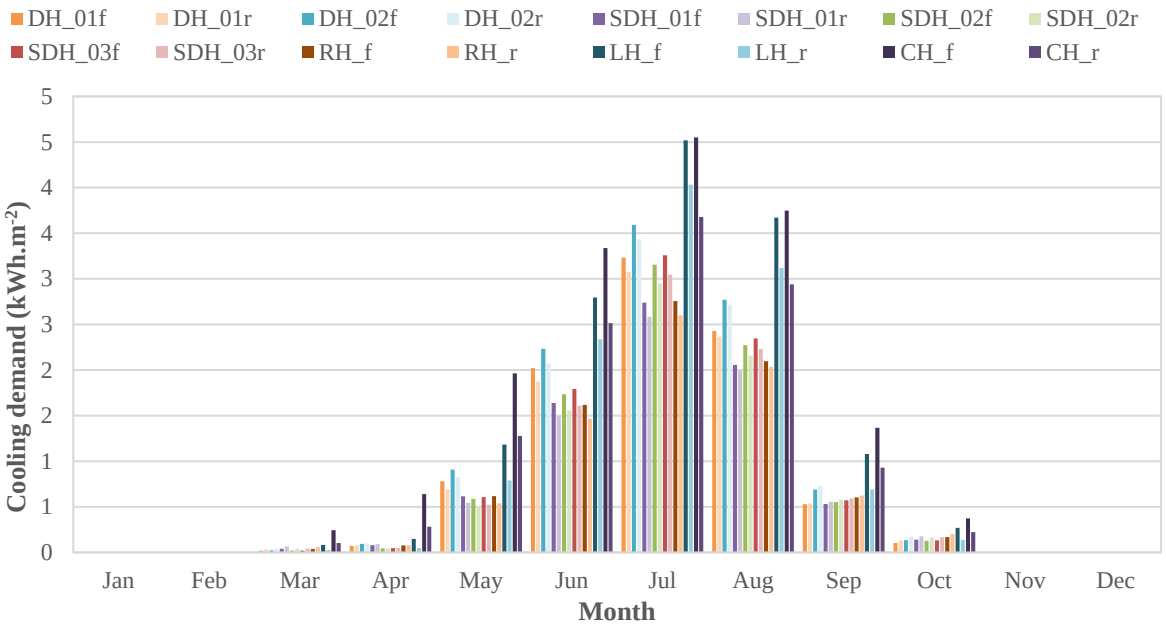

Figure 56. Comparison of simulated cooling demand (kWh.m^{-2}) of WWW=45% (N-S), Berlin climate, LFT construction system

Figure 57 represents the monthly heating demand for all morphologies, in the case of light-frame timber construction system and a percentage of WWR 60% for the North-South oriented façades scenario. The heating demand in each month shows a slight decrease for almost all morphologies, except LH_$_f$ and LH_$_r$, CH_$_f$ and CH_$_r$. *Figure 58* the monthly heating demand for all morphologies, in the case of light-frame timber construction system and WWR 60% scenario. The cooling demand in each month shows a sight increment for all morphologies except LH_$_f$ and LH_$_r$, CH_$_f$ and CH_$_r$, putting in question their efficiency for Berlin climate.

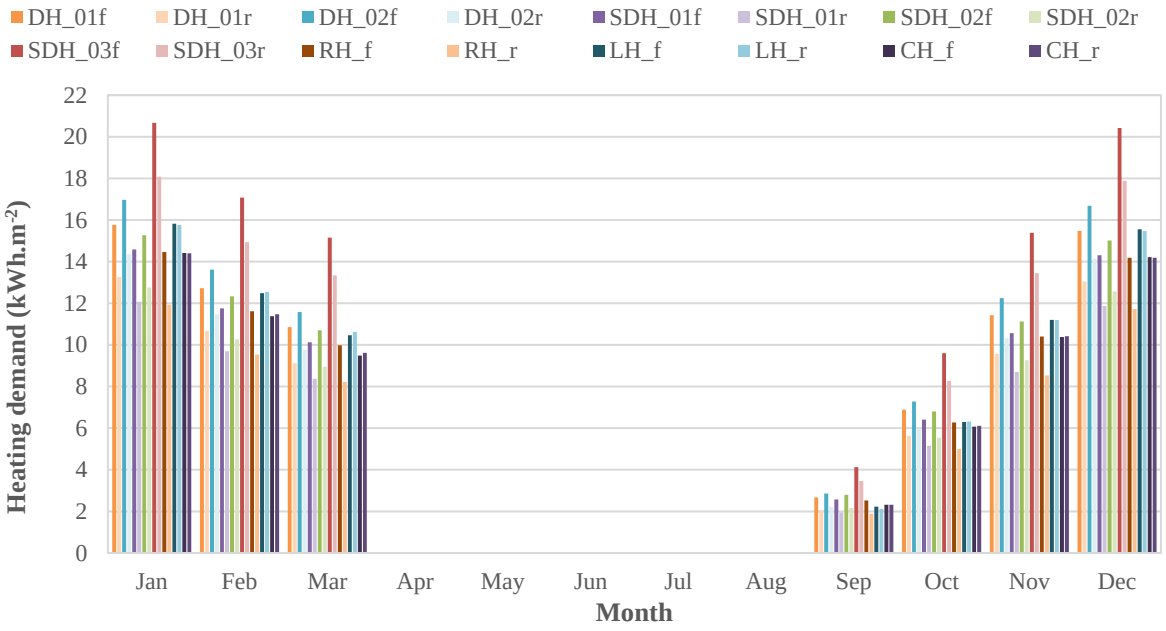

Figure 57. Comparison of simulated heating demand (kWh.m^{-2}) of WWW=60% (N-S), Berlin climate, LFT construction system

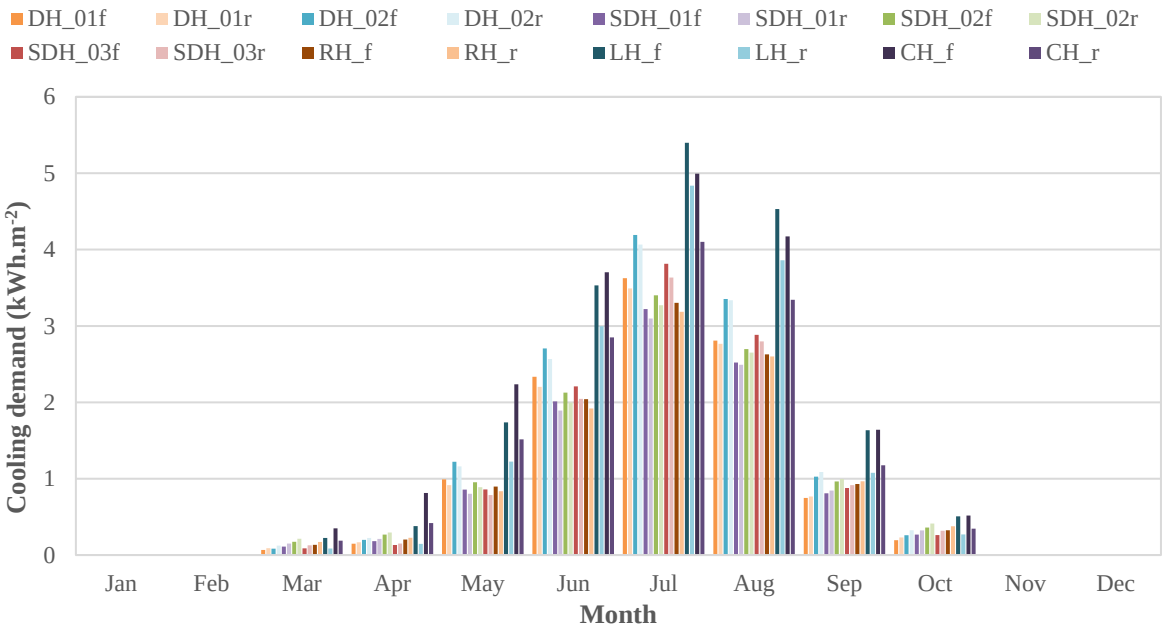

Figure 58. Comparison of simulated cooling demand (kWh.m^{-2}) of WWW=60% (N-S), Berlin climate, LFT construction system

Figure 59 represents the monthly heating demand for all morphologies, in the case of light-frame timber construction system and a percentage of WWR 75% scenario. The heating demand in each month shows a slight decrease for almost all morphologies, except LH_$_f$ and LH_$_r$, CH_$_f$ and CH_$_r$. *Figure 60* the monthly heating demand for all morphologies, in the case of light-frame timber construction system and WWR 75% scenario. The cooling demand in each month shows a sight increment for all morphologies except LH_$_f$ and LH_$_r$, CH_$_f$ and CH_$_r$, putting in question their efficiency for Berlin climate, even this scenario of transparency.

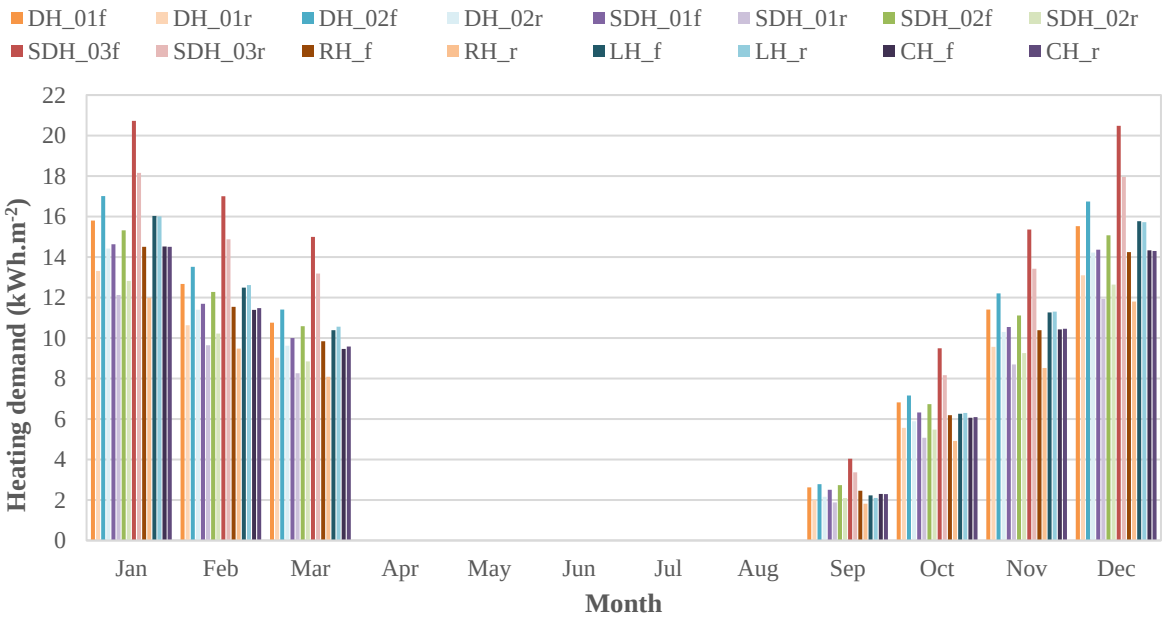

Figure 59. Comparison of simulated heating demand (kWh.m^{-2}) of WWW=75% (N-S), Berlin climate, LFT construction system

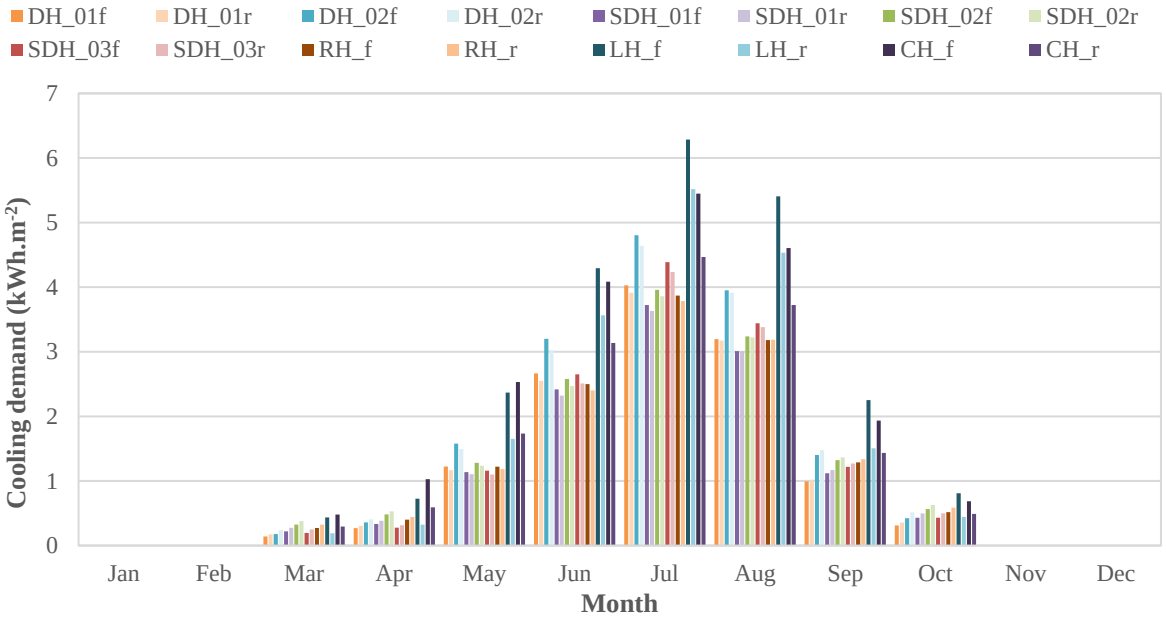

Figure 60. Comparison of simulated cooling demand (kWh.m^{-2}) of WWW=75% (N-S), Berlin climate, LFT construction system

5.3 Climate of Garoua

To determine the impact of the tropical savanna climate of Garoua in the computed morphologies, a comparison between yearly active energy consumption is run and represented in the illustrations below.

4.1.1 Energy performance

The graphical charts below illustrate the relationship of annual energy consumption for heating and cooling loads of all sixteen low-rise single housing morphologies.

4.1.1.1 Energy performance of mass timber construction

The graph illustrated in *Figure 61* shows heating demand in each month for all morphologies, in the case of mass timber construction system and a percentage of WWR 45% for the North-South oriented façades scenario. It is noticeable that all morphologies in the climate of Garoua, require a low heating demand compared to the previous climates of the same scenario. Although SDH_03$_f$ and SDH_03$_r$ continue to have a poorer performance compared to other models, whereas LH_$_r$, LH_$_f$ and DH_01$_r$, DH_01$_f$ display the best performance among all. *Figure 62* shows the monthly cooling demand in each month for all morphologies, in the case of mass timber construction system and a percentage of WWR 45% scenario. It is noticed that overall, morphologies require a great energy for monthly cooling loads in the climate of Garoua. LH_$_f$, LH_$_r$ and SDH_03$_f$, SDH_03$_r$ display the poorest performance, whereas RH_$_r$ and RH_$_f$, have the best performance.

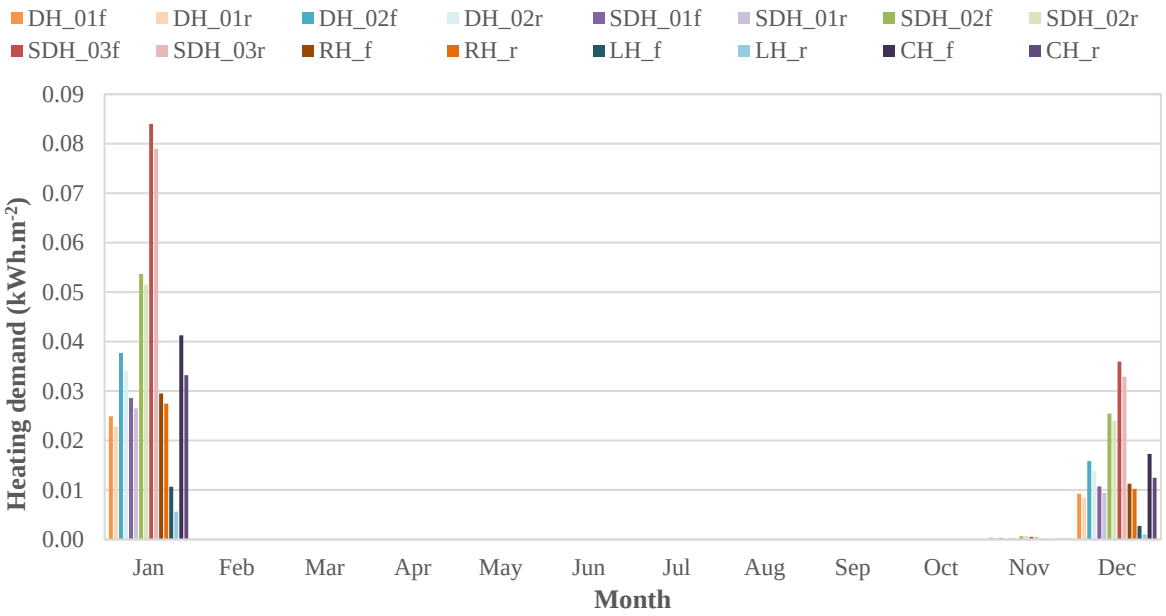

Figure 61. Comparison of simulated heating demand (kWh.m^{-2}) of WWW=45% (N-S), Garoua climate, MTC system

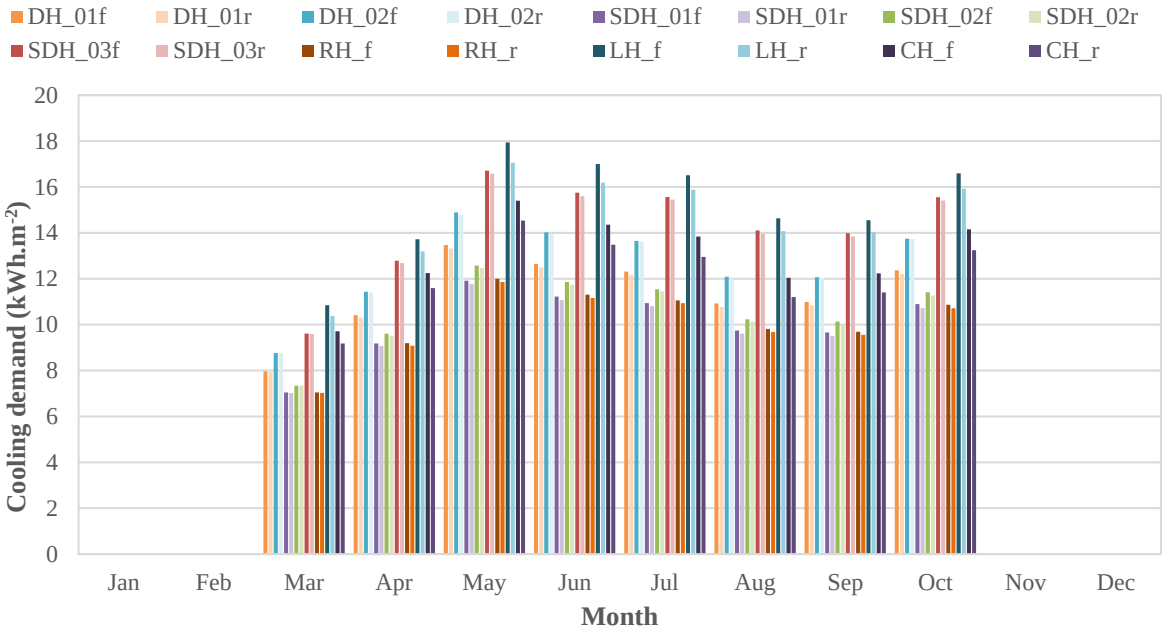

Figure 62. Comparison of simulated cooling demand (kWh.m^{-2}) of WWW=45% (N-S), Garoua climate, MTC system

Figure 63 represents the heating demand in each month for all morphologies, in the case of mass timber construction system and a percentage of WWR 45% for

the North-South oriented façades scenario. In general, it is noticed an increment in the heating demand in each month for all morphologies, except CH_f. *Figure 64* represents the cooling demand in each month for all morphologies, in the case of mass timber construction system and a percentage of WWR 45% scenario. It is seen a slight increment of cooling demand in each month, due a higher transparency scenario compared to the previous one, except LH_f.

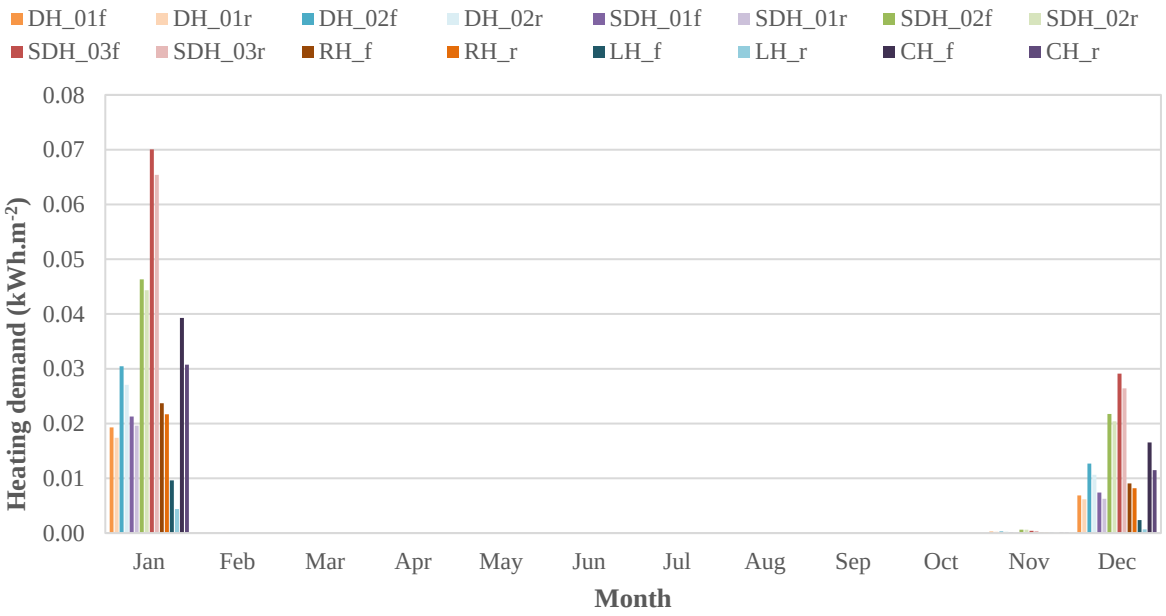

Figure 63. Comparison of simulated heating demand (kWh.m^{-2}) of WWW=60% (N-S), Garoua climate, MTC system

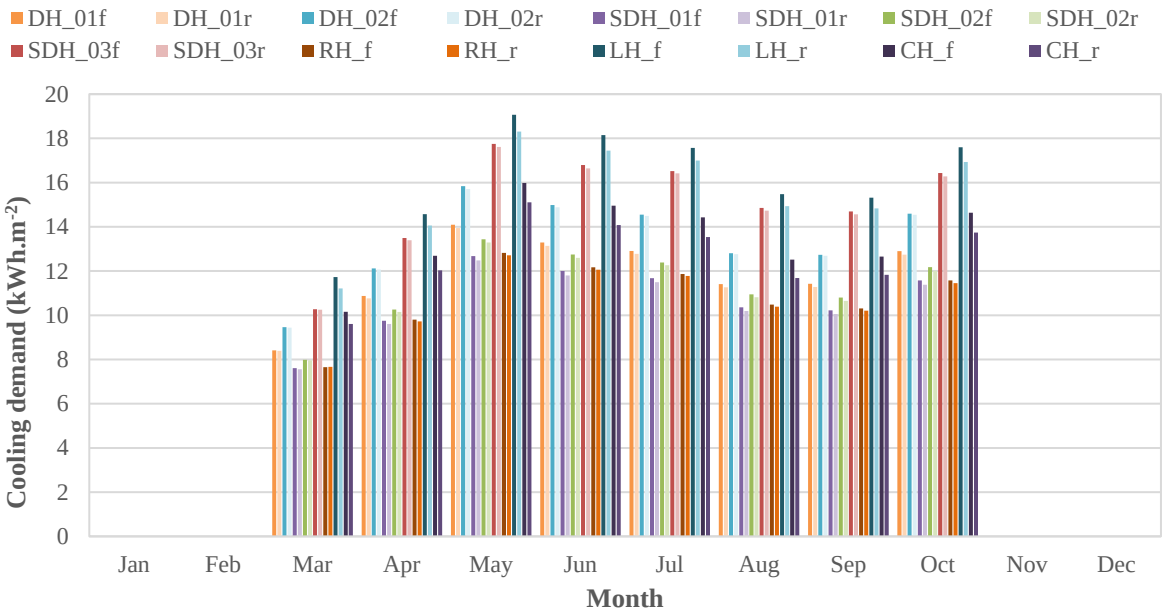

Figure 64. Comparison of simulated cooling demand (kWh.m^{-2}) of WWW=60% (N-S), Garoua climate, MTC system

Figure 65 represents the monthly heating demand for all morphologies, in the case of mass timber construction system and a percentage of WWR 75% scenario. It is seen that the heating demand in each month has increased very slightly for all morphologies, except for LH_r. *Figure 66* represents the monthly cooling demand for all morphologies, in the case of mass timber construction system and a percentage of WWR 75% scenario. It shows an increment of cooling load for all morphologies, except CH_f.

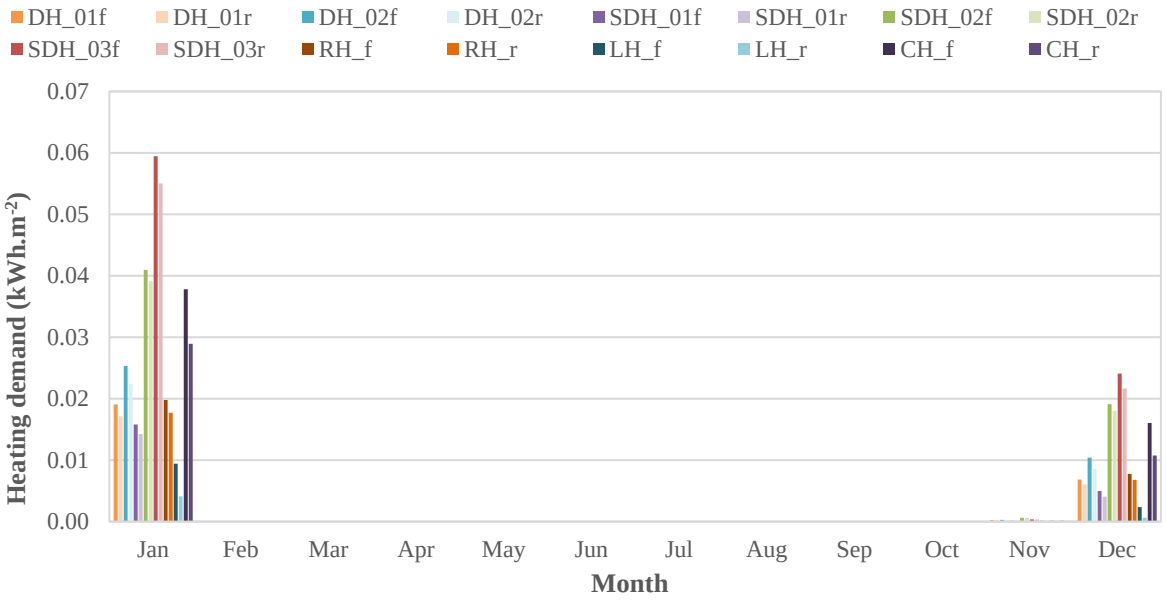

Figure 65. Comparison of simulated heating demand (kWh.m^{-2}) of WWW=75% (N-S), Garoua climate, MTC system

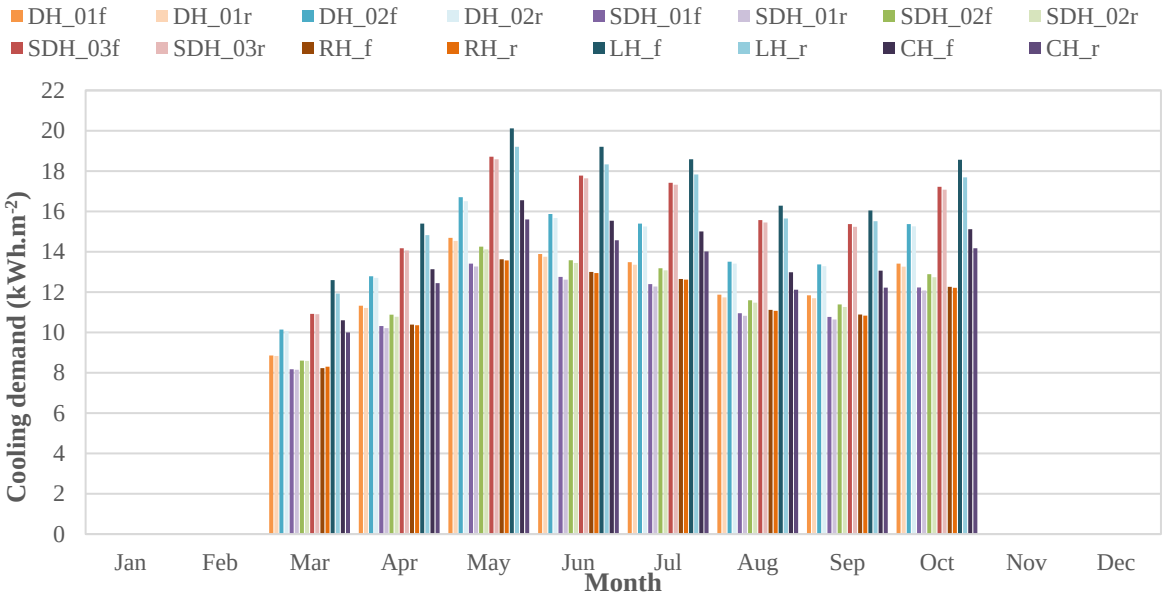

Figure 66. Comparison of simulated cooling demand (kWh.m^{-2}) of WWW=75% (N-S), Garoua climate, MTC system

4.1.1.2 Energy performance of light-frame timber construction

The graph shown in *Figure 67* show heating demand in each month for all morphologies, in the case of light-frame timber construction system and a percentage of WWR 45% for the North-South oriented façades scenario. Overall, in the case of light-frame construction system, all morphologies have a poorer performance than mass timber construction system. It is noticeable a low heating demand in all month for every morphology. *Figure 68* represents the monthly cooling demand for all morphologies, in the case of light-frame timber construction system and WWR 45% scenario. It displays a great need of every morphology for cooling demand.

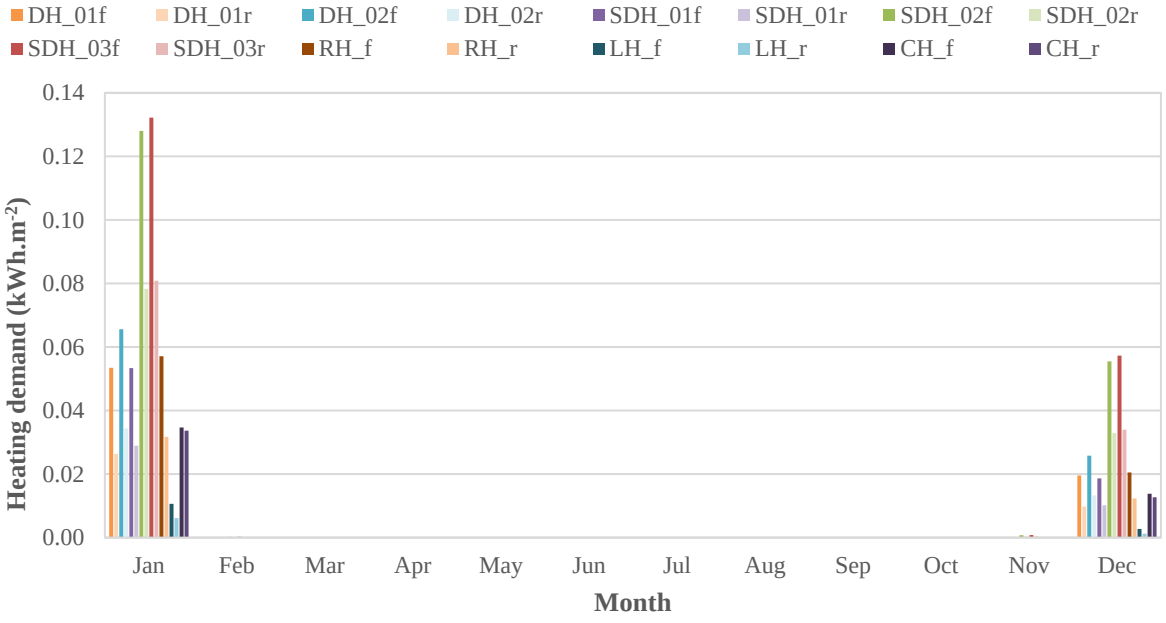

Figure 67. Comparison of simulated heating demand (kWh.m^{-2}) of WWW=45% (N-S), Garoua climate, LFT construction system

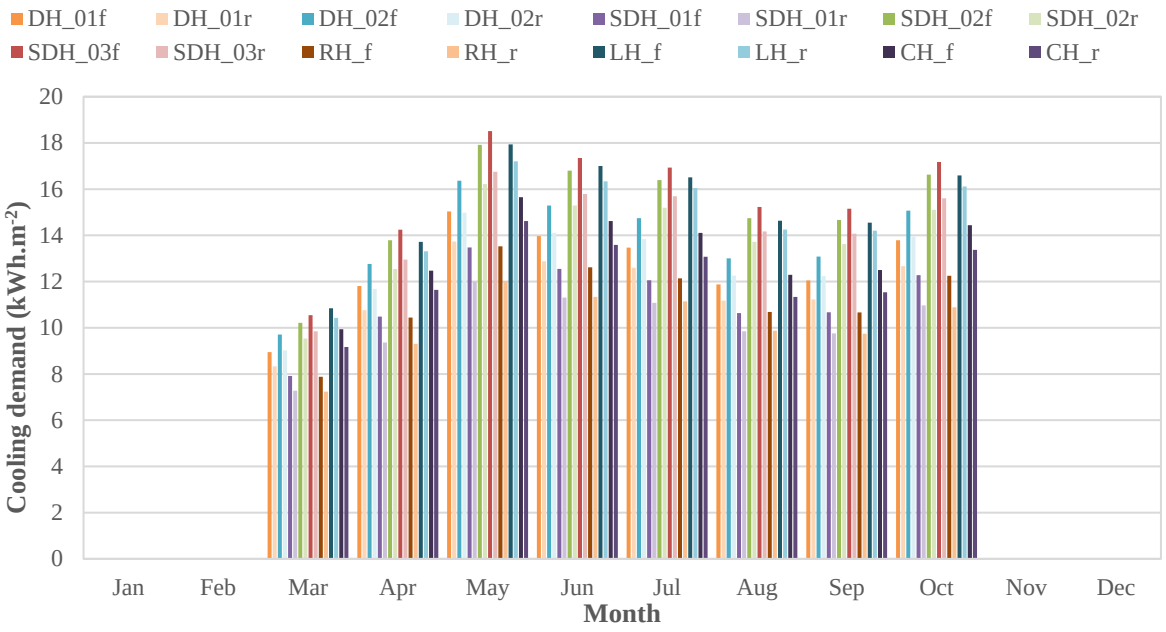

Figure 68. Comparison of simulated cooling demand (kWh.m^{-2}) of WWW=45% (N-S), Garoua climate, LFT construction system

In *Figure 69* it is shown the monthly heating demand for all morphologies, in the case of light-frame timber construction system and a percentage of WWR 60% scenario. It is noticed a slight decrease in the heating demand for each morphology, except CH_r. In *Figure 70* it's shown the monthly cooling demand for all morphologies, in the case of light-frame timber construction system and a percentage of WWR 60% scenario. The cooling loads experience an increment for each morphology.

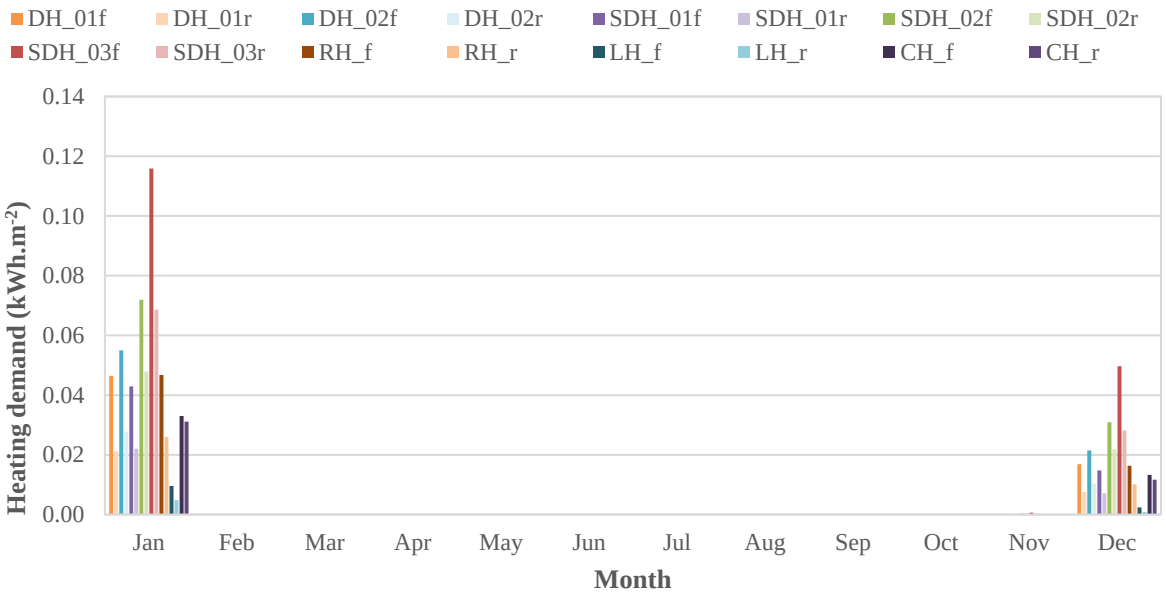

Figure 69. Comparison of simulated heating demand (kWh.m^{-2}) of WWW=60% (N-S), Garoua climate, LFT construction system

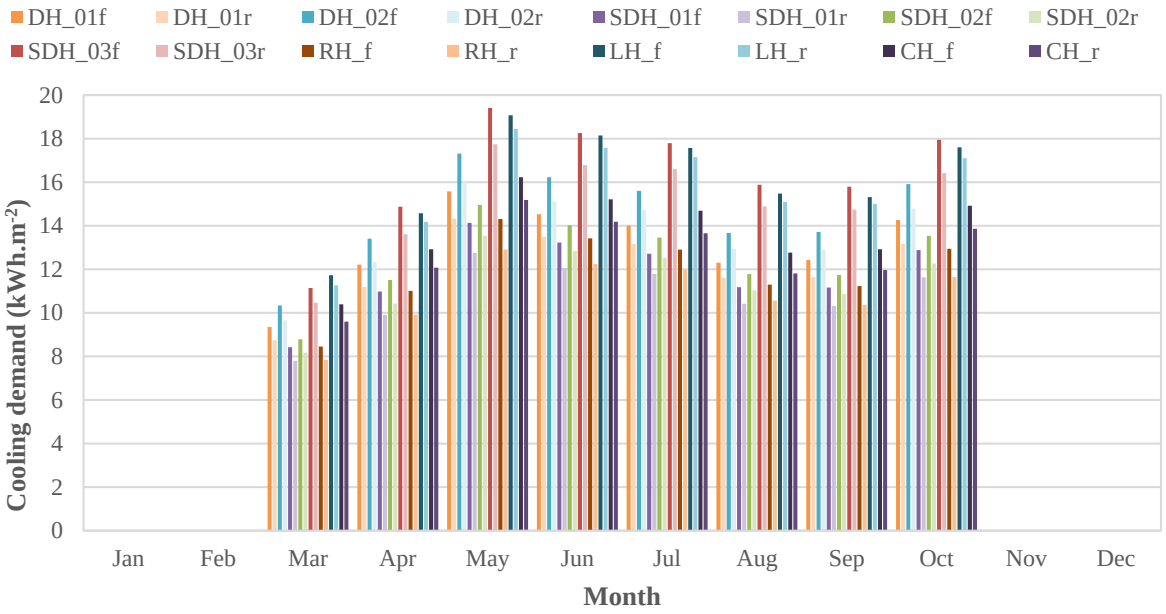

Figure 70. Comparison of simulated cooling demand (kWh.m^{-2}) of WWW=60% (N-S), Garoua climate, LFT construction system

In *Figure 71* it is represented the monthly heating demand for all morphologies, in the case of light-frame timber construction system and a percentage of WWR 75% scenario. It is noticed a slight decrease in the heating demand for each morphology. *Figure 72* represent the monthly cooling demand for all morphologies, in the case of light-frame timber construction system and a percentage of WWR 75% scenario, where the cooling loads experience an increment for all morphologies.

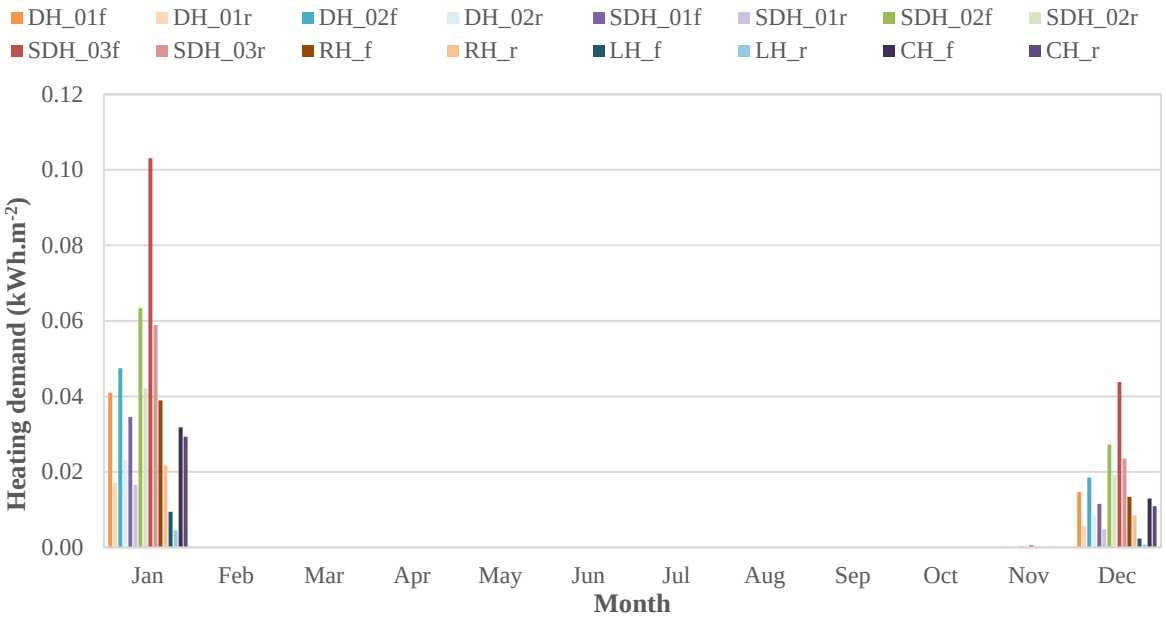

Figure 71. Comparison of simulated heating demand (kWh.m^{-2}) of WWW=75% (N-S), Garoua climate, LFT construction system

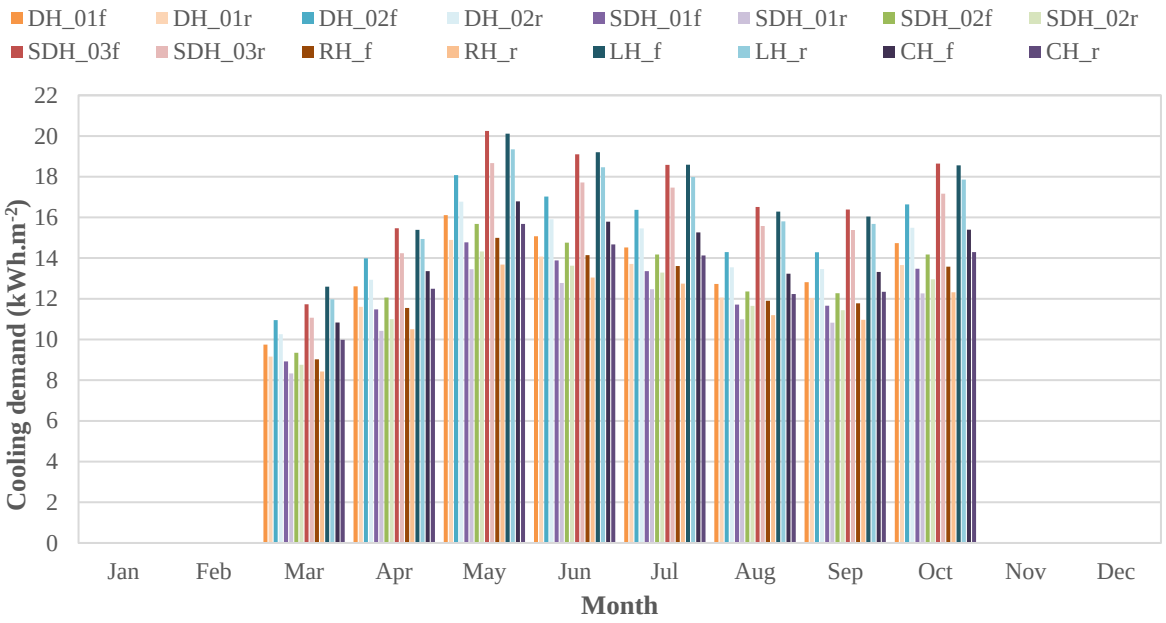

Figure 72. Comparison of simulated cooling demand ($kWh.m^{-2}$) of WWW=75% (N-S), Garoua climate, LFT construction system

CHAPTER 6

DISCUSSION

6.1 Climate of Athens

To determine the morphology effectiveness of each low-rise single housing, in the Mediterranean climate of Athens a comparison of annual active energy consumption for every scenario of WWR and the indoor passive thermal comfort for the worst performing morphology is conducted.

6.1.1 Energy performance of mass timber construction

As illustrated in *Figure 73*, the comparison of annual energy consumption in terms of transparency in the case of mass timber construction, shows an incrementing trend when the house gains more transparency from 45%, 60% to 75%, which correspond to the North and South oriented rooms. The most notable impact of transparency is visible in morphologies LH_$_f$, LH_$_r$, due to the L-shape layout and SDH_03$_f$, SDH_03$_r$, due to the dual occupancy within one unit. In LH_$_f$ morphology, energy consumption is subject to an increase of 14.66 kWh.m^{-2} a^{-1}, when transparency is 60% and 20.86 kWh.m^{-2} a^{-1}, when WWR is 75%. As for LH_$_r$ morphology, energy consumption is subject to an increase of 14.15 kWh.m^{-2} a^{-1}, when transparency is 60% and 18.86 kWh.m^{-2} a^{-1}, when WWR is 75%, due to the roof insulating attributes. In SDH_03$_f$ model, energy demand is subject to in increment of 3.81 kWh.m^{-2} a^{-1}, when WWR is 60% and 7.89, when WWR is 75%. As for its akin, SDH_03$_r$ model han an energy increment of 3.75 kWh.m^{-2} a^{-1}, when WWR is 60% and 7.70 kWh.m^{-2} a^{-1}, when WWR is 75%.

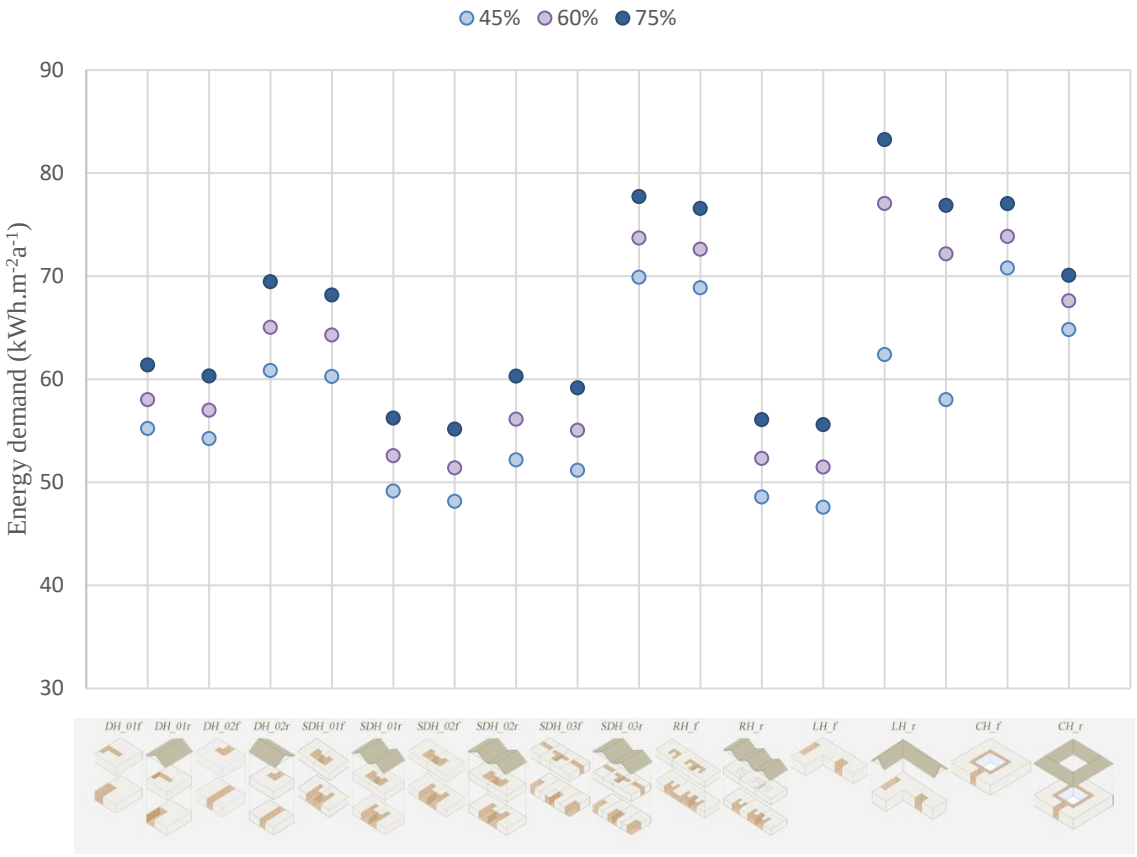

Figure 73. Comparison of simulated annual energy demand (kWh.m^{-2} a^{-1}), Athens climate context, MTC system

Table 11 summarizes the obtained simulation results from Design Builder for all transparency scenarios in the climate of Athens. A maximum of 13.84% of total energy consumption can be reduced, if the proper morphology is selected for the studied climatic region. The typology with the worst performance in terms of heating and cooling loads is SDH_03$_f$ and SDH_03$_r$, meanwhile LH_$_f$ and LH_$_r$, have the worst performance in terms of cooling loads. The L-shape houses, LH_$_f$ and LH_$_r$ save 10.78 kWh.m^{-2} a^{-1} and 11.03 kWh.m^{-2} a^{-1} respectively in heating loads with a morphology effectiveness of 51.83% and 55.14% compared to the relatively compact and organic shapes. Their high demand for conditioned air in summer months increases the cooling demand and reduces the morphology effectiveness by 44.97% and 33.74% respectively. Among the low-rise single housing it is noted that the best performing model is RH_$_r$ with 13.84% effectiveness, followed by another model, SDH_01$_r$ with 12.78% effectiveness. Meanwhile the model with the poorest performance is CH_$_f$ with -28.2% effectiveness.

Table 11. Simulation results obtained for all scenarios in the climate of Athens, MTC system

	Annual heating demand		**Annual cooling demand**		**Annual energy demand**	
Scenarios	Heating/ conditioned area [kWh.m^{-2} a^{-1}]	**Morphology effectiveness [%]**	Cooling/ Conditioned area [kWh.m^{-2} a^{-1}]	**Morphology effectiveness [%]**	Total energy/ conditioned area [kWh.m^{-2} a^{-1}]	**Total morphology effectiveness [%]**
DH_01$_f$ (45%)	18.23	_	36.98	_	55.21	_
DH_01$_r$ (45%)	17.85	**2.07**	36.38	**1.64**	54.23	**1.78**
DH_02$_f$ (45%)	20.07	**-10.08**	40.77	**-10.24**	60.84	**-10.19**
DH_02$_r$ (45%)	19.80	**-8.61**	40.46	**-9.39**	60.25	**-9.13**
SDH_01$_f$ (45%)	17.47	**4.16**	31.66	**14.38**	49.13	**11.01**
SDH_01$_r$ (45%)	17.06	**6.42**	31.09	**15.92**	48.15	**12.78**
SDH_02$_f$ (45%)	19.02	**-4.31**	33.15	**10.37**	52.16	**5.52**
SDH_02$_r$ (45%)	18.60	**-2.03**	32.56	**11.95**	51.16	**7.33**
SDH_03$_f$ (45%)	29.31	**-60.76**	40.57	**-9.71**	69.88	**-26.57**
SDH_03$_r$ (45%)	28.88	**-58.45**	39.97	**-8.08**	68.86	**-24.71**
RH_$_f$ (45%)	16.97	**0.00**	31.60	**14.56**	48.57	**12.03**
RH_$_r$ (45%)	16.54	**9.26**	31.03	**16.10**	47.57	**13.84**
LH_$_f$ (45%)	8.78	**51.83**	53.61	**-44.97**	62.39	**-13.01**
LH_$_r$ (45%)	8.54	**53.14**	49.46	**-33.74**	58.00	**-5.05**
CH_$_f$ (45%)	20.72	**-13.65**	50.06	**-35.37**	70.78	**-28.20**
CH_$_r$ (45%)	20.66	**-13.31**	44.15	**-19.38**	64.80	**-17.37**
DH_01$_f$ (60%)	60.10	_	40.30	_	100.40	_
DH_01$_r$ (60%)	59.29	**1.35**	39.68	**1.54**	98.97	**1.43**
DH_02$_f$ (60%)	66.61	**-10.83**	45.88	**-13.83**	112.49	**-12.04**
DH_02$_r$ (60%)	66.22	**-10.19**	45.45	**-12.77**	111.67	**-11.23**
SDH_01$_f$ (60%)	56.81	**5.47**	35.84	**11.06**	92.65	**7.72**
SDH_01$_r$ (60%)	55.92	**6.96**	35.10	**12.91**	91.01	**9.35**
SDH_02$_f$ (60%)	60.52	**-0.70**	37.85	**6.09**	98.37	**2.03**
SDH_02$_r$ (60%)	59.69	**0.69**	37.23	**7.62**	96.92	**3.47**
SDH_03$_f$ (60%)	88.23	**-46.81**	45.38	**-12.60**	133.61	**-33.07**
SDH_03$_r$ (60%)	87.40	**-45.42**	44.75	**-11.04**	132.15	**-31.62**
RH_$_f$ (60%)	56.17	**0.00**	36.07	**10.49**	92.24	**8.13**
RH_$_r$ (60%)	55.29	**8.01**	35.75	**11.29**	91.04	**9.32**
LH_$_f$ (60%)	74.05	**-23.21**	57.49	**-42.64**	131.53	**-31.01**
LH_$_r$ (60%)	72.99	**-21.44**	52.58	**-30.45**	125.56	**-25.06**
CH_$_f$ (60%)	68.57	**-14.10**	53.49	**-32.72**	122.06	**-21.57**
CH_$_r$ (60%)	68.27	**-13.60**	47.40	**-17.61**	115.67	**-15.21**

DH_01$_f$ (75%)	17.77	_	43.60	_	61.37	_
DH_01$_r$ (75%)	17.35	**2.38**	42.96	**1.47**	60.31	**1.73**
DH_02$_f$ (75%)	18.37	**-3.36**	51.09	**-17.17**	69.46	**-13.17**
DH_02$_r$ (75%)	18.04	**-1.52**	50.12	**-14.95**	68.16	**-11.06**
SDH_01$_f$ (75%)	16.08	**9.53**	40.15	**7.93**	56.22	**8.39**
SDH_01$_r$ (75%)	15.60	**12.20**	39.54	**9.31**	55.15	**10.15**
SDH_02$_f$ (75%)	17.66	**0.62**	42.63	**2.23**	60.29	**1.77**
SDH_02$_r$ (75%)	17.17	**3.40**	41.99	**3.69**	59.16	**3.61**
SDH_03$_f$ (75%)	27.46	**-54.50**	50.25	**-15.25**	77.71	**-26.62**
SDH_03$_r$ (75%)	26.96	**-51.71**	49.60	**-13.75**	76.56	**-24.74**
RH_$_f$ (75%)	15.66	**0.00**	40.40	**7.34**	56.06	**8.66**
RH_$_r$ (75%)	15.00	**15.57**	40.59	**6.91**	55.59	**9.42**
LH_$_f$ (75%)	18.89	**-6.30**	64.36	**-47.60**	83.25	**-35.64**
LH_$_r$ (75%)	19.02	**-7.01**	57.84	**-32.65**	76.86	**-25.23**
CH_$_f$ (75%)	20.05	**-12.80**	56.98	**-30.69**	77.03	**-25.51**
CH_$_r$ (75%)	19.83	**-11.59**	50.25	**-15.24**	70.08	**-14.19**

6.1.2 Thermal performance of mass timber construction

The worst energy performing morphology in the case of mass timber construction was chosen to simulate the indoor air temperature, in order to determine the impact of three window-to-wall ratio scenarios.

Figure 74 demonstrates the simulated indoor temperature during summer, with all three window-to-wall ratio scenarios, with the worst performing morphology, LH_$_f$ in the case of mass timber construction. Altogether with the outside dry-bulb temperature, are calculated using the Athens weather data. It is noted, when the outdoor temperature fluctuates, the indoor air temperature of LH_$_f$, stays linear throughout three WWR scenarios. LH_$_f$ in the 45% window-to-wall ratio scenario displays a closer performance to the comfort zone. Meanwhile in the other two scenarios of 60% and 75% window-to wall ratio, the morphology displays temperatures a little further away from the comfort zone. There is a tendency of the indoor temperatures to go lower after 9:00 AM to 17:00 PM, approaching the comfort values.

Table 12 summarizes the simulation results for the indoor air temperature, calculated in the climate context of Athens on July 22. Hence obtaining the worst performance, LH_$_f$ with the living room exposed to north and south, it gains 13.57 °C

when WWR is 45%, 14.6°C when WWR is 60% and 14.62°C when WWR is 75%.

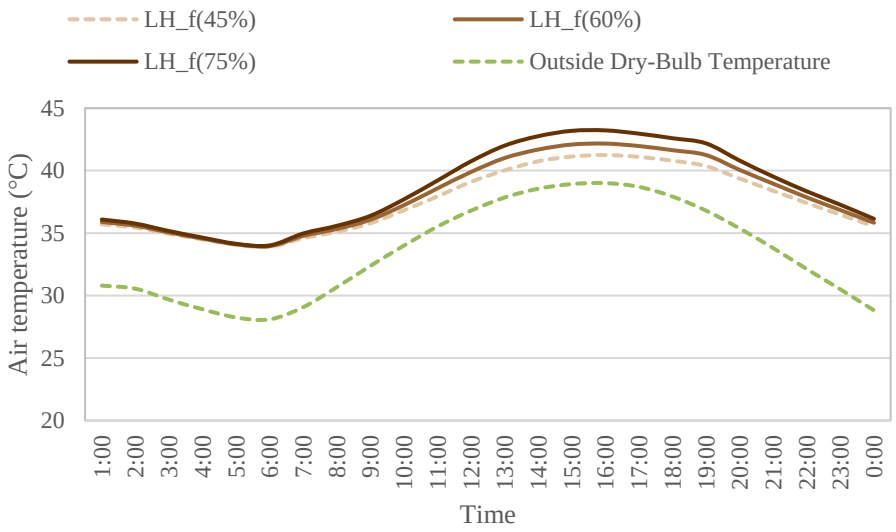

Figure 74. Simulated indoor air temperatures of living room for the worst energy performance morphology, together with the dry-bulb temperature for 22 of July, Athens climate, MTC system

Table 12. Simulation results for the air temperature calculated on the 22th of July, Athens climate, MTC system

T [°C]	45%			60%			75%		
	Min	Max	**OH_m**	Min	Max	**OH_m**	Min	Max	**OH_m**
LH_f	33.90	41.25	**13.57**	33.96	42.16	**14.06**	34.01	43.22	**14.62**

Figure 75 depicts the simulated indoor temperature during winter, with all three window-to-wall ratio scenarios, with the worst performing morphology, LH_f in the case of mass timber construction. Altogether with the outside dry-bulb temperature, are calculated using the Athens weather data for January 18. It is noted that even during winter, when the outdoor temperature fluctuates, the indoor air temperature of LH_f, stays

linear throughout three WWR scenarios. LH_f in all three window-to-wall ratio scenarios, stays further way from the comfort temperatures. Thus, requiring for more heating loads during winter months and putting in doubt its effectiveness in this climate.

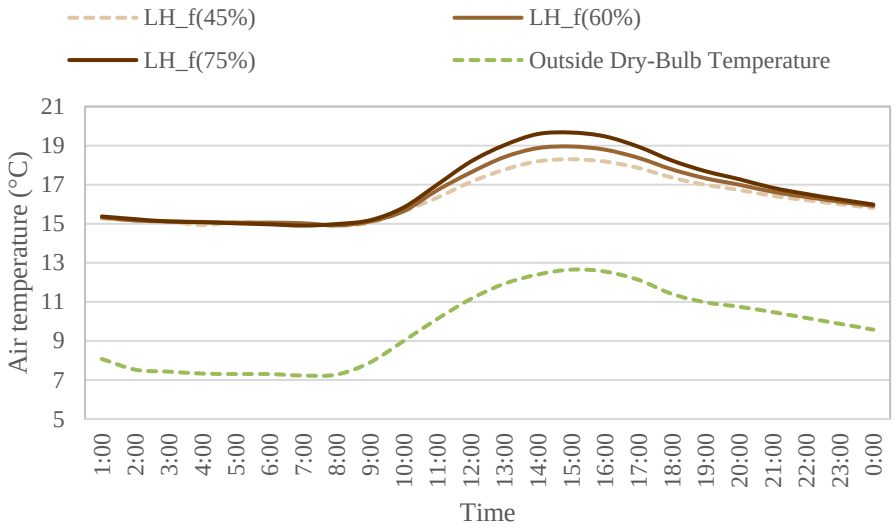

Figure 75. Simulated indoor air temperatures of living room for the worst energy performance morphology, together with the dry-bulb temperature for 18 of January, Athens climate, MTC system

6.1.3 Energy performance of light-timber construction

As illustrated in *Figure 76*, the comparison of annual energy consumption in terms of transparency in the case of mass timber construction, shows a varying trend when the house gains more transparency from 45%, 60% to 75%, which correspond to the North and South oriented rooms. The most notable impact of transparency is visible in morphologies SDH_02$_f$, SDH_02$_r$, due to the square layouts and LH_$_f$, LH_$_r$, due to the L-shape layouts. In SDH_02$_f$ morphology, energy consumption increases with 3.39 kWh.m^{-2} a^{-1}, when transparency is 60% and increases with 3.62 kWh.m^{-2} a^{-1}, when transparency is 75%. In SDH_01$_r$ morphology, energy consumption is subject to an increase of 3.13 kWh.m^{-2} a^{-1}, when transparency is 60% and 3.35 kWh.m^{-2} a^{-1}, when WWR is 75%. In SDH_01$_f$ model, energy consumption is subject to an increase of 2.93 kWh.m^{-2} a^{-1}, when transparency is 60% and 3.15 kWh.m^{-2} a^{-1}, when transparency is

75%. As for LH_f morphology, energy consumption is subject to an increase of 5.85 kWh.m^{-2} a^{-1}, when transparency is 60% and 6.20 kWh.m^{-2} a^{-1}, when WWR is 75%, meanwhile LH_r experiences a smaller increase, from 5.21 kWh.m^{-2} a^{-1} to 4.68 kWh.m^{-2} a^{-1}, due to the roof insulating attributes. In SDH_03$_f$ model, energy demand is subject to in increment of 3.27 kWh.m^{-2} a^{-1}, when WWR is 60% and 3.48 kWh.m^{-2} a^{-1}, when WWR is 75%. As for its akin, SDH_03$_r$ model has an energy increment of 3.46 kWh.m^{-2} a^{-1}, when WWR is 60% and 3.67 kWh.m^{-2} a^{-1}, when WWR is 75%.

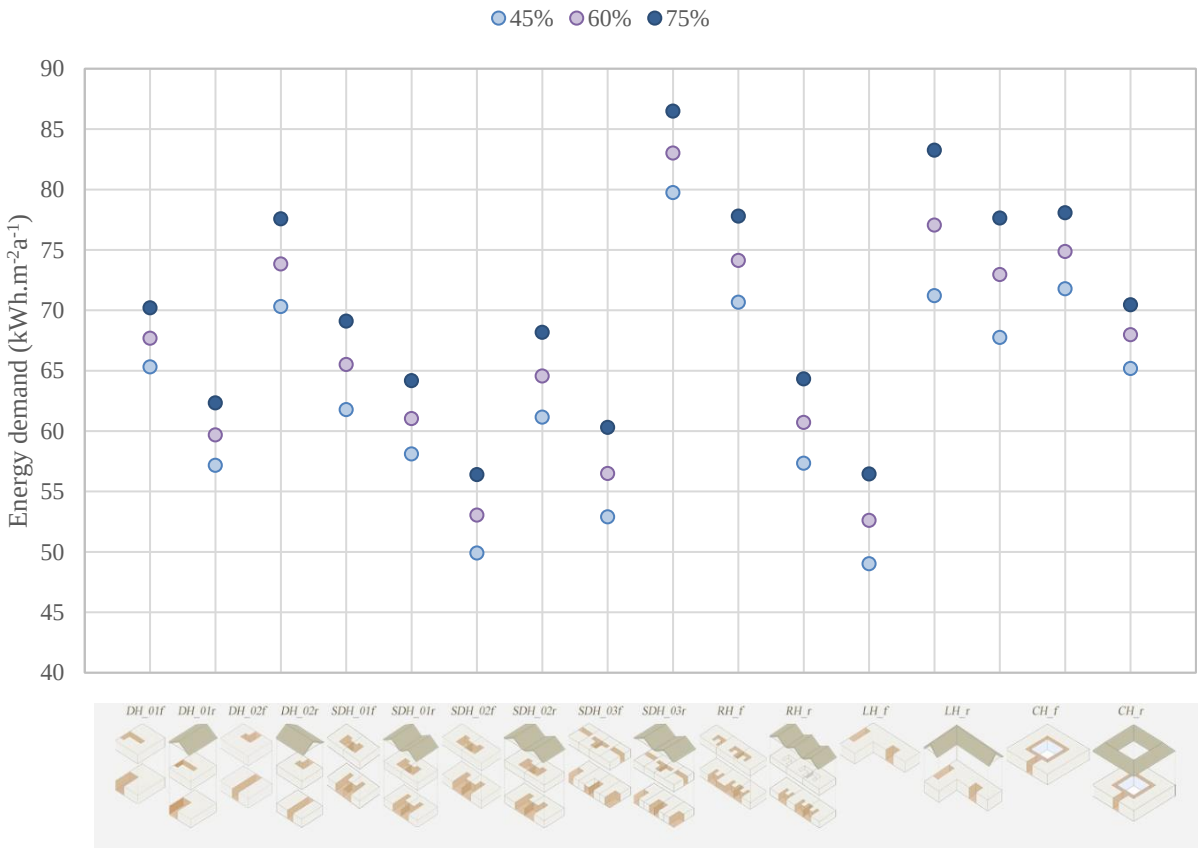

Figure 76. Comparison of simulated annual energy demand (kWh.m^{-2} a^{-1}), Athens climate context, LFT construction system

Table 13 summarizes the obtained simulation results from Design Builder for all transparency scenarios in the climate of Athens. A maximum of 24.95% of total energy consumption can be reduced, if the right morphology is selected for the studied climatic region. The typology with the worst performance in terms of heating loads is SDH_03$_f$

and SDH_03$_r$, meanwhile CH_$_f$ and LH_$_f$, have the worst performance in terms of cooling loads, followed by LH_$_f$ and CH_$_r$. The row house RH_$_r$ saves 5.85 kWh.m^{-2} a^{-1} and 6.20 kWh.m^{-2} a^{-1}, when WWR is 60% and 75% respectively. Its heating demand in winter months, displays a morphology effectiveness of 1689%. On the other hand, it is noted that CH_$_f$ cooling demand reduces the morphology effectiveness with -25.93 % and LH_$_f$ with -24.35 % (WWR=45%). Among the timber low-rise single housing it is depicted that the best performing model is RH_$_r$ with 24.95% effectiveness, followed by another type, SDH_01$_r$ with 23.58% and DH_01$_r$ with 12.47%. Meanwhile the morphology with the poorest performance is SDH_03$_f$ with -22.11% effectiveness, followed by CH_$_f$ with -9.91% and LH_$_f$ with -9.03% effectiveness.

Table 13. Simulation results obtained for all scenarios in the climate of Athens, LFT construction system

	Annual heating demand		**Annual cooling demand**		**Annual energy demand**	
Scenarios	Heating/ conditioned area [kw.h^{-1}m^{-2}]	**Morphology effectiveness [%]**	Cooling/ conditioned area [kw.h^{-1}m^{-2}]	**Morphology effectiveness [%]**	Total energy/ conditioned area [kw.h^{-1}m^{-2}]	**Total morphology effectiveness [%]**
DH_01$_f$ (45%)	24.47	_	40.84	_	65.30	_
DH_01$_r$ (45%)	19.22	**21.44**	37.94	**7.09**	57.16	**12.47**
DH_02$_f$ (45%)	25.89	**-5.82**	44.41	**-8.76**	70.30	**-7.66**
DH_02$_r$ (45%)	20.44	**16.44**	41.32	**-1.19**	61.77	**5.42**
SDH_01$_f$ (45%)	22.98	**6.08**	35.12	**14.00**	58.10	**11.03**
SDH_01$_r$ (45%)	17.71	**27.61**	32.19	**21.17**	49.90	**23.58**
SDH_02$_f$ (45%)	24.54	**-0.31**	36.61	**10.34**	61.15	**6.35**
SDH_02$_r$ (45%)	19.23	**21.39**	33.66	**17.58**	52.89	**19.01**
SDH_03$_f$ (45%)	35.21	**-43.91**	44.53	**-9.05**	79.74	**-22.11**
SDH_03$_r$ (45%)	29.57	**-20.88**	41.09	**-0.62**	70.66	**-8.21**
RH_$_f$ (45%)	22.44	**8.29**	34.89	**14.55**	57.33	**12.21**
RH_$_r$ (45%)	17.07	**30.21**	31.94	**21.79**	49.01	**24.95**
LH_$_f$ (45%)	20.42	**16.53**	50.78	**-24.35**	71.20	**-9.03**
LH_$_r$ (45%)	20.72	**15.32**	47.02	**-15.15**	67.74	**-3.74**
CH_$_f$ (45%)	20.35	**16.82**	51.43	**-25.93**	71.78	**-9.91**
CH_$_r$ (45%)	20.73	**15.26**	44.45	**-8.84**	65.18	**0.19**
DH_01$_f$ (60%)	23.85	_	43.83	_	67.68	_
DH_01$_r$ (60%)	18.61	**21.98**	41.06	**6.30**	59.67	**11.83**
DH_02$_f$ (60%)	24.85	**-4.16**	48.99	**-11.77**	73.83	**-9.09**

DH_02$_r$ (60%)	19.44	**18.52**	46.07	**-5.12**	65.51	**3.21**
SDH_01$_f$ (60%)	22.16	**7.12**	38.87	**11.32**	61.02	**9.84**
SDH_01$_r$ (60%)	16.89	**29.17**	36.14	**17.54**	53.03	**21.64**
SDH_02$_f$ (60%)	23.71	**0.61**	40.84	**6.82**	64.55	**4.63**
SDH_02$_r$ (60%)	18.40	**22.88**	38.09	**13.09**	56.48	**16.54**
SDH_03$_f$ (60%)	34.14	**-43.11**	48.87	**-11.51**	83.01	**-22.65**
SDH_03$_r$ (60%)	28.49	**-19.45**	45.63	**-4.11**	74.12	**-9.52**
RH_$_f$ (60%)	21.55	**9.67**	39.16	**10.66**	60.70	**10.31**
RH_$_r$ (60%)	16.18	**32.16**	36.42	**16.89**	52.60	**22.27**
LH_$_f$ (60%)	19.57	**17.98**	57.49	**-31.17**	77.05	**-13.85**
LH_$_r$ (60%)	19.98	**16.25**	52.97	**-20.87**	72.95	**-7.79**
CH_$_f$ (60%)	20.00	**16.17**	54.86	**-25.18**	74.86	**-10.61**
CH_$_r$ (60%)	20.28	**14.99**	47.70	**-8.83**	67.98	**-0.44**
DH_01$_f$ (75%)	23.30	**_**	46.89	**_**	70.20	**_**
DH_01$_r$ (75%)	18.07	**22.47**	44.26	**5.61**	62.33	**11.21**
DH_02$_f$ (75%)	23.94	**-2.71**	53.63	**-14.36**	77.57	**-10.49**
DH_02$_r$ (75%)	18.59	**20.23**	50.51	**-7.70**	69.10	**1.57**
SDH_01$_f$ (75%)	21.42	**8.11**	42.76	**8.83**	64.17	**8.59**
SDH_01$_r$ (75%)	16.17	**30.63**	40.22	**14.24**	56.38	**19.68**
SDH_02$_f$ (75%)	23.00	**1.33**	45.17	**3.68**	68.17	**2.90**
SDH_02$_r$ (75%)	17.69	**24.10**	42.61	**9.13**	60.30	**14.10**
SDH_03$_f$ (75%)	33.19	**-42.43**	53.29	**-13.64**	86.49	**-23.20**
SDH_03$_r$ (75%)	27.55	**-18.20**	50.24	**-7.14**	77.79	**-10.81**
RH_$_f$ (75%)	20.77	**10.88**	43.55	**7.14**	64.32	**8.38**
RH_$_r$ (75%)	15.41	**33.88**	41.03	**12.50**	56.44	**19.60**
LH_$_f$ (75%)	18.89	**18.94**	64.36	**-37.24**	83.25	**-18.59**
LH_$_r$ (75%)	19.42	**16.69**	58.21	**-24.14**	77.63	**-10.58**
CH_$_f$ (75%)	19.70	**15.47**	58.36	**-24.46**	78.06	**-11.20**
CH_$_r$ (75%)	19.91	**14.59**	50.55	**-7.79**	70.45	**-0.36**

6.1.4 Thermal performance of light-timber construction

The worst energy performing morphology in the case of and light-frame timber construction was chosen to simulate the indoor air temperature, in order to determine the impact of three window-to-wall ratio scenarios.

Figure 77 demonstrates the simulated indoor temperature during summer, with all three window-to-wall ratio scenarios, with the worst performing morphology, SDH_03$_f$

in the case of light-frame timber construction. Altogether with the outside dry-bulb temperature, are calculated using the Athens weather data. It is noted, when the outdoor temperature fluctuates, the indoor air temperature of SDH_03$_f$, stays linear throughout three WWR scenarios. SDH_03$_f$ in the 45% window-to-wall ratio scenario displays a closer performance to the comfort temperatures. The other two scenarios of 60% and 75% window-to wall ratio have similar performances. There is a tendency of the indoor temperatures to go lower after 10:00 AM to 20:00 PM, approaching the comfort values, even going down and staying within the comfort zone.

Table 14 summarizes the simulation results for the indoor air temperature, calculated in the climate context of Athens on July 22. Hence obtaining the worst performance, SDH_03$_f$ with the living room exposed to north, it gains 8.70 °C when WWR is 45%, 9.08°C when WWR is 60% and 9.46°C when WWR is 75%.

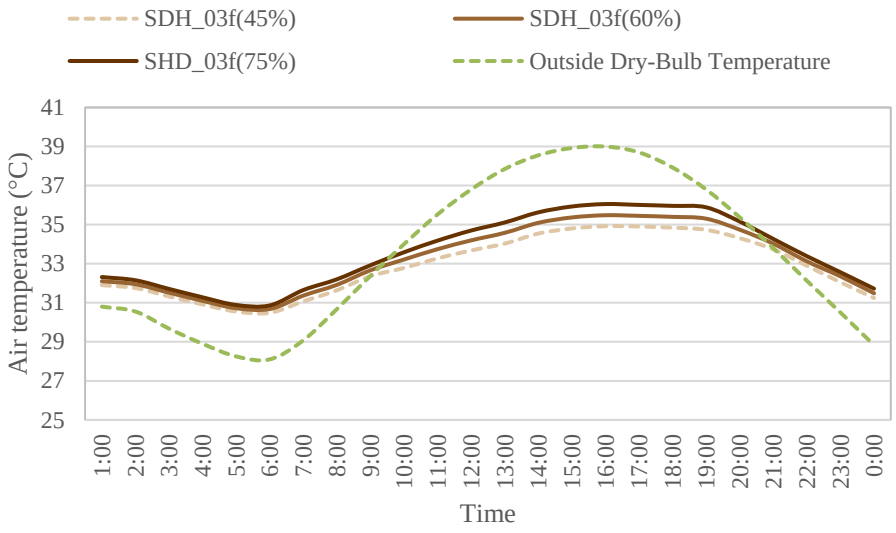

Figure 77. Simulated indoor air temperatures of living room for the worst energy performance morphology, together with the dry-bulb temperature for 22 of July, Athens climate, LFT construction system

Table 14. Simulation results for the air temperature calculated on the 22th of July, Athens climate, LFT construction system

T [°C]	45%			60%			75%		
	Min	Max	**OH_m**	Min	Max	**OH_m**	Min	Max	**OH_m**
SDH_03_f	30.48	34.92	**8.70**	30.68	35.48	**9.08**	30.86	36.05	**9.46**

Figure 78 depicts the simulated indoor temperature during winter, with all three window-to-wall ratio scenarios, with the worst performing morphology, SDH_03_f in the case of light-timber construction. Altogether with the outside dry-bulb temperature, are calculated using the Athens weather data for January 18. It is noted that even during winter, when the outdoor temperature fluctuates, the indoor air temperature of SDH_03_f, stays linear throughout three WWR scenarios. SDH_03f in all three window-to-wall ratio scenarios, stays further way from the comfort temperatures, compared even to the mass timber SDH_03_f scenarios. Thus, requiring for more heating loads during winter months and putting in doubt its effectiveness in this climate.

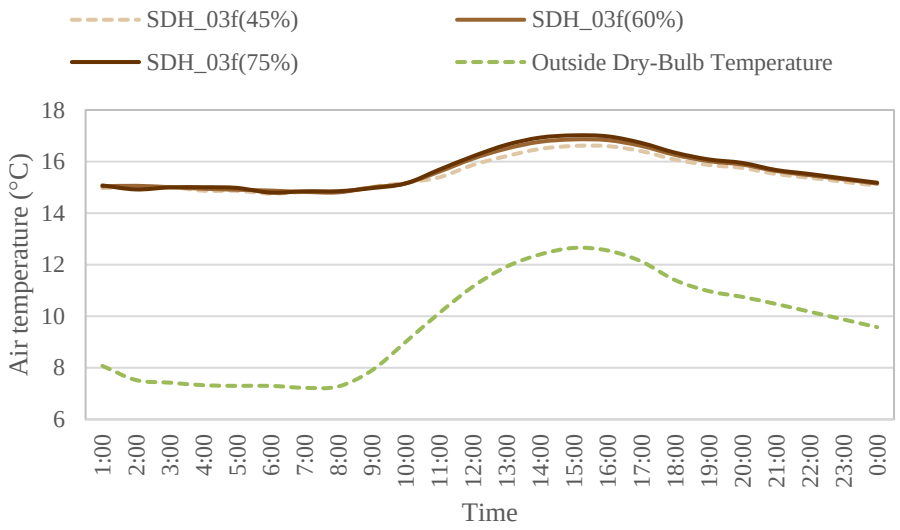

Figure 78. Simulated indoor air temperatures of living room for the worst energy performance morphology, together with the dry-bulb temperature for 18 of January, Athens climate, LFT construction system

6.2 Climate of Berlin

To determine the morphology effectiveness of each low-rise single housing, in the continental climate of Berlin a comparison of annual active energy consumption for every scenario of WWR and the indoor passive thermal comfort for the worst performing morphology is conducted.

6.2.1 Energy performance of mass timber construction

As illustrated in *Figure 79* the comparison of annual energy consumption in terms of transparency in the case of mass timber construction, shows an increasing trend when the house gains more transparency from 45%, 60% to 75%, which correspond to the North and South oriented rooms. In the same time, it is noted an increase in the annual energy demand for all morphologies, compared to the Athens climate conditions. RH_r and RH_f remains the best at energy performance, due to the horizontal layout orientation. Same with Athens, even in Berlin, the most significant impact of transparency is visible in the L-shape layouts, LH_f and LH_r. energy consumption of LH_f increases from 29.25 $kWh.m^{-2} a^{-1}$, when WWR IS 60% and 34.28 $kWh.m^{-2} a^{-1}$, when WWR is 75%. In LH_r morphology the energy is subject to an increase of 28.80 $kWh.m^{-2} a^{-1}$ and 32.63 $kWh.m^{-2} a^{-1}$, when WWR is 60% and 75% respectively.

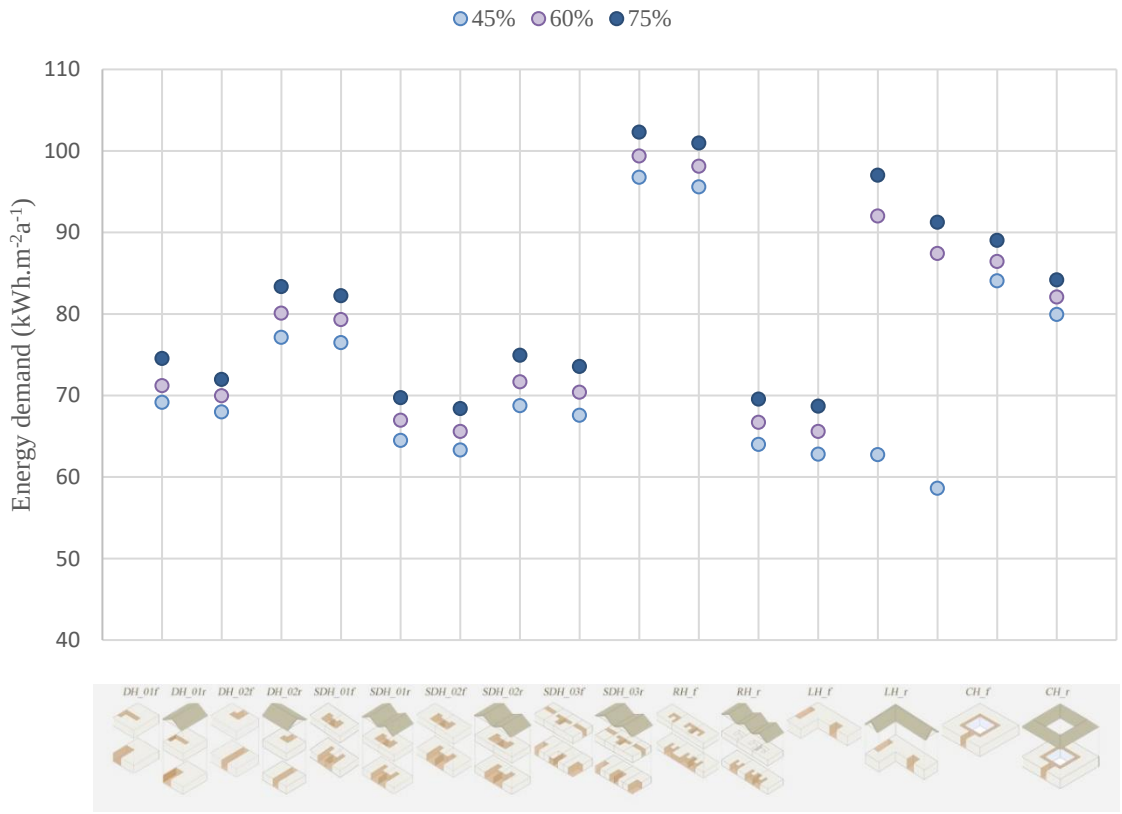

Figure 79. Comparison of simulated annual energy demand (kWh.m^{-2} a^{-1}), Berlin climate context, MTC system

Table 15 summarizes the obtained simulation results from Design Builder for all transparency scenarios in the climate of Berlin. A maximum of 15.25% of total energy consumption can be reduced, if the right morphology is selected for the studied climatic region. The typology with the worst performance in terms of heating loads is SDH_03$_f$ and SDH_03$_r$, meanwhile LH_$_f$ and LH_$_r$, have the worst performance in terms of cooling loads, followed by CH_$_f$ and CH_$_r$. The row houses, RH_$_f$ and RH_$_r$ save 2.64 kWh.m^{-2} a^{-1} and 2.76 kWh.m^{-2} a^{-1} respectively in cooling loads with a morphology effectiveness of 13.58% and 17.56% respectively, compared to the other houses. Their sightly high demand for heating loads in winter months, displays a morphology effectiveness by 6.55% and 7.92% respectively. On the other hand, it is noted that LH_$_f$ cooling demand reduces the morphology effectiveness with -90.83 kWh.m^{-2} a^{-1} and CH_$_f$ with -71.79 kWh.m^{-2} a^{-1}. Among the timber low-rise single housing it is depicted that the best performing model is LH_$_r$ with 15.25% effectiveness, followed by another type, RH_$_r$

with 9.19% and SDH_01$_r$ with 8.46%. Meanwhile the morphology with the poorest performance is SDH_03$_f$ with -39.92 effectiveness, followed by CH_$_f$ with -21.55% effectiveness.

Table 15. Simulation results obtained for all scenarios in the climate of Berlin, MTC system

Scenarios	**Annual heating demand**		**Annual cooling demand**		**Annual energy demand**	
	Heating/ conditioned area [kw.h^{-1}m^{-2}]	**Morphology effectiveness [%]**	Cooling/ conditioned area [kw.h^{-1}m^{-2}]	**Morphology effectiveness [%]**	Total energy/ conditioned area [kw.h^{-1}m^{-2}]	**Total morphology effectiveness [%]**
DH_01$_f$ (45%)	60.02	_	9.12	_	69.14	_
DH_01$_r$ (45%)	59.22	**1.32**	8.74	**4.24**	67.96	**1.71**
DH_02$_f$ (45%)	66.63	**-11.02**	10.49	**-15.02**	77.12	**-11.55**
DH_02$_r$ (45%)	66.28	**-10.43**	10.19	**-11.73**	76.47	**-10.60**
SDH_01$_f$ (45%)	56.77	**0.00**	7.70	**15.58**	64.47	**6.76**
SDH_01$_r$ (45%)	55.95	**6.78**	7.35	**19.47**	63.29	**8.46**
SDH_02$_f$ (45%)	60.43	**-0.69**	8.29	**9.10**	68.73	**0.60**
SDH_02$_r$ (45%)	59.64	**0.64**	7.92	**13.21**	67.55	**2.30**
SDH_03$_f$ (45%)	88.25	**-47.04**	8.49	**6.91**	96.74	**-39.92**
SDH_03$_r$ (45%)	87.44	**-45.69**	8.14	**10.81**	95.58	**-38.23**
RH_$_f$ (45%)	56.09	**6.55**	7.88	**13.58**	63.97	**7.47**
RH_$_r$ (45%)	55.27	**7.92**	7.52	**17.57**	62.79	**9.19**
LH_$_f$ (45%)	45.33	**24.48**	17.41	**-90.83**	62.73	**9.27**
LH_$_r$ (45%)	44.00	**26.68**	14.59	**-59.96**	58.59	**15.25**
CH_$_f$ (45%)	68.37	**13.91**	15.67	**-71.79**	84.04	**-21.55**
CH_$_r$ (45%)	68.13	**-13.52**	11.79	**-29.25**	79.92	**-15.59**
DH_01$_f$ (60%)	60.10	_	11.09	_	71.19	_
DH_01$_r$ (60%)	59.29	**1.35**	10.67	**3.83**	69.96	**1.73**
DH_02$_f$ (60%)	66.61	**-10.83**	13.47	**-21.46**	80.08	**-12.49**
DH_02$_r$ (60%)	66.22	**-10.19**	13.08	**-17.92**	79.30	**-11.39**
SDH_01$_f$ (60%)	56.81	**0.00**	10.14	**8.59**	66.95	**5.96**
SDH_01$_r$ (60%)	55.92	**6.96**	9.65	**13.00**	65.56	**7.90**
SDH_02$_f$ (60%)	60.52	**-0.70**	11.14	**-0.43**	71.66	**-0.66**
SDH_02$_r$ (60%)	59.69	**0.69**	10.70	**3.53**	70.39	**1.13**
SDH_03$_f$ (60%)	88.23	**-46.81**	11.12	**-0.30**	99.35	**-39.56**
SDH_03$_r$ (60%)	87.40	**-45.42**	10.70	**3.50**	98.10	**-37.80**
RH_$_f$ (60%)	56.17	**6.54**	10.52	**5.14**	66.69	**6.32**
RH_$_r$ (60%)	55.29	**8.01**	10.28	**7.29**	65.57	**7.89**

LH_$_f$ (60%)	74.05	**-23.21**	17.94	**-61.75**	91.99	**-29.21**
LH_$_r$ (60%)	72.99	**-21.44**	14.41	**-29.93**	87.40	**-22.77**
CH_$_f$ (60%)	68.57	**14.10**	17.86	**-60.99**	86.43	**-21.41**
CH_$_r$ (60%)	68.27	**-13.60**	13.78	**-24.24**	82.05	**-15.26**
DH_01$_f$ (75%)	61.39	_	13.13	_	74.52	_
DH_01$_r$ (75%)	60.56	**1.35**	12.67	**3.54**	73.23	**1.73**
DH_02$_f$ (75%)	66.64	**-8.54**	16.71	**-27.26**	83.35	**-11.84**
DH_02$_r$ (75%)	66.24	**-7.89**	15.98	**-21.71**	82.22	**-10.33**
SDH_01$_f$ (75%)	56.87	**0.00**	12.84	**2.22**	69.71	**6.45**
SDH_01$_r$ (75%)	56.00	**8.78**	12.38	**5.75**	68.38	**8.25**
SDH_02$_f$ (75%)	60.67	**1.17**	14.24	**-8.42**	74.91	**-0.52**
SDH_02$_r$ (75%)	59.80	**2.59**	13.74	**-4.59**	73.54	**1.32**
SDH_03$_f$ (75%)	88.26	**-43.76**	14.03	**-6.80**	102.28	**-37.25**
SDH_03$_r$ (75%)	87.40	**-42.37**	13.54	**-3.13**	100.94	**-35.45**
RH_$_f$ (75%)	56.31	**8.28**	13.24	**-0.79**	69.55	**6.68**
RH_$_r$ (75%)	55.35	**9.83**	13.33	**-1.50**	68.68	**7.84**
LH_$_f$ (75%)	74.42	**-21.22**	22.58	**-71.93**	97.00	**-30.15**
LH_$_r$ (75%)	73.55	**-19.81**	17.67	**-34.55**	91.22	**-22.41**
CH_$_f$ (75%)	68.79	**12.06**	20.21	**-53.88**	89.00	**-19.43**
CH_$_r$ (75%)	68.45	**-11.51**	15.71	**-19.65**	84.17	**-12.94**

6.2.2 Thermal performance of mass timber construction

The worst energy performing morphology in the case of and mass timber construction was chosen to simulate the indoor air temperature, in order to determine the impact of three window-to-wall ratio scenarios.

Figure 80 demonstrates the simulated indoor temperature during summer, with all three window-to-wall ratio scenarios, with the worst performing morphology, SDH_03$_f$ in the case of mass timber construction. Altogether with the outside dry-bulb temperature, are calculated using the Berlin weather data. It is noted, when the outdoor temperature fluctuates, the indoor air temperature of SDH_03$_f$, stays linear throughout three WWR scenarios. SDH_03$_f$ in the 45% window-to-wall ratio scenario displays a closer performance to the comfort temperatures. The other two scenarios of 60% and 75% window-to wall ratio have similar performances, but further away from the comfort zone. There is a tendency of the indoor temperatures to go lower after 13:00 PM to 17:00 PM,

approaching the comfort values.

Table 16 summarizes the simulation results for the indoor air temperature, calculated in the climate context of Berlin on July 22. Hence obtaining the worst performance, SDH_03$_f$ with the living room exposed to north, it requires to gain heat of 3.30 °C when WWR is 45%, 2.96 when WWR is 60% and 2.66 when WWR is 75%. Compared to Athens climate, here the temperatures don't exceed the comfort temperature of 24°C, resulting in no overheating, despite the poor performance of the morphology compared to others.

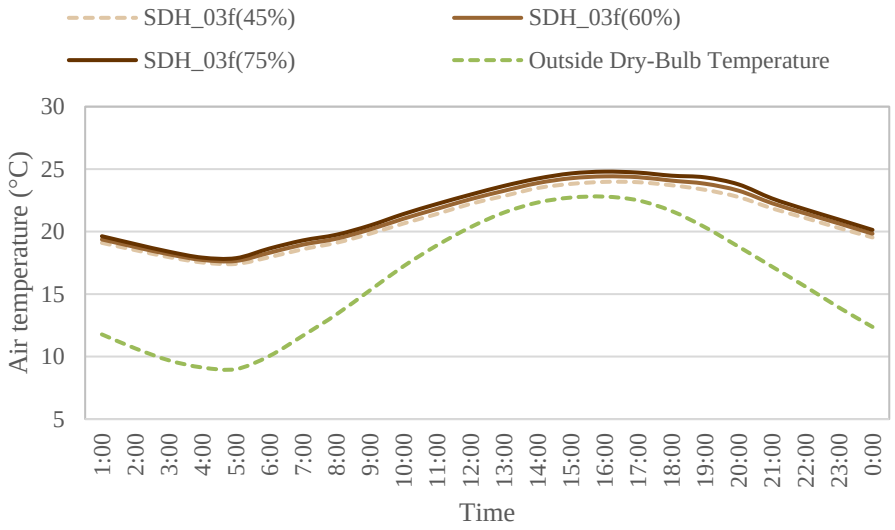

Figure 80. Simulated indoor air temperatures of living room for the worst energy performance morphology, together with the dry-bulb temperature for 22 of July, Berlin climate, MTC system

Table 16. Simulation results for the air temperature calculated on the 22th of July, Berlin climate, MTC system

T [°C]	45%			60%			75%		
	Min	Max	**OH$_m$**	Min	Max	**OH$_m$**	Min	Max	**OH$_m$**
SDH_03$_f$	17.41	23.98	**-3.30**	17.65	24.42	**-2.96**	17.87	24.80	**-2.66**

Figure 81 depicts the simulated indoor temperature during winter, with all three window-to-wall ratio scenarios, with the worst performing morphology, SDH_03$_f$ in the case of mass timber construction. Altogether with the outside dry-bulb temperature, are calculated using the Berlin weather data for January 18. It is noted that even during winter, when the outdoor temperature fluctuates, the indoor air temperature of SDH_03$_f$, stays linear throughout three WWR scenarios. SDH_03$_f$ in all three window-to-wall ratio scenarios, stays way further from the comfort temperatures, compared even to the mass timber SDH_03$_f$ scenarios. Thus, requiring for higher heating loads during winter months and putting in doubt its effectiveness in this climate.

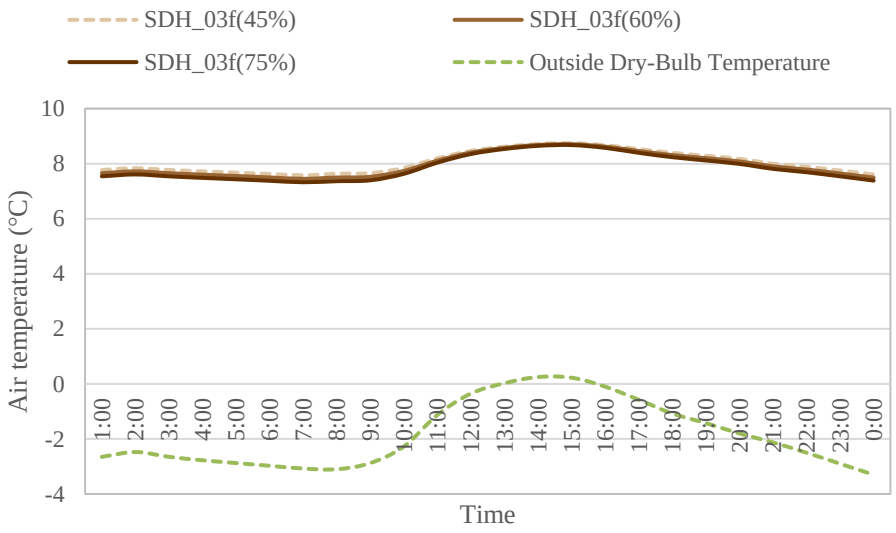

Figure 81. Simulated indoor air temperatures of living room for the worst energy performance morphology, together with the dry-bulb temperature for 18 of January, Berlin climate, MTC system

6.2.3 Energy performance of light-frame timber construction

As illustrated in *Figure 82* the comparison of annual energy consumption in terms of transparency in the case of light-frame timber construction, shows a varying trend when the house gains more transparency from 45%, 60% to 75%, which correspond to the North and South oriented rooms.in the same time values of the energy consumption are higher than in the case of mass-timber construction for all scenarios. The most notable impact of transparency is visible in morphologies SDH_02$_f$, SDH_02$_r$, due to the square

layout and LH_f, LH_r, due to the L-shape layout. In SDH_02f morphology, energy consumption increases with 2.46 kWh.m^{-2} a^{-1}, when transparency is 60% and 2.58 kWh.m^{-2} a^{-1}, when transparency is 75%. In SDH_01r morphology, energy consumption is subject to an increase of 1.85 kWh.m^{-2} a^{-1}, when transparency is 60% and 2.14 kWh.m^{-2} a^{-1}, when WWR is 75%. As for LH_f morphology, energy consumption is subject to an increase of 4.55 kWh.m^{-2} a^{-1}, when transparency is 60% and 5.01 kWh.m^{-2} a^{-1}, when WWR is 75%, meanwhile LH_r experiences a smaller increase, from 3.38 kWh.m^{-2} a^{-1}to 3.79 kWh.m^{-2} a^{-1}, due to the roof insulating attributes. Even in SDH_03f model, energy demand is subject to an increase of 1.94 kWh.m^{-2} a^{-1}, when WWR is 60% and 2.28 kWh.m^{-2} a^{-1}, when WWR is 75%.

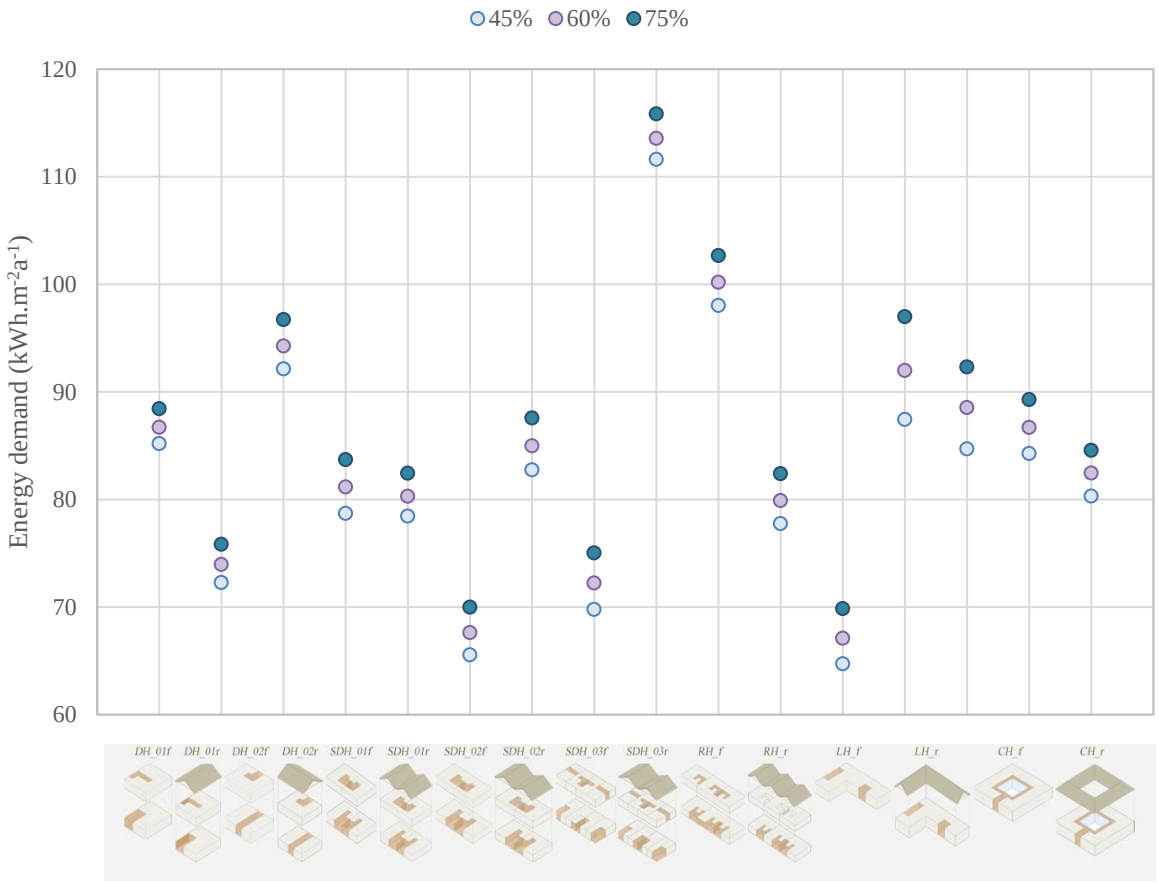

Figure 82. Comparison of simulated annual energy demand (kWh.m^{-2} a^{-1}), Berlin climate context, LFT construction system

Table 17 summarizes the obtained simulation results from Design Builder for all transparency scenarios in the climate of Berlin. A maximum of 24.04% of total energy

consumption can be reduced, if the right morphology is selected for the studied climatic region. The typology with the worst performance in terms of heating loads is SDH_03f, meanwhile CH_$_f$ and LH_$_f$, have the worst performance in terms of cooling loads. The row house RH_r saves 0.29 kWh.m^{-2} a^{-1} and 0.51 kWh.m^{-2} a^{-1}, when WWR is 60% and 75% respectively. Their heating demand in winter months, displays a morphology effectiveness of 24.85%. On the other hand, it is noted that CH_$_f$ cooling demand reduces the morphology effectiveness with -76.55 % and LH_$_f$ with -49.63 %. Among the timber low-rise single housing it is depicted that the best performing model is RH_$_r$ with 24.04% effectiveness, followed by another type, SDH_01$_r$ with 23.05% and DH_01$_r$ with 15.15%. Meanwhile the morphology with the poorest performance is SDH_03$_f$ with -31.01% effectiveness, followed by another morphology DH_02$_f$ with -8.15% effectiveness.

Table 17. Simulation results obtained for all scenarios in the climate of Berlin, LFT construction system

	Annual heating demand		**Annual cooling demand**		**Annual energy demand**	
Scenarios	Heating/ Conditioned Area [kw.h^{-1}m^{-2}]	**Morphology effectiveness [%]**	Cooling/ conditioned area [kw.h$_{-1}$m^{-2}]	**Morphology effectiveness [%]**	Total energy/ conditioned area [kw.h^{-1}m^{-2}]	**Total morphology effectiveness [%]**
DH_01$_f$ (45%)	76.01	_	9.19	_	85.19	_
DH_01$_r$ (45%)	63.50	**16.46**	8.79	**4.38**	72.28	**15.15**
DH_02$_f$ (45%)	81.69	**-7.48**	10.45	**-13.69**	92.14	**-8.15**
DH_02$_r$ (45%)	68.62	**9.72**	10.09	**-9.86**	78.71	**7.61**
SDH_01$_f$ (45%)	70.62	**7.09**	7.84	**14.68**	78.45	**7.91**
SDH_01$_r$ (45%)	58.06	**23.61**	7.50	**18.41**	65.56	**23.05**
SDH_02$_f$ (45%)	74.34	**2.19**	8.41	**8.43**	82.75	**2.86**
SDH_02$_r$ (45%)	61.75	**18.75**	8.02	**12.68**	69.77	**18.10**
SDH_03$_f$ (45%)	102.84	**-35.30**	8.77	**4.49**	111.62	**-31.01**
SDH_03$_r$ (45%)	89.77	**-18.11**	8.26	**10.13**	98.03	**-15.07**
RH_$_f$ (45%)	69.78	**8.19**	7.97	**13.24**	77.75	**8.74**
RH_$_r$ (45%)	57.12	**24.85**	7.60	**17.27**	64.72	**24.04**
LH_$_f$ (45%)	73.69	**3.05**	13.75	**-49.63**	87.44	**-2.64**
LH_$_r$ (45%)	73.52	**3.27**	11.18	**-21.73**	84.70	**0.58**
CH_$_f$ (45%)	68.05	**10.47**	16.22	**-76.55**	84.27	**1.08**
CH_$_r$ (45%)	68.37	**10.04**	11.94	**-29.99**	80.32	**5.73**
DH_01$_f$ (60%)	75.80	_	10.92	_	86.72	_

DH_01_r (60%)	63.33	**16.45**	10.63	**2.62**	73.96	**14.71**
DH_02_f (60%)	81.23	**-7.17**	13.04	**-19.45**	94.27	**-8.71**
DH_02_r (60%)	68.27	**9.93**	12.89	**-18.05**	81.16	**6.41**
SDH_01_f (60%)	70.32	**7.23**	9.98	**8.56**	80.31	**7.39**
SDH_01_r (60%)	57.82	**23.72**	9.81	**10.13**	67.63	**22.01**
SDH_02_f (60%)	74.05	**2.31**	10.94	**-0.23**	84.99	**1.99**
SDH_02_r (60%)	61.51	**18.85**	10.72	**1.78**	72.23	**16.70**
SDH_03_f (60%)	102.43	**-35.14**	11.13	**-1.91**	113.56	**-30.95**
SDH_03_r (60%)	89.42	**-17.97**	10.77	**1.33**	100.19	**-15.54**
$RH\_{\_f}$ (60%)	69.44	**8.39**	10.46	**4.20**	79.90	**7.86**
$RH\_{\_r}$ (60%)	56.83	**25.02**	10.28	**5.86**	67.11	**22.61**
$LH\_{\_f}$ (60%)	74.05	**2.31**	17.94	**-64.31**	91.99	**-6.08**
$LH\_{\_r}$ (60%)	74.04	**2.32**	14.50	**-32.79**	88.54	**-2.10**
$CH\_{\_f}$ (60%)	68.26	**9.94**	18.43	**-68.77**	86.69	**0.03**
$CH\_{\_r}$ (60%)	68.52	**9.60**	13.94	**-27.64**	82.46	**4.91**
DH_01_f (75%)	75.61	**_**	12.83	**_**	88.44	**_**
DH_01_r (75%)	63.18	**16.44**	12.66	**1.34**	75.84	**14.25**
DH_02_f (75%)	80.82	**-6.89**	15.90	**-23.91**	96.72	**-9.36**
DH_02_r (75%)	67.99	**10.08**	15.71	**-22.44**	83.70	**5.36**
SDH_01_f (75%)	70.05	**7.36**	12.39	**3.42**	82.44	**6.78**
SDH_01_r (75%)	57.59	**23.83**	12.39	**3.43**	69.99	**20.87**
SDH_02_f (75%)	73.82	**2.36**	13.75	**-7.16**	87.57	**0.98**
SDH_02_r (75%)	61.34	**18.87**	13.69	**-6.73**	75.04	**15.16**
SDH_03_f (75%)	102.08	**-35.00**	13.76	**-7.25**	115.84	**-30.98**
SDH_03_r (75%)	89.12	**-17.87**	13.56	**-5.69**	102.68	**-16.10**
$RH\_{\_f}$ (75%)	69.15	**8.55**	13.25	**-3.27**	82.40	**6.83**
$RH\_{\_r}$ (75%)	56.60	**25.14**	13.25	**-3.29**	69.85	**21.02**
$LH\_{\_f}$ (75%)	74.42	**1.58**	22.58	**-75.97**	97.00	**-9.67**
$LH\_{\_r}$ (75%)	74.59	**1.35**	17.73	**-38.21**	92.32	**-4.39**
$CH\_{\_f}$ (75%)	68.49	**9.42**	20.80	**-62.10**	89.29	**-0.96**
$CH\_{\_r}$ (75%)	68.70	**9.14**	15.87	**-23.71**	84.57	**4.38**

6.2.4 Thermal performance of light-frame timber construction

The worst energy performing morphology in the case of and light-frame timber construction was chosen to simulate the indoor air temperature, in order to determine the impact of three window-to-wall ratio scenarios.

Figure 83 demonstrates the simulated indoor temperature during summer, with all three window-to-wall ratio scenarios, with the worst performing morphology, SDH_03f

in the case of light-frame timber construction. Altogether with the outside dry-bulb temperature, are calculated using the Berlin weather data. It is noted, when the outdoor temperature fluctuates, the indoor air temperature of SDH_03f, stays linear throughout three WWR scenarios. SDH_03f in the 45% window-to-wall ratio scenario displays a closer performance to the comfort temperatures. The other two scenarios of 60% and 75% window-to wall ratio have similar performances, but a little further away from the comfort zone. There is a tendency of the indoor temperatures to go lower after 13:00 PM to 16:00 PM, approaching the comfort values.

Table 18 summarizes the simulation results for the indoor air temperature, calculated in the climate context of Berlin on July 22. Hence obtaining the worst performance, SDH_03f with the living room exposed to north, it requires to gain heat of 15.47 °C when WWR is 45%, 15.55 when WWR is 60% and 15.63 when WWR is 75%. Compared to Athens climate, here the temperatures don't exceed the comfort temperature of 24°C, resulting in no overheating, despite the poor performance of the morphology compared to others.

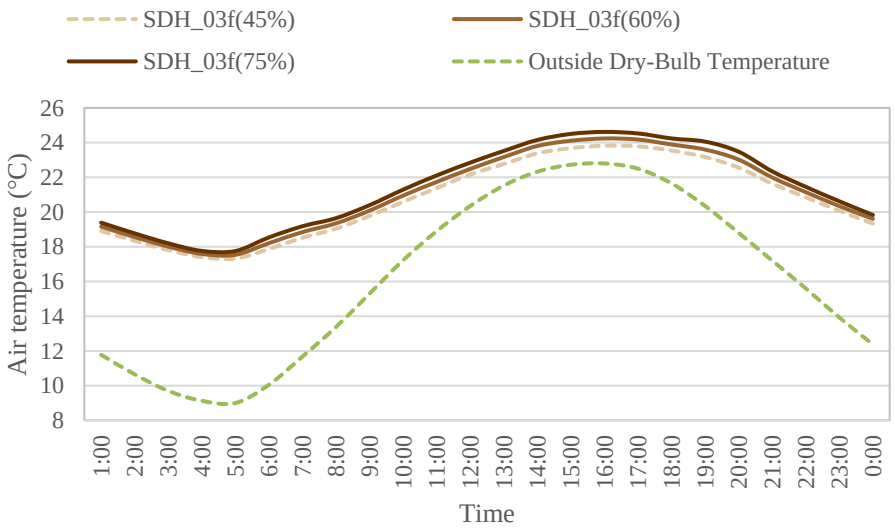

Figure 83. Simulated indoor air temperatures of living room for the worst energy performance morphology, together with the dry-bulb temperature for 22 of July, Berlin climate, LFT construction system

Table 18. Simulation results for the air temperature calculated on the 22th of July, Berlin

climate, LFT construction system

T [°C]	45%			60%			75%		
	Min	Max	**OH_m**	Min	Max	**OH_m**	Min	Max	**OH_m**
SDH_03_f	7.95	9.11	**-15.47**	7.83	9.07	**-15.55**	7.70	9.03	**-15.63**

Figure 84 depicts the simulated indoor temperature during winter, with all three window-to-wall ratio scenarios, with the worst performing morphology, SDH_03_f in the case of mass timber construction. Altogether with the outside dry-bulb temperature, are calculated using the Berlin weather data for January 18. It is noted that even during winter, when the outdoor temperature fluctuates, the indoor air temperature of SDH_03_f, stays linear throughout three WWR scenarios. SDH_03_f in all three window-to-wall ratio scenarios, stays way further from the comfort temperatures, compared even to the mass timber SDH_03_f scenarios. Thus, requiring for higher heating loads during winter months and putting in doubt its effectiveness in this climate.

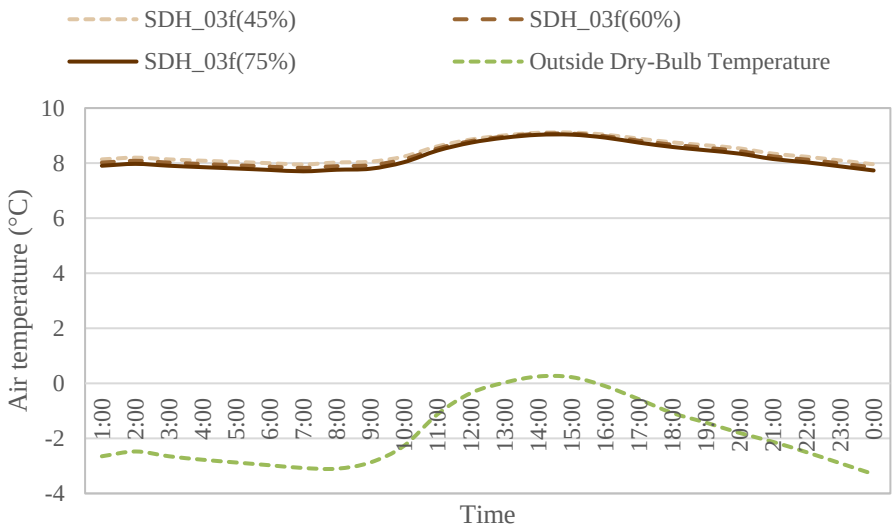

Figure 84. Simulated indoor air temperatures of living room for the worst energy performance morphology, together with the dry-bulb temperature for 18 of January, Berlin climate, LFT construction system

6.3 Climate of Garoua

To determine the morphology effectiveness of each low-rise single housing, in the tropical climate of Garoua, a comparison of annual active energy consumption for every scenario of WWR and the indoor passive thermal comfort for the worst performing morphology is conducted.

6.3.1 Energy performance of mass timber construction

As illustrated in *Figure 85* the comparison of annual energy consumption in terms of transparency in the case of mass timber construction, shows an increasing trend when the house gains more transparency from 45%, 60% to 75%, which correspond to the North and South oriented rooms. In the same time, it is noted an increase in the annual energy demand for all morphologies, compared to the Athens and Berlin climate conditions. The most significant impact of transparency is visible is the L-shape layouts, LH_f and LH_r, dual occupancy within one-unit SDH_03f and SDH_03r, rectangular box detached house DH_02f and DH_02r. Energy consumption of LH_f increases from 7.68 $kWh.m^{-2}\ a^{-1}$, when WWR is 60% and 14.98 $kWh.m^{-2}\ a^{-1}$, when WWR is 75%. In LH_r morphology the energy is subject to an increase of 7.99 $kWh.m^{-2}\ a^{-1}$, when WWR is 60% and 14.25 $kWh.m^{-2}\ a^{-1}$, when WWR is 75%. RH_f and RH_r, stay in the range of the best performance in energy consumption.

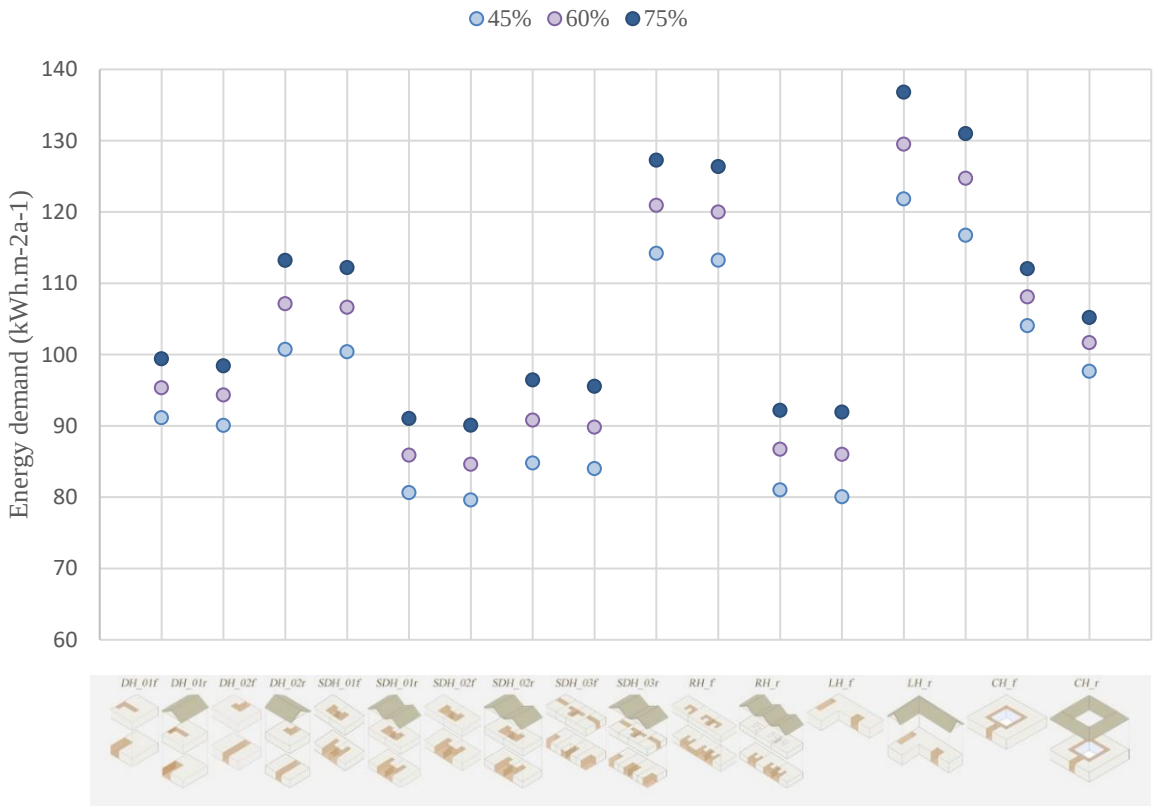

Figure 85. Comparison of simulated annual energy demand (kWh.m^{-2} a^{-1}), Garoua climate context, MTC system

Table 19 summarizes the obtained simulation results from Design Builder for all transparency scenarios in the climate of Garoua. A maximum of 11.26% of total energy consumption can be reduced, if the right morphology is selected for the studied climatic region. The typology with the worst performance in terms of heating loads is SDH_03$_f$ and SDH_03$_r$, meanwhile LH_$_f$ and LH_$_r$, have the worst performance in terms of cooling loads. The row house, RH_$_r$ demands the same energy of 0.01 kWh.m^{-2} a^{-1} for heating loads in all three transparency scenarios and a morphology effectiveness of 81.89 %, when WWR is 75%. Same approach happens in the courtyard house with a roof, CH_$_r$, with a morphology effectiveness of 111.80%, when WWR is 60%. The LH_$_r$ high demand for air-conditioning during summer months, reduces the morphology effectiveness by 32.82%. On the other hand, it is noted that the heating demand of SDH_03$_f$ and SDH_03$_r$ reduces the morphology effectiveness with -221.16% and -191.74% respectively. Among the timber low-rise single housing it is depicted that the

best performing model is SDH_01$_r$ and SDH_01$_f$ with 12.65% and 11.51% effectiveness respectively, followed by another type, RH_$_r$ with 12.15%. Meanwhile the morphology with the poorest performance is LH_$_f$ with -33.67% effectiveness, followed by LH_$_r$ with -28.10% effectiveness. Next in worst ranking is SDH_03$_f$ with a -25.31% effectiveness.

Table 19. Simulation results obtained for all scenarios in the climate of Berlin, MTC system

	Annual heating demand		**Annual cooling demand**		**Annual energy demand**	
Scenarios	Heating/ conditioned Area [kw.h^{-1}m^{-2}]	**Morphology effectiveness [%]**	Cooling/ conditioned area [kw.h^{-1}m^{-2}]	**Morphology effectiveness [%]**	Total energy/ conditioned Area [kw.h^{-1}m^{-2}]	**Total morphology effectiveness [%]**
DH_01$_f$ (45%)	0.03	_	91.09	_	91.12	_
DH_01$_r$ (45%)	0.03	**8.32**	90.03	**1.16**	90.06	**1.16**
DH_02$_f$ (45%)	0.05	**-56.27**	100.66	**-10.51**	100.72	**-10.53**
DH_02$_r$ (45%)	0.05	**-39.76**	100.33	**-10.14**	100.38	**-10.15**
SDH_01$_f$ (45%)	0.04	**0.00**	80.60	**11.52**	80.64	**11.51**
SDH_01$_r$ (45%)	0.04	**-4.69**	79.56	**12.65**	79.60	**12.65**
SDH_02$_f$ (45%)	0.08	**-131.76**	84.71	**7.01**	84.79	**6.95**
SDH_02$_r$ (45%)	0.08	**-121.20**	83.92	**7.87**	83.99	**7.83**
SDH_03$_f$ (45%)	0.12	**-249.91**	114.06	**-25.22**	114.18	**-25.31**
SDH_03$_r$ (45%)	0.11	**-226.31**	113.10	**-24.16**	113.21	**-24.24**
RH_$_f$ (45%)	0.04	**-18.72**	80.97	**11.11**	81.01	**11.09**
RH_$_r$ (45%)	0.04	**-9.75**	80.01	**12.16**	80.05	**12.15**
LH_$_f$ (45%)	0.01	**61.15**	121.79	**-33.71**	121.81	**-33.67**
LH_$_r$ (45%)	0.01	**80.70**	116.72	**-28.14**	116.73	**-28.10**
CH_$_f$ (45%)	0.06	**70.42**	103.97	**-14.14**	104.03	**-14.16**
CH_$_r$ (45%)	0.05	**-33.02**	97.60	**-7.15**	97.65	**-7.16**
DH_01$_f$ (60%)	0.03	_	95.30	_	95.33	_
DH_01$_r$ (60%)	0.02	**9.89**	94.29	**1.06**	94.31	**1.07**
DH_02$_f$ (60%)	0.04	**-64.40**	107.07	**-12.35**	107.12	**-12.37**
DH_02$_r$ (60%)	0.04	**-43.69**	106.58	**-11.84**	106.62	**-11.85**
SDH_01$_f$ (60%)	0.03	**0.00**	85.86	**9.91**	85.89	**9.90**
SDH_01$_r$ (60%)	0.03	**1.55**	84.57	**11.26**	84.60	**11.26**
SDH_02$_f$ (60%)	0.07	**-160.14**	90.72	**4.81**	90.79	**4.76**
SDH_02$_r$ (60%)	0.07	**-147.44**	89.74	**5.84**	89.80	**5.80**
SDH_03$_f$ (60%)	0.10	**-276.89**	120.81	**-26.77**	120.91	**-26.83**
SDH_03$_r$ (60%)	0.09	**-249.06**	119.88	**-25.79**	119.97	**-25.85**
RH_$_f$ (60%)	0.03	**-24.47**	86.67	**9.06**	86.70	**9.05**

RH_r (60%)	0.03	**-13.51**	85.97	**9.79**	86.00	**9.78**
LH_f (60%)	0.01	**54.38**	129.48	**-35.86**	129.49	**-35.83**
LH_r (60%)	0.01	**80.83**	124.72	**-30.87**	124.72	**-30.83**
CH_f (60%)	0.06	**111.80**	108.02	**-13.34**	108.07	**-13.37**
CH_r (60%)	0.04	**-60.20**	101.61	**-6.62**	101.65	**-6.63**
DH_01f (75%)	0.03	_	99.36	_	99.38	_
DH_01r (75%)	0.02	**10.51**	98.38	**0.98**	98.41	**0.99**
DH_02f (75%)	0.04	**-37.70**	113.15	**-13.88**	113.19	**-13.89**
DH_02r (75%)	0.03	**-19.35**	112.15	**-12.87**	112.18	**-12.88**
SDH_01f (75%)	0.02	**20.04**	90.99	**8.42**	91.01	**8.43**
SDH_01r (75%)	0.02	**29.41**	90.06	**9.36**	90.08	**9.36**
SDH_02f (75%)	0.06	**-132.26**	96.36	**3.02**	96.42	**2.98**
SDH_02r (75%)	0.06	**-121.04**	95.47	**3.91**	95.53	**3.88**
SDH_03f (75%)	0.08	**-221.16**	127.17	**-27.99**	127.25	**-28.04**
SDH_03r (75%)	0.08	**-194.74**	126.27	**-27.09**	126.35	**-27.13**
RH_f (75%)	0.03	**-5.89**	92.15	**7.26**	92.17	**7.26**
RH_r (75%)	0.02	**5.84**	91.90	**7.51**	91.92	**7.51**
LH_f (75%)	0.01	**54.39**	136.78	**-37.66**	136.79	**-37.64**
LH_r (75%)	0.00	**81.89**	130.97	**-31.82**	130.98	**-31.79**
CH_f (75%)	0.05	**-106.47**	111.98	**-12.70**	112.03	**-12.72**
CH_r (75%)	0.04	**-52.26**	105.13	**-5.81**	105.17	**-5.83**

6.3.2 Thermal performance of mass timber construction

The worst energy performing morphology in the case of mass timber construction was chosen to simulate the indoor air temperature, in order to determine the impact of three window-to-wall ratio scenarios.

Figure 86 demonstrates the simulated indoor temperature during summer, with all three window-to-wall ratio scenarios, with the worst performing morphology, LH_f in the case of mass timber construction. Altogether with the outside dry-bulb temperature, are calculated using the Garoua weather data. It is noted, when the outdoor temperature fluctuates, the indoor air temperature of LH_f, stays linear throughout three WWR scenarios. LH_f in the 45% window-to-wall ratio scenario displays a closer performance to the comfort zone. Meanwhile in the other two scenarios of 60% and 75% window-to wall ratio, the morphology displays temperatures a little further away from the comfort zone. There is a tendency of the indoor temperatures to go lower from 11:00 AM to 16:00

PM, approaching the comfort values.

Table 20 summarizes the simulation results for the indoor air temperature, calculated in the climate context of Garoua on May 3. Hence obtaining the worst performance, LH_f with the living room exposed to north and south, it gains 13.16 °C when WWR is 45%, 13.77°C when WWR is 60% and 14.30°C when WWR is 75%.

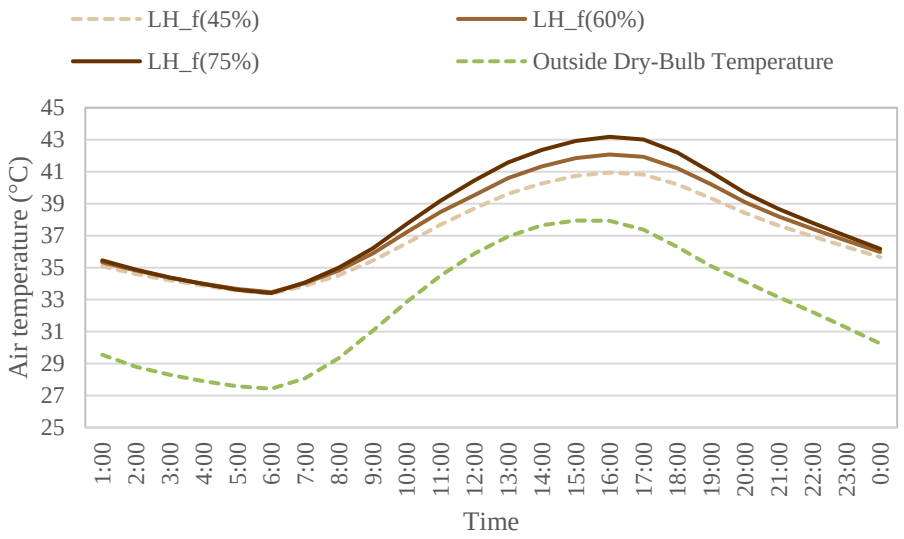

Figure 86. Simulated indoor air temperatures of living room for the worst energy performance morphology, together with the dry-bulb temperature for 3rd of May, Garoua climate, MTC system

Table 20. Simulation results for the air temperature calculated on the 3rd of May, Garoua climate, MTC system

T [°C]	45%			60%			75%		
	Min	Max	**OH_m**	Min	Max	**OH_m**	Min	Max	**OH_m**
LH_f	33.38	40.95	**13.16**	33.46	42.08	**13.77**	33.41	43.18	**14.30**

Figure 87 depicts the simulated indoor temperature during winter, with all three window-to-wall ratio scenarios, with the worst performing morphology, LH_f in the case of mass timber construction. Altogether with the outside dry-bulb temperature, are calculated using the Berlin weather data for January 4. It is noted that even during winter, when the outdoor temperature fluctuates, the indoor air temperature of LH_f, stays linear throughout three WWR scenarios. SDH_03f in all three window-to-wall ratio scenarios, stays a little further from the comfort temperatures. Thus, requiring for more heating loads during winter months and putting in doubt its effectiveness in this climate.

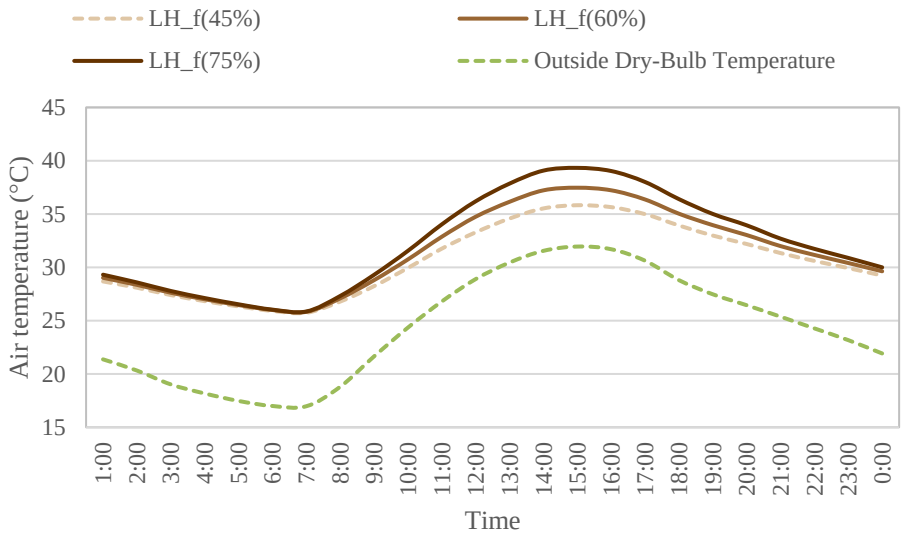

Figure 87. Simulated indoor air temperatures of living room for the worst energy performance morphology, together with the dry-bulb temperature for 4th of January, Garoua climate, MTC system

6.3.3 Energy performance of light-frame timber construction

As illustrated in *Figure 88* he comparison of annual energy consumption in terms of transparency in the case of light-frame timber construction, shows varying trend when the house gains more transparency from 45%, 60% to 75%, which correspond to the North and South oriented rooms. The most notable impact of transparency is visible in the semi-detached morphologies SDH_03f, SDH_03r and L-shape layouts LH_f, LH_r. In SDH_02f morphology, energy consumption is subject to an increase of 5.23 $kWh.m^{-2} a^{-1}$, when transparency is 60% and an increase of 5.64 $kWh.m^{-2} a^{-1}$, when WWR is 75%.

As for SDH_02$_r$ morphology, energy consumption is subject to an increase of 5.03 kWh.m^{-2} a^{-1}, when transparency is 60% and it increases to 5.36 kWh.m^{-2} a^{-1}1, when WWR is 75%. In LH_$_f$ model, energy demand is subject to in increment of 7.68 kWh.m^{-2} a^{-1}, when WWR is 60% and 14.98 kWh.m^{-2} a^{-1}, when WWR is 75%. As for its akin, LH_$_r$ model has an increase in energy demand by 7.93 kWh.m^{-2} a^{-1}, when WWR is 60% and 14.15 kWh.m^{-2} a^{-1}, when WWR is 75%. Meanwhile SDH_03$_f$ is subject to an increase of 5.91 kWh.m^{-2} a^{-1}, when WWR is 60% and 5.75 kWh.m^{-2} a^{-1}, when WWR is 75%.

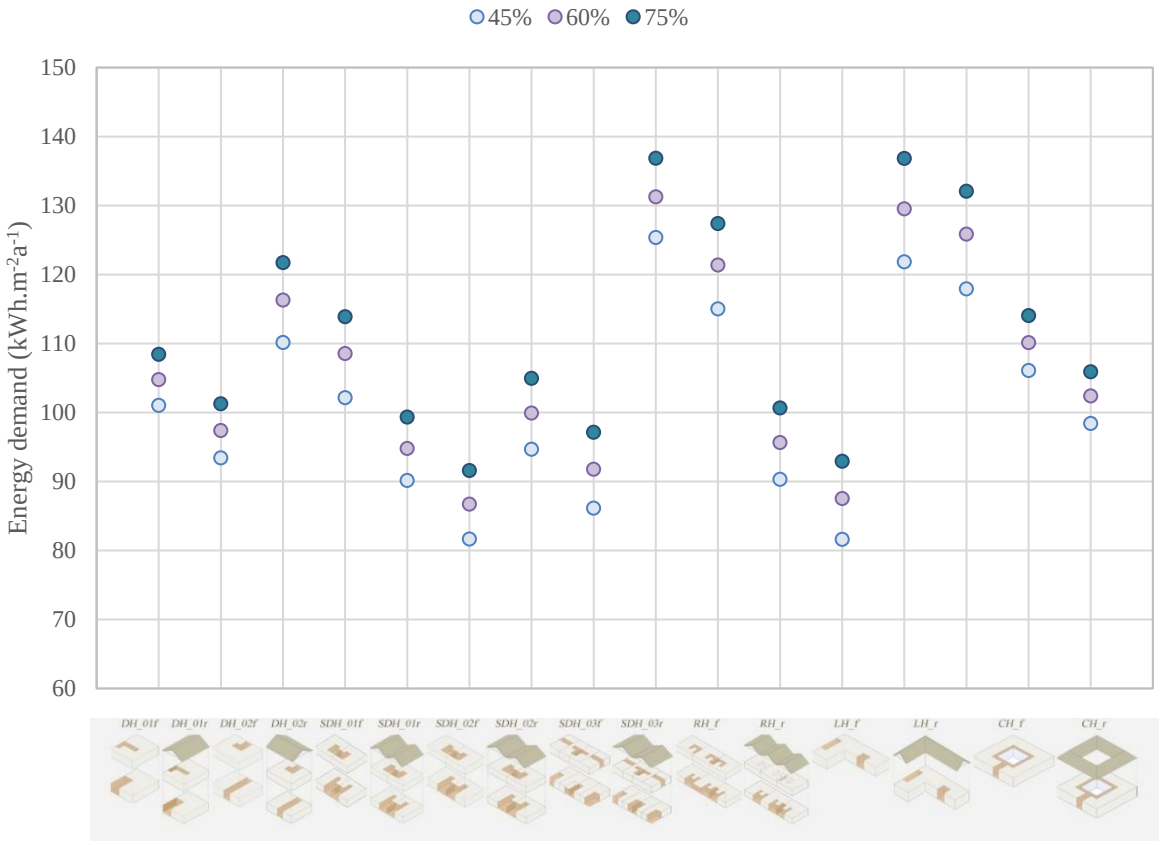

Figure 88. Comparison of simulated annual energy demand (kWh.m^{-2} a^{-1}), Garoua climate context, LFT construction system

Table 21 summarizes the obtained simulation results from Design Builder for all transparency scenarios in the climate of Garoua. A maximum of 19.23% of total energy consumption can be reduced, if the right morphology is selected for the studied climatic region. The typology with the worst performance in terms of heating and cooling loads

is SDH_03f. The semi-detached type, SDH_01r with its heating demand, increasing the morphology effectiveness to 46.52% and 17.16% in cooling demand, when transparency is 45%. The low demand for heating demand in LH_r, increases the morphology effectiveness by 89.97%, but its high demand for air-conditioning during summer months, reduces the morphology effectiveness by 16.71%. On the other hand, it is noted that the heating demand of SDH_02f and SDH_03f, reduces the morphology effectiveness with -63.33% and –160.70% respectively. Among the timber low-rise single housing it is depicted that the best performing model is SDH_01r and RH_r with 19.18% and 19.23% effectiveness respectively, followed by their akin types, RH_f with 10.62% and SDH_01f with 10.78%. Meanwhile the morphology with the poorest performance is SDH_03f with -24.07% effectiveness, followed by LH_f with -20.58% effectiveness.

Table 21. Simulation results obtained for all scenarios in the climate of Berlin, LFT construction system

	Annual heating demand		**Annual cooling demand**		**Annual energy demand**	
Scenarios	Heating/ conditioned area [kw.h^{-1}m^{-2}]	**Morphology effectiveness [%]**	Cooling/ conditioned area [kw.h^{-1}m^{-2}]	**Morphology effectiveness [%]**	Total energy/ conditioned Area [kw.h^{-1}m^{-2}]	**Total morphology effectiveness [%]**
DH_01f (45%)	0.07	_	100.94	_	101.02	_
DH_01r (45%)	0.04	**50.51**	93.37	**7.50**	93.41	**7.53**
DH_02f (45%)	0.09	**-25.21**	110.03	**-9.00**	110.12	**-9.01**
DH_02r (45%)	0.05	**34.81**	102.07	**-1.12**	102.12	**-1.09**
SDH_01f (45%)	0.07	**1.47**	90.06	**10.79**	90.13	**10.78**
SDH_01r (45%)	0.04	**46.52**	81.60	**19.16**	81.64	**19.18**
SDH_02f (45%)	0.12	**-63.33**	94.54	**6.35**	94.66	**6.30**
SDH_02r (45%)	0.08	**-11.02**	86.02	**14.78**	86.10	**14.76**
SDH_03f (45%)	0.19	**-160.70**	125.14	**-23.97**	125.33	**-24.07**
SDH_03r (45%)	0.12	**-57.59**	114.88	**-13.81**	115.00	**-13.84**
RH_f (45%)	0.08	**-6.14**	90.21	**10.63**	90.29	**10.62**
RH_r (45%)	0.04	**39.82**	81.55	**19.22**	81.59	**19.23**
LH_f (45%)	0.01	**81.69**	121.79	**-20.65**	121.81	**-20.58**
LH_r (45%)	0.01	**89.97**	117.89	**-16.79**	117.90	**-16.71**
CH_f (45%)	0.05	**33.58**	106.02	**-5.03**	106.07	**-5.00**
CH_r (45%)	0.05	**36.46**	98.34	**2.58**	98.39	**2.60**
DH_01f (60%)	0.06	_	104.68	_	104.75	_
DH_01r (60%)	0.03	**54.69**	97.34	**7.01**	97.37	**7.04**

DH_02$_f$ (60%)	0.08	**-20.99**	116.18	**-10.98**	116.26	**-10.99**
DH_02$_r$ (60%)	0.04	**39.63**	108.48	**-3.62**	108.52	**-3.60**
SDH_01$_f$ (60%)	0.06	**8.86**	94.70	**9.54**	94.76	**9.54**
SDH_01$_r$ (60%)	0.03	**53.81**	86.66	**17.22**	86.69	**17.24**
SDH_02$_f$ (60%)	0.10	**-63.01**	99.79	**4.68**	99.89	**4.64**
SDH_02$_r$ (60%)	0.07	**-10.69**	91.67	**12.43**	91.74	**12.42**
SDH_03$_f$ (60%)	0.17	**-162.72**	131.08	**-25.21**	131.24	**-25.29**
SDH_03$_r$ (60%)	0.10	**-53.19**	121.25	**-15.83**	121.35	**-15.85**
RH_$_f$ (60%)	0.06	**0.36**	95.56	**8.71**	95.62	**8.71**
RH_$_r$ (60%)	0.04	**42.96**	87.47	**16.45**	87.50	**16.46**
LH_$_f$ (60%)	0.01	**80.96**	129.48	**-23.68**	129.49	**-23.62**
LH_$_r$ (60%)	0.01	**91.09**	125.82	**-20.19**	125.83	**-20.13**
CH_$_f$ (60%)	0.05	**26.75**	110.04	**-5.12**	110.09	**-5.10**
CH_$_r$ (60%)	0.04	**32.29**	102.34	**2.24**	102.38	**2.26**
DH_01$_f$ (75%)	0.06	**_**	108.34	**_**	108.40	**_**
DH_01$_r$ (75%)	0.02	**58.93**	101.21	**6.58**	101.23	**6.61**
DH_02$_f$ (75%)	0.07	**-18.86**	121.63	**-12.26**	121.69	**-12.27**
DH_02$_r$ (75%)	0.03	**43.20**	113.84	**-5.07**	113.87	**-5.05**
SDH_01$_f$ (75%)	0.05	**17.05**	99.27	**8.37**	99.32	**8.37**
SDH_01$_r$ (75%)	0.02	**61.55**	91.54	**15.51**	91.56	**15.53**
SDH_02$_f$ (75%)	0.09	**-63.63**	104.83	**3.24**	104.92	**3.20**
SDH_02$_r$ (75%)	0.06	**-10.88**	97.05	**10.42**	97.11	**10.41**
SDH_03$_f$ (75%)	0.15	**-165.20**	136.67	**-26.15**	136.82	**-26.22**
SDH_03$_r$ (75%)	0.08	**-48.59**	127.28	**-17.48**	127.36	**-17.50**
RH_$_f$ (75%)	0.05	**5.90**	100.59	**7.15**	100.64	**7.15**
RH_$_r$ (75%)	0.03	**45.70**	92.89	**14.26**	92.92	**14.28**
LH_$_f$ (75%)	0.01	**78.57**	136.78	**-26.25**	136.79	**-26.19**
LH_$_r$ (75%)	0.01	**90.55**	132.04	**-21.88**	132.05	**-21.82**
CH_$_f$ (75%)	0.04	**19.38**	113.97	**-5.20**	114.02	**-5.19**
CH_$_r$ (75%)	0.04	**27.60**	105.83	**2.32**	105.87	**2.33**

6.3.4 Thermal performance of light-frame timber construction

The worst energy performing morphology in the case of light-frame timber construction was chosen to simulate the indoor air temperature, in order to determine the impact of three window-to-wall ratio scenarios.

Figure 89 demonstrates the simulated indoor temperature during summer, with all three window-to-wall ratio scenarios, with the worst performing morphology, SDH_03$_f$

in the case of mass timber construction. Altogether with the outside dry-bulb temperature, are calculated using the Garoua weather data. It is noted, when the outdoor temperature fluctuates, the indoor air temperature of SDH_03$_f$, stays linear throughout three WWR scenarios. SDH_03$_f$ in the 45% window-to-wall ratio scenario displays a closer performance to the comfort temperatures. The other two scenarios of 60% and 75% window-to wall ratio have similar performances. There is a tendency of the indoor temperatures to go lower after 10:00 AM to 20:00 PM, approaching the comfort values, even going down and staying within the comfort zone.

Table 22 summarizes the simulation results for the indoor air temperature, calculated in the climate context of Garoua on May 3. Hence obtaining the worst performance, SDH_03$_f$ with the living room exposed to north, it gains 8.66°C when WWR is 45%, 9.15°C when WWR is 60% and 9.65°C when WWR is 75%.

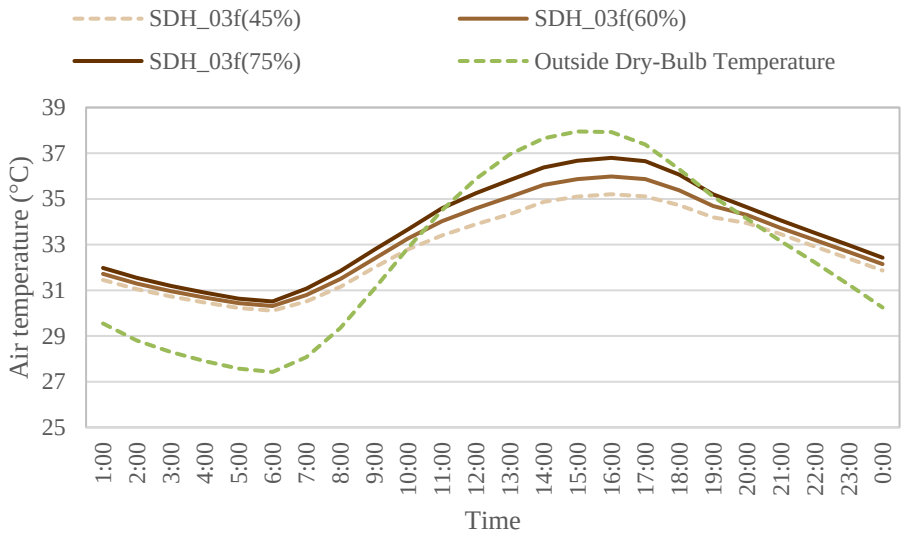

Figure 89. Simulated indoor air temperatures of living room for the worst energy performance morphology, together with the dry-bulb temperature for 3rd of May, Garoua climate, LFT construction system

Table 22. Simulation results for the air temperature calculated on the 3rd of May, Garoua climate, MTC system

T [°C]	45%			60%			75%		
	Min	Max	**OH_m**	Min	Max	**OH_m**	Min	Max	**OH_m**
SDH_03_f	30.11	35.20	**8.66**	30.31	35.98	**9.15**	30.51	36.80	**9.65**

Figure 90 depicts the simulated indoor temperature during winter, with all three window-to-wall ratio scenarios, with the worst performing morphology, SDH_03_f in the case of mass timber construction. Altogether with the outside dry-bulb temperature, are calculated using the Garoua weather data for January 4. It is noted that even during winter, when the outdoor temperature fluctuates, the indoor air temperature of SDH_03_f, stays linear throughout three WWR scenarios. SDH_03_f in all three window-to-wall ratio scenarios, stays a little far from the comfort temperatures, but above 11:00 AM to 18:00 PM stays within the comfort zone. Thus, requiring for few heating loads during winter months.

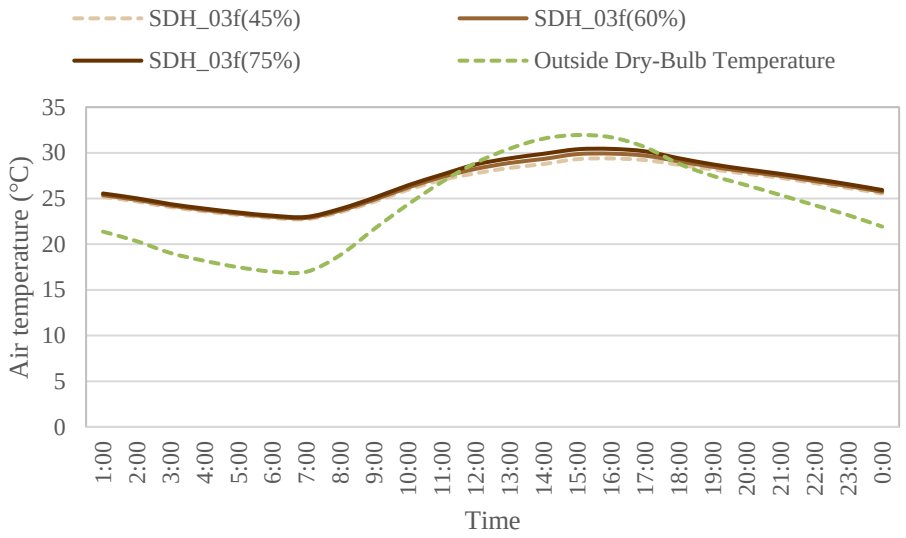

Figure 90. Simulated indoor air temperatures of living room for the worst energy performance morphology, together with the dry-bulb temperature for 4th of January, Garoua climate, LFT construction system

6.4 Climate comparison

Figure 91 illustrates the comparison of the simulated energy consumption (kWh.m^{-2} a^{-1}) for window-to-wall ratio 45% (North-South oriented façades), in three climate contexts, in the case of mass timber construction. Three climates are located in different contexts, thus their energy requirements are not the same. The tropical climate of Garoua displays the highest demand of energy, due to the influence of the local steppe climate. The temperate climate of Berlin displays less energy demand than Garoua, generally with a more average stand. Meanwhile, Athens has the best energy demand, due to its Mediterranean climate with hot-summer weather and slightly higher temperatures than Berlin.

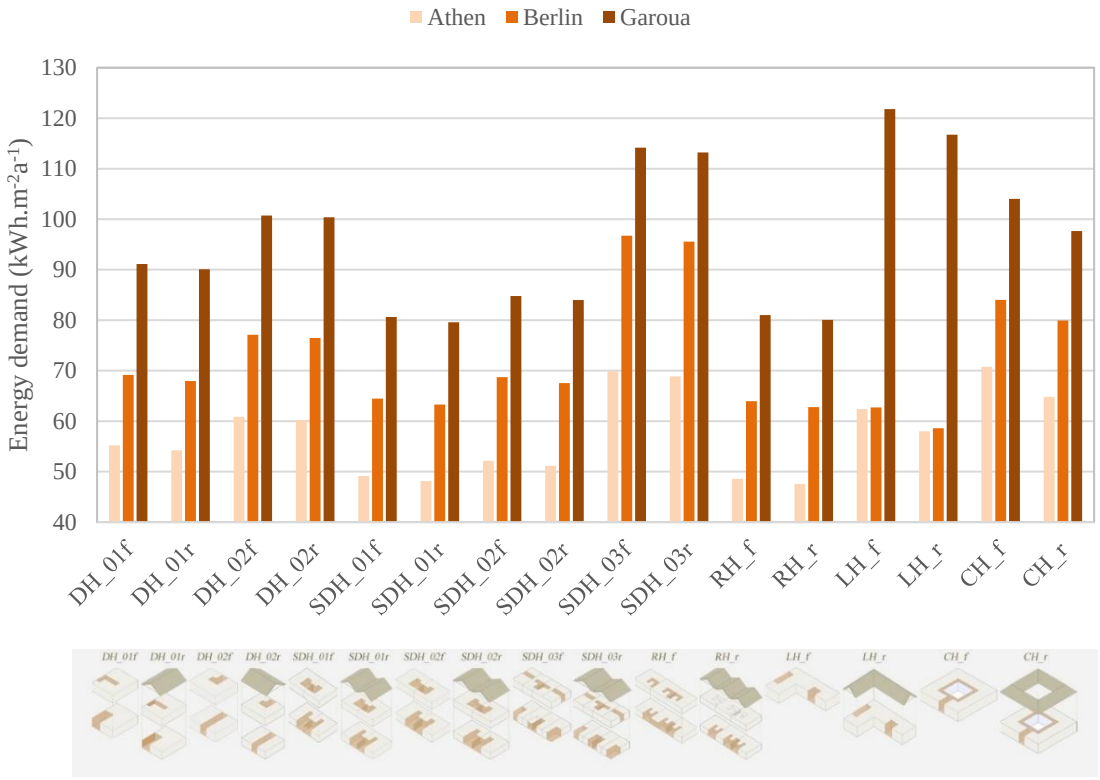

Figure 91. Annual simulated energy demand (kWh.m^{-2} a $^{-1}$) for all WWR=45% morphology scenario, in 3 climatic contexts, MTC system

According to the efficiency gradient of *Figure 92* settled based on the simulated results of all scenarios, in the case of mass timber construction, LH_$_f$, LH_$_r$ and SDH_03$_f$, SDH_03$_r$ morphologies are the least favorable for locations that exhibit similar climatic

condition to Garoua and Berlin, hence further needs of optimizing are required to deliver a better energetic performance. In all three climates it is noted that the most suitable morphologies are SDH_01$_r$, SDH_01$_f$ and RH_$_r$, RH_$_f$, ranking higher than others.

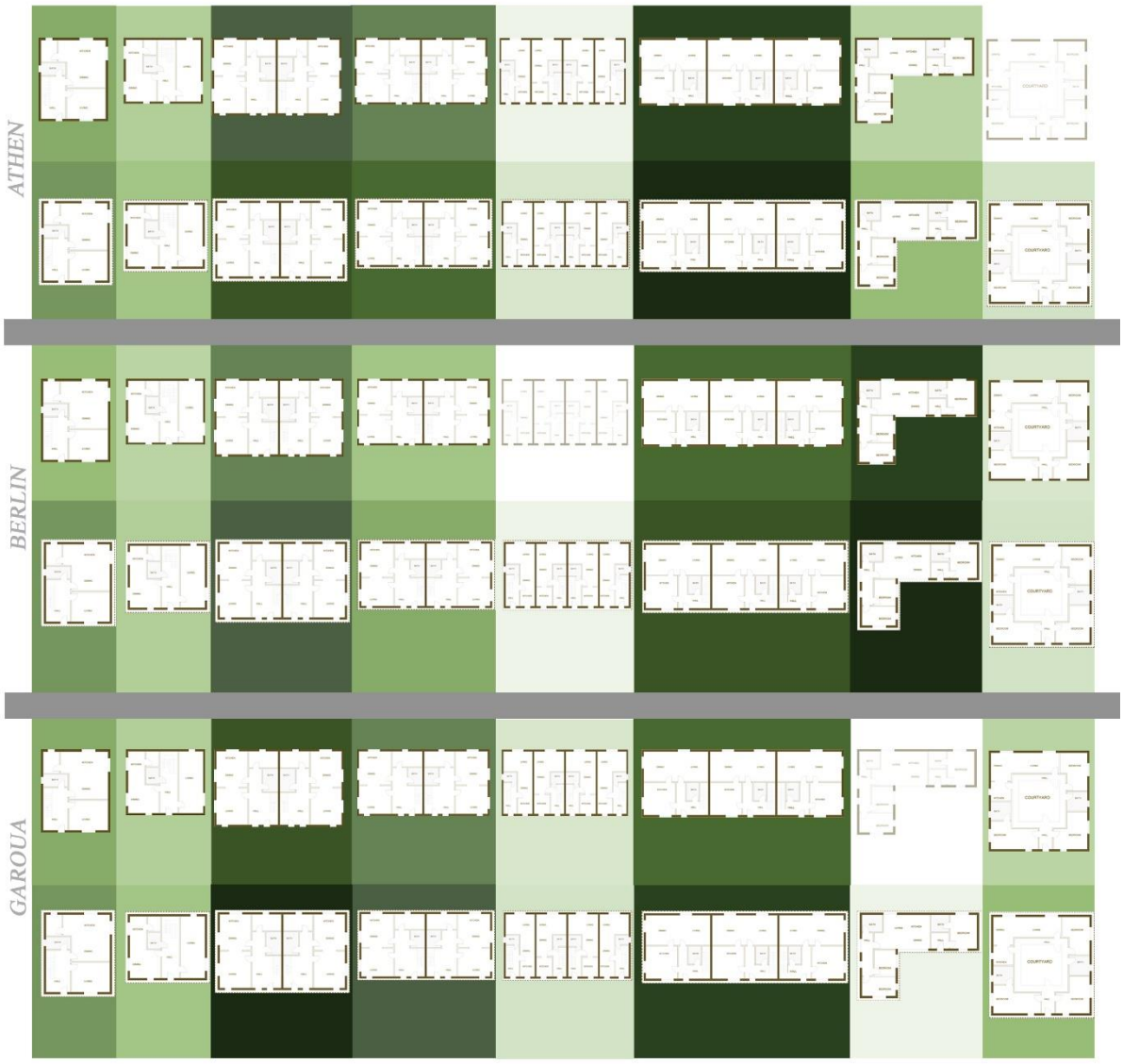

Figure 92. Suitability gradient of timber low-rise single housing morphologies in all climatic contexts, MTC system

Evaluation of results shows that a higher optimization of energy consumption for cooling, is required in hot climates like Garoua, then Athens, but also a higher optimization of energy consumption for heating is required in Berlin, so morphologies

can obtain a better performance. *Table 23* illustrates the morphology effectiveness of each scenario in all three studied climates in the case of mass timber construction. 13.84% is the highest value optimized that is reached in the climate of Athens, due to its best performance in energy demand for heating and cooling. Table 24 illustrates the overheating values of the worst performing morphologies in the climates of Athens and Garoua in the case of mass timber construction, since in Berlin the worst energy performing morphology manages to stay within the comfort temperature.

Table 23. Total morphology effectiveness (%) for three studied climates, MTC system

Scenario	Athens	Berlin	Garoua
DH_01$_f$ (45%)	__	__	__
DH_01$_r$ (45%)	1.78	1.71	1.16
DH_02$_f$ (45%)	-10.19	-11.55	-10.53
DH_02$_r$ (45%)	-9.13	-10.60	-10.15
SDH_01$_f$ (45%)	11.01	6.76	11.51
SDH_01$_r$ (45%)	12.78	8.46	12.65
SDH_02$_f$ (45%)	5.52	0.60	6.95
SDH_02$_r$ (45%)	7.33	2.30	7.83
SDH_03$_f$ (45%)	-26.57	-39.92	-25.31
SDH_03$_r$ (45%)	-24.71	-38.23	-24.24
RH_$_f$ (45%)	12.03	7.47	11.09
RH_$_r$ (45%)	13.84	9.19	12.15
LH_$_f$ (45%)	-13.01	9.27	-33.67
LH_$_r$ (45%)	-5.05	15.25	-28.10
CH_$_f$ (45%)	-28.20	-21.55	-14.16
CH_$_r$ (45%)	-17.37	-15.59	-7.16
DH_01$_f$ (60%)	_	_	_
DH_01$_r$ (60%)	1.43	1.73	1.07
DH_02$_f$ (60%)	-12.04	-12.49	-12.37
DH_02$_r$ (60%)	-11.23	-11.39	-11.85
SDH_01$_f$ (60%)	7.72	5.96	9.90
SDH_01$_r$ (60%)	9.35	7.90	11.26
SDH_02$_f$ (60%)	2.03	-0.66	4.76
SDH_02$_r$ (60%)	3.47	1.13	5.80
SDH_03$_f$ (60%)	-33.07	-39.56	-26.83
SDH_03$_r$ (60%)	-31.62	-37.80	-25.85

RH_f (60%)	8.13	6.32	9.05
RH_r (60%)	9.32	7.89	9.78
LH_f (60%)	-31.01	-29.21	-35.83
LH_r (60%)	-25.06	-22.77	-30.83
CH_f (60%)	-21.57	-21.41	-13.37
CH_r (60%)	-15.21	-15.26	-6.63
DH_01f (75%)	_	_	_
DH_01r (75%)	1.73	1.73	0.99
DH_02f (75%)	-13.17	-11.84	-13.89
DH_02r (75%)	-11.06	-10.33	-12.88
SDH_01f (75%)	8.39	6.45	8.43
SDH_01r (75%)	10.15	8.25	9.36
SDH_02f (75%)	1.77	-0.52	2.98
SDH_02r (75%)	3.61	1.32	3.88
SDH_03f (75%)	-26.62	-37.25	-28.04
SDH_03r (75%)	-24.74	-35.45	-27.13
RH_f (75%)	8.66	6.68	7.26
RH_r (75%)	9.42	7.84	7.51
LH_f (75%)	-35.64	-30.15	-37.64
LH_r (75%)	-25.23	-22.41	-31.79
CH_f (75%)	-25.51	-19.43	-12.72
CH_r (75%)	-14.19	-12.94	-5.83

Table 24. Timber low-rising single housing overheating in the 22 of July and 3 of May in the case of MTC system

T [°C]		45%			60%			75%		
		Min	Max	**OH_m**	Min	Max	**OH_m**	Min	Max	**OH_m**
Athen	**LH_f**	33.90	41.25	**13.57**	33.96	42.16	**14.06**	34.01	43.22	**14.62**
Garoua	**LH_f**	33.38	40.95	**13.16**	33.46	42.08	**13.77**	33.41	43.18	**14.30**

Figure 93 illustrates the comparison of the simulated energy consumption ($kWh.m^{-2}\ a^{-1}$) for window-to-wall ratio 45% (North-South oriented façades), in three

climate contexts, in the case of light-frame timber construction. Three climates are located in different contexts, thus their energy requirements are not the same. Compared to the mass timber construction, morphologies constructed with light-frame timber demand higher energy consumption. The tropical climate of Garoua displays the highest demand of energy, due to the influence of the local steppe climate. The temperate climate of Berlin displays less energy demand than Garoua, generally with a more average stand. Meanwhile, Athens has the best energy demand, due to its Mediterranean climate with hot-summer weather and slightly higher temperatures than Berlin.

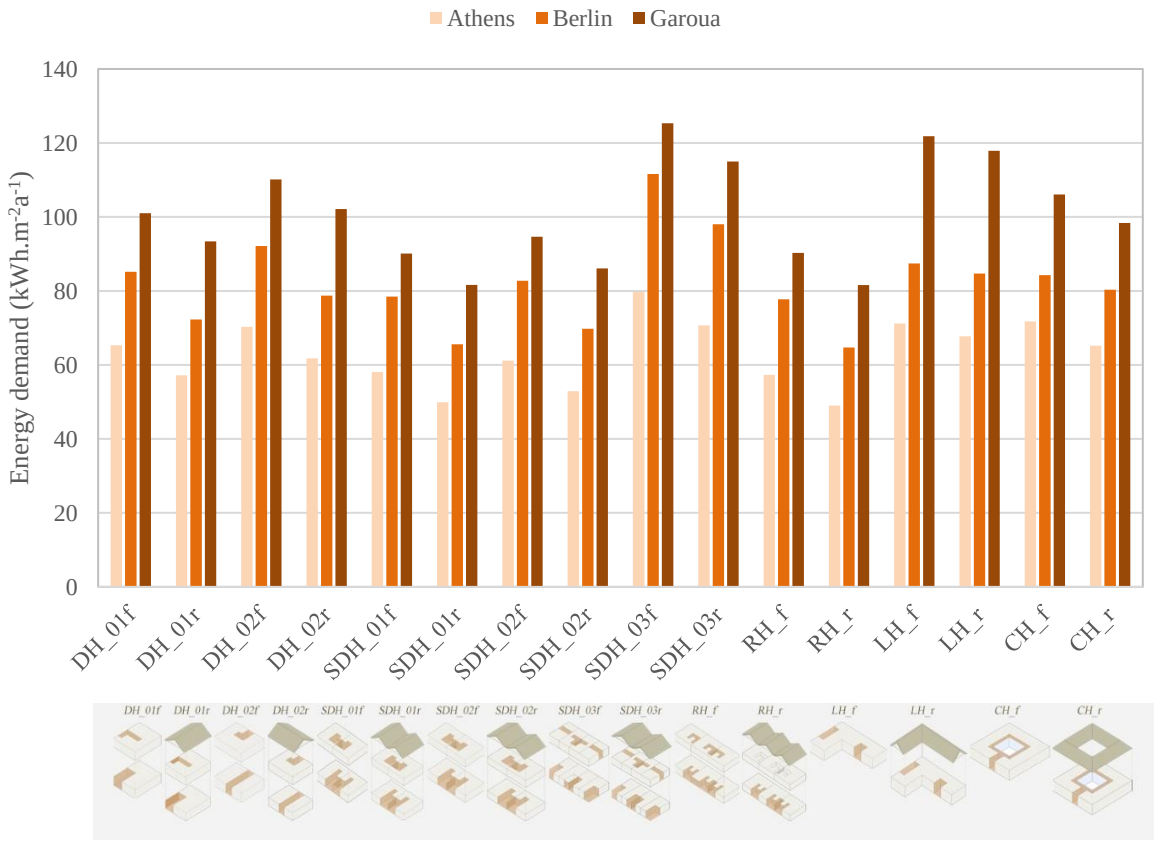

Figure 93. Annual simulated energy demand (kWh.m^{-2} a $^{-1}$) for all WWR=45% morphology scenario, in 3 climatic contexts, LFT construction system

According to the efficiency gradient of *Figure 94* settled based on the simulated results of all scenarios, in the case of mass timber construction, LH_$_f$, LH_$_r$ and SDH_03$_f$, SDH_03$_r$ even CH_$_f$, CH_$_r$ morphologies are the least favorable for locations that exhibit

similar climatic condition to Garoua and Berlin, hence further needs of optimizing are required to deliver a better energetic performance. In all three climates it is noted that the most suitable morphologies are SDH_01$_r$, SDH_01$_f$ and RH_$_r$, RH_$_f$, ranking higher than others.

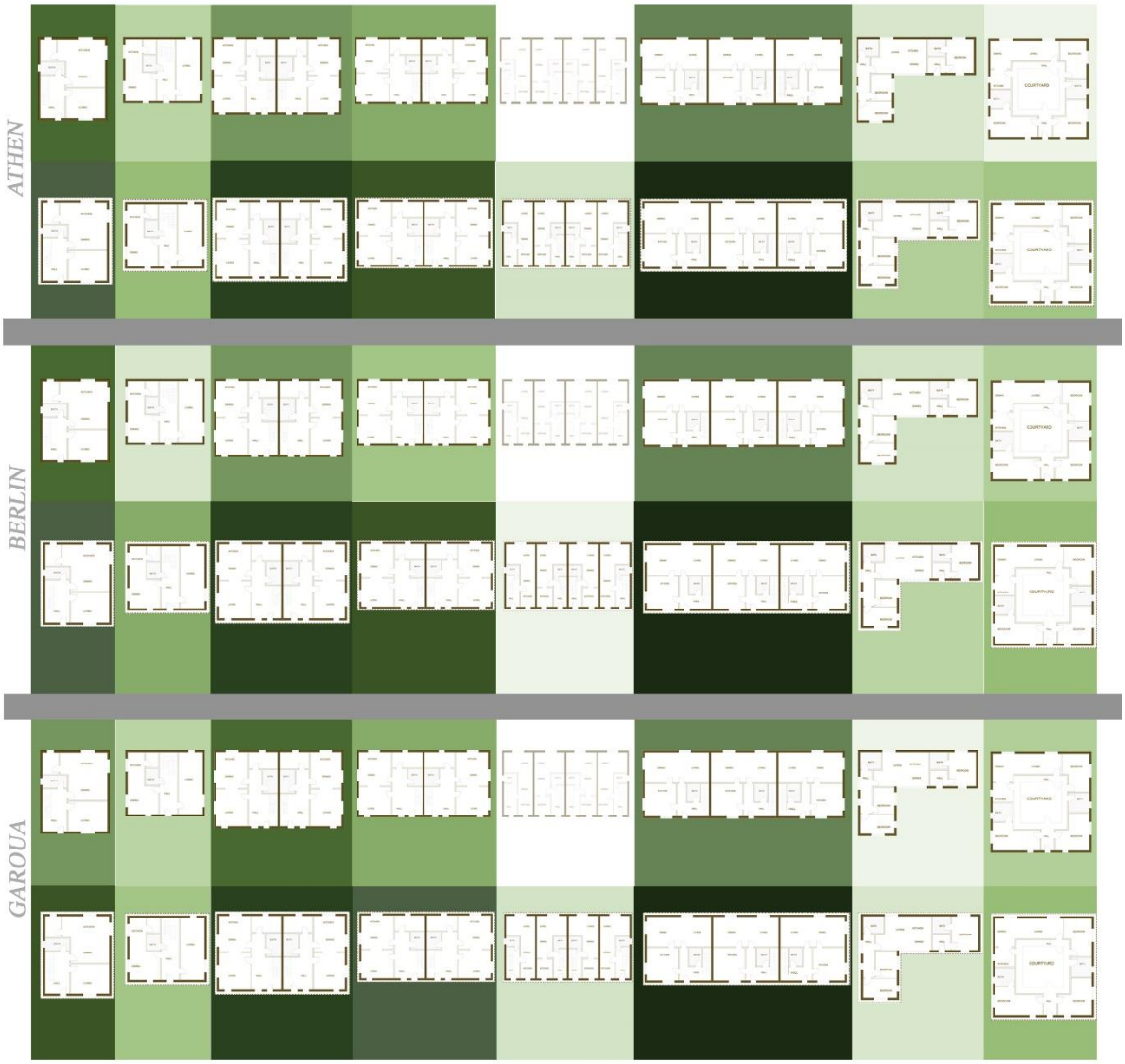

Figure 94. Suitability gradient of timber low-rise single housing morphologies in all climatic contexts, LFT construction system

Evaluation of results shows that a higher optimization of energy consumption for cooling, is required in hot climates like Garoua, then Athen, but also a higher optimization of energy consumption for heating is required in Berlin, so morphologies can obtain a

better performance. *Table 25* illustrates the morphology effectiveness of each scenario in all three studied climates. 24.95% is the highest value optimized that is reached in the climate of Athens, due to its best performance in energy demand for heating and cooling. *Table 26* illustrates the overheating values of the worst performing morphologies in the climates of Athens and Garoua in the case of mass timber construction, since in Berlin the worst energy performing morphology manages to stay within the comfort temperature.

Table 25. Total morphology effectiveness (%) for three studied climates, LFT construction system

Scenario	Athens	Berlin	Garoua
DH_01_f (45%)	_	_	_
DH_01_r (45%)	12.47	15.15	7.53
DH_02_f (45%)	-7.66	-8.15	-9.01
DH_02_r (45%)	5.42	7.61	-1.09
SDH_01_f (45%)	11.03	7.91	10.78
SDH_01_r (45%)	23.58	23.05	19.18
SDH_02_f (45%)	6.35	2.86	6.30
SDH_02_r (45%)	19.01	18.10	14.76
SDH_03_f (45%)	-22.11	-31.01	-24.07
SDH_03_r (45%)	-8.21	-15.07	-13.84
RH_{f} (45%)	12.21	8.74	10.62
RH_{r} (45%)	24.95	24.04	19.23
LH_{f} (45%)	-9.03	-2.64	-20.58
LH_{r} (45%)	-3.74	0.58	-16.71
CH_{f} (45%)	-9.91	1.08	-5.00
CH_{r} (45%)	0.19	5.73	2.60
DH_01_f (60%)	_	_	_
DH_01_r (60%)	11.83	14.71	7.04
DH_02_f (60%)	-9.09	-8.71	-10.99
DH_02_r (60%)	3.21	6.41	-3.60
SDH_01_f (60%)	9.84	7.39	9.54
SDH_01_r (60%)	21.64	22.01	17.24
SDH_02_f (60%)	4.63	1.99	4.64
SDH_02_r (60%)	16.54	16.70	12.42
SDH_03_f (60%)	-22.65	-30.95	-25.29

SDH_03$_r$ (60%)	-9.52	-15.54	-15.85
RH_$_f$ (60%)	10.31	7.86	8.71
RH_$_r$ (60%)	22.27	22.61	16.46
LH_$_f$ (60%)	-13.85	-6.08	-23.62
LH_$_r$ (60%)	-7.79	-2.10	-20.13
CH_$_f$ (60%)	-10.61	0.03	-5.10
CH_$_r$ (60%)	-0.44	4.91	2.26
DH_01$_f$ (75%)	_	_	_
DH_01$_r$ (75%)	11.21	7.04	6.61
DH_02$_f$ (75%)	-10.49	-10.99	-12.27
DH_02$_r$ (75%)	1.57	-3.60	-5.05
SDH_01$_f$ (75%)	8.59	9.54	8.37
SDH_01$_r$ (75%)	19.68	17.24	15.53
SDH_02$_f$ (75%)	2.90	4.64	3.20
SDH_02$_r$ (75%)	14.10	12.42	10.41
SDH_03$_f$ (75%)	-23.20	-25.29	-26.22
SDH_03$_r$ (75%)	-10.81	-15.85	-17.50
RH_$_f$ (75%)	8.38	8.71	7.15
RH_$_r$ (75%)	19.60	16.46	14.28
LH_$_f$ (75%)	-18.59	-23.62	-26.19
LH_$_r$ (75%)	-10.58	-20.13	-21.82
CH_$_f$ (75%)	-11.20	-5.10	-5.19
CH_$_r$ (75%)	-0.36	2.26	2.33

Table 26. Timber low-rising single housing overheating in the 22 of July and 3 of May in the case of LFT construction system

T [°C]		45%			60%			75%		
		Min	Max	**OH$_m$**	Min	Max	**OH$_m$**	Min	Max	**OH$_m$**
Athen	**SDH_03$_f$**	30.48	34.92	**8.70**	30.68	35.48	**9.08**	30.86	36.05	**9.46**
Garoua	**SDH_03$_f$**	30.11	35.20	**8.66**	30.31	35.98	**9.15**	30.51	36.80	**9.65**

6.5 Embodied carbon of timber morphologies

The estimated embodied carbon footprint of the morphologies is shown in *Figure 95*. It expresses the carbon of the operating house, the amount of the emissions, constructed of mass timber system. It is noticed that the morphology with the lowest carbon footprint is the L-shape morphology, LH_r. Whilst *Table 27* indicates embodied carbon footprint of the morphologies (KgCO2-e/m^2) and the equivalent CO_2 data in $kgCO_2$.

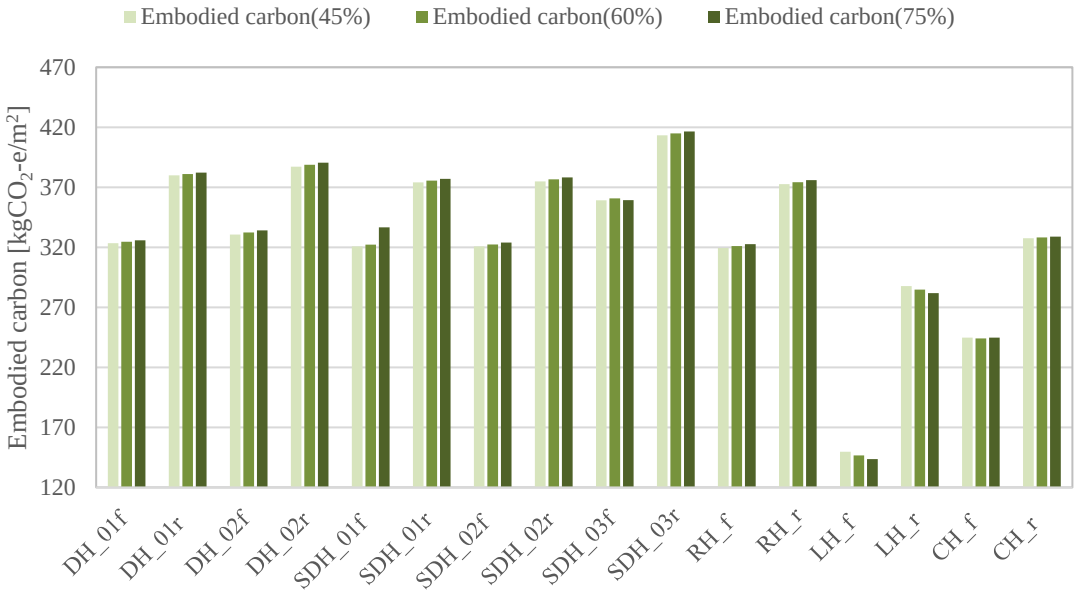

Figure 95. Embodied carbon footprint of morphologies (KgCO2-e/m^2), MTC system

Table 27. Embodied carbon footprint of the morphologies (KgCO2-e/m^2) and the equivalent CO_2 data in $kgCO_2$, MTC system

	WWR=45%		WWR=60%		WWR=75%	
	Embodied Carbon [$kgCO_2$-e/m^2]	**Equivalent CO_2 [kgCO2]**	**Embodied Carbon [$kgCO_2$]**	**Equivalent CO_2 [kgCO2]**	**Embodied Carbon [$kgCO_2$]**	**Equivalent CO_2 [kgCO2]**
DH_01_f	323	40435	325	40556	326	40677
DH_01_r	380	47565	381	47686	382	47807
DH_02_f	331	41316	332	41493	334	41670
DH_02_r	387	48446	389	48623	391	48800
SDH_01_f	321	80190	322	80494	337	80797

SDH_01_r	374	93638	376	93941	377	94245
SDH_02_f	321	80172	322	80505	324	80839
SDH_02_r	375	93842	377	94176	378	94509
SDH_03_f	359	89767	361	90098	359	89810
SDH_03_r	413	103437	415	103768	417	104099
$RH\_{\_f}$	319	119757	321	120242	323	120768
$RH\_{\_r}$	373	139887	374	140393	376	140898
$LH\_{\_f}$	150	20880	147	20200	144	19521
$LH\_{\_r}$	288	38565	285	37927	282	37289
$CH\_{\_f}$	245	401	244	48261	245	48369
$CH\_{\_r}$	328	342	328	65010	329	65117

The estimated embodied carbon footprint of the morphologies is shown in *Figure 96.* It expresses the carbon of the operating house, the amount of the emissions, constructed of light-frame timber system. It is noticed that the morphology with the lowest carbon footprint is the L-shape morphology, LH_r. Whilst *Table 28* indicates embodied carbon footprint of the morphologies (KgCO2-e/m^2) and the equivalent CO_2 data in $kgCO_2$.

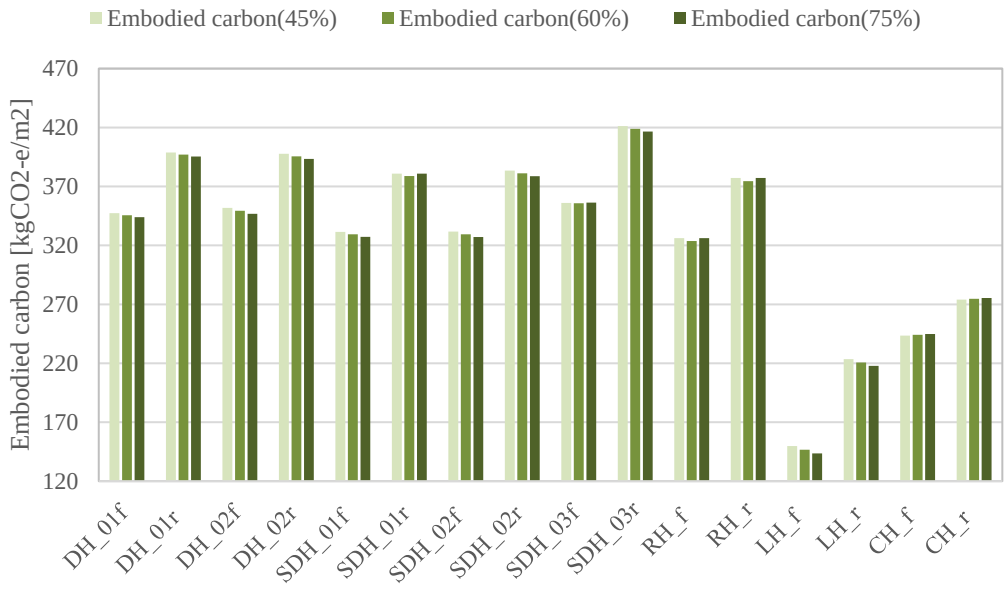

Figure 96. Embodied carbon footprint of morphologies (KgCO2-e/m^2), LFT construction system

Table 28. Embodied carbon footprint of the morphologies (KgCO2-e/m^2) and the equivalent CO_2 data in $kgCO_2$, LFT construction system

	WWR=45%		**WWR=60%**		**WWR=75%**	
	Embodied Carbon [$kgCO_2$-e/m^2]	**Equivalent CO_2 [kgCO2]**	**Embodied Carbon [$kgCO_2$]**	**Equivalent CO_2 [kgCO2]**	**Embodied Carbon [$kgCO_2$]**	**Equivalent CO_2 [kgCO2]**
DH_01_f	347	44068	346	43785	344	43501
DH_01_r	399	50688	397	50405	395	50121
DH_02_f	352	44588	349	44174	347	43760
DH_02_r	398	50461	396	50097	393	49732
SDH_01_f	331	79043	329	83063	327	82354
SDH_01_r	381	96468	379	95759	381	96468
SDH_02_f	332	83836	329	83056	327	82276
SDH_02_r	383	97131	381	96351	379	95571
SDH_03_f	356	89500	356	89291	356	89543
SDH_03_r	421	106584	419	86195	417	105038
RH_{f}	326	123472	324	122290	326	123472
RH_{r}	377	143158	375	141836	377	143158
LH_{f}	150	20880	147	20200	144	19521
LH_{r}	224	30671	221	30033	218	29395
CH_{f}	243	48154	244	48261	245	48369
CH_{r}	274	54663	275	54770	275	54877

CHAPTER 7

CONCLUSIONS

7.1 Conclusions

Architectural design of low-rise single housing, driven by energy performance and thermal performance simulations are not fully explored. In these conditions, this research paper brings forward a new comprehensive methodology that includes the building morphology, benefits of using timber in designing houses, presence of roof, courtyard and glazing properties for different transparency options. The methodology framework combines quantitative and analytical process to evaluate and optimize energy and thermal comfort performance of one and two story low-rise single housing in three different climatic conditions. Hence contributing to the awareness of architects and designers and assisting in decision-making process. The worthy novel contribution of this paper is proposing the optimal choices in timber low-rise single housing, by providing a set of scenarios and guidelines, together with benefits of using timber in early stages of design. The proposed body of work is an added contribution to the existing literature and provides to following conclusions:

- Garoua's Tropical savanna climate with steppe climate influence requires the highest energy demand, followed by Berlin ranked second with an average decrease 24.78 $kWh.m^{-2}$ a^{-1} in case of mass timber system The proposed timber low-rise single housing models appear to perform better in the hot-summer Mediterranean climate of Athens, thus being the most efficient in terms of energy consumption of 7.70 $kWh.m^{-2}$ less then Berlin.

- Even in the case of light frame timber construction Garoua requires the highest energy demand, followed by Berlin ranked in second place with an average decrease 16.87 $kWh.m^{-2}$ a^{-1}. The hypothetical timber low-rise single housing models display a better performance in the hot-summer Mediterranean climate of Athens, thus being the most efficient in terms of energy consumption of 15.71 $kWh.m^{-2}$ a^{-1} less than Berlin.

- As stated from the simulation results low-rise single housing with courtyard and square box detached houses are less suitable for climates similar to Athens, Berlin and Garoua.

However, further optimization of aspect ratios of the morphology is needed in order to obtain a better energetic performance. Semi-detached houses type two and one are ranked second in energy performance in the case of mass timber construction, due to the rectangular shape of the box model. Row houses display the best performance contributed to the longitudinal stretch of the house, no matter the transparency variables.

- Semi-detached houses type three, SDH_03_f, SDH_03_r display the worst energy performance due to dual occupancy within one module in both construction systems.

- The proper selection of the timber low-rise single housing, accounting to the climatic context, can obtain 13.84% of the total energy consumption in Athens, scenario WWR (45%). Followed by climate of Berlin with 15.25% and Garoua with 12.15% in case of mass timber construction. In the case of light-frame timber, models can obtain 24.95% in Athens, followed by Berlin with 24.04% and Garoua 19.23%.

- In terms of window-to-wall ratio scenarios, yearly simulated energy demands for the three climatic contexts exhibit an increasing trend when the houses gain higher transparency values (respectively from 45% to 60% to 75%). The highest shift in values happens in the l-shape house due to the compactness and footprint of the morphology. The best performing window-to-wall (WWR) scenario in all cases it appears to be 45%.

7.2 Recommendations for Future Work

The presented framework of this study calls attention to the promising use of timber in low-rise single housing, to achieve energy efficient houses and thermal comfort further highlighted by the building morphology and window- to wall ratio impact. The hypothetical proposed house models in the chosen three climates are developed bases on previous studies related to timber and low-rise single housing. The validity of this research paper is credited to the software's computation and simulation methods such as: Design Builder, Energy Plus, Meteonorm. The geometrical characteristics of the timber low-rise single housing are based on the construction details, occupancy schedule, HVAC for cooling and heating schedules, natural ventilation schedules, glazing properties (WWR) and energy loads are virtually generated through a total of 372 simulations. Moreover, this research paper sets forward important principles for future studies to be

aimed towards the field mentioned below:

- Farther investigation of timber in low-rise single housing in terms of shape related properties
- Observation of the proposed morphologies in other different climatic conditions
- Further exploration and evaluation of the internal layouts in the assessment of simulation results
- Including shading devise variables as inputs to generate simulation results
- Including roof variables as inputs to generate simulation results
- Optimizing the glazing properties of proposed morphologies
- Encouraging the usage of more sustainable materials such as timber and its elements from the early stages of design

Essentially, the original work of this paper emphasizes once again the benefits of timber in energy efficiency, but not only. Furthermore, it makes clear the appropriate use of a building morphology and how impactful the shape and glazing properties can be to optimize the energy efficiency of timber low-rise single housing, from the early phases of design. Finally, it can be of service to architects and designers, as a sustainable guideline for future implementations to achieve desired efficiency.

7.3 Limitation of the research

The presented research, regardless the noble contribution to the body of literature, there are a few limitations that call for further attention. The selected building morphology, low-rise single housing is proposed in three climatic contexts for comparison reasons through a set of simulation variables. Thus, there is a need for a further specification, if terms of location, geography and terrain, in the case of Athens.

In this study only two main types of timber construction systems are studied. It is essential to explore the possibility of other attainable options for timber construction systems, to see if there is any difference in terms of energy and thermal performance.

REFERENCES

Filipović, S., Lior, N., & Radovanović, M. (2022). The green deal – just transition and sustainable development goals Nexus. *Renewable and Sustainable Energy Reviews, 168*. https://doi.org/10.1016/j.rser.2022.112759

Haines, A., & Scheelbeek, P. (2020, April 25). European Green Deal: a major opportunity for health improvement. *The Lancet*. Lancet Publishing Group. https://doi.org/10.1016/S0140-6736(20)30109-4

Weitzel, M., Vandyck, T., Rey Los Santos, L., Tamba, M., Temursho, U., & Wojtowicz, K. (2023). A comprehensive socio-economic assessment of EU climate policy pathways. *Ecological Economics, 204*. https://doi.org/10.1016/j.ecolecon.2022.107660

Arbulu, M., Oregi, X., Etxepare, L., & Hernández-Minguillón, R. J. (2022). Barriers and challenges of the assessment framework of the Commission Recommendation (EU) 2019/786 on building renovation by European RTD projects. *Energy and Buildings, 269*. https://doi.org/10.1016/j.enbuild.2022.112267

Duan, Z., Huang, Q., Sun, Q., & Zhang, Q. (2022). Comparative life cycle assessment of a reinforced concrete residential building with equivalent cross laminated timber alternatives in China. *Journal of Building Engineering, 62*. https://doi.org/10.1016/j.jobe.2022.105357

Eurostat-European Union. (2020). *Energy, transport and environment statistics*. *Publications Office of the European Union* (p. 188). Publications Office of the European Union. Retrieved from https://ec.europa.eu/eurostat/documents/3217494/11478276/KS-DK-20-001-EN-N.pdf/06ddaf8d-1745-76b5-838e-013524781340?t=1605526083000

Jaysawal, R. K., Chakraborty, S., Elangovan, D., & Padmanaban, S. (2022, December 1). Concept of net zero energy buildings (NZEB) - A literature review. *Cleaner Engineering and Technology*. Elsevier Ltd. https://doi.org/10.1016/j.clet.2022.100582

Frank, E. W., Dahy, H., & Vibæk, K. S. (2022). Challenges in creating a sustainable building certificate for single-family housing in Denmark through an Actor-Network Theory (ANT) lens. *Current Research in Environmental Sustainability*, *4*. https://doi.org/10.1016/j.crsust.2022.100144

Maria, J. R. G., Renata, K., (2021). A New European Bauhaus for a Culture of Transversality and Sustainability. *European Union New European Bauhaus* https://europa.eu/new-european-bauhaus/index_en

Huo, T., Xu, L., Liu, B., Cai, W., & Feng, W. (2022). China's commercial building carbon emissions toward 2060: An integrated dynamic emission assessment model. *Applied Energy*, *325*. https://doi.org/10.1016/j.apenergy.2022.119828

Vita, G., Lundström, J. R., Hertwich, E. G., Quist, J., Ivanova, D., Stadler, K., & Wood, R. (2019). The Environmental Impact of Green Consumption and Sufficiency Lifestyles Scenarios in Europe: Connecting Local Sustainability Visions to Global Consequences. *Ecological Economics*, *164*. https://doi.org/10.1016/j.ecolecon.2019.05.002

Asdrubali, F., & Grazieschi, G. (2020). Life cycle assessment of energy efficient buildings. *Energy Reports*, *6*, 270–285. https://doi.org/10.1016/j.egyr.2020.11.144

Ding, G. K. C. (2020). Lifecycle Assessment of Building Materials – A Cradle-to-Gate Approach. In *Encyclopedia of Renewable and Sustainable Materials* (pp. 476–488). Elsevier. https://doi.org/10.1016/b978-0-12-803581-8.10542-9

Bukauskas, A., Mayencourt, P., Shepherd, P., Sharma, B., Mueller, C., Walker, P., & Bregulla, J. (2019, July 20). Whole timber construction: A state of the art review. *Construction and Building Materials*. Elsevier Ltd. https://doi.org/10.1016/j.conbuildmat.2019.03.043

Duan, Z., Huang, Q., & Zhang, Q. (2022, August 1). Life cycle assessment of mass timber construction: A review. *Building and Environment*. Elsevier Ltd. https://doi.org/10.1016/j.buildenv.2022.109320

Fabrizio, M., Thorsten, S. (2022). Hybrid timber-based systems for low-carbon, deep renovation of aged buildings: Three exemplary buildings in the Republic of Korea. *Building and Environment*. Elsevier Ltd. https://doi.org/10.1016/j.buildenv.2022.108889

Andersen, J. H., Rasmussen, N. L., & Ryberg, M. W. (2022). Comparative life cycle assessment of cross laminated timber building and concrete building with special focus on biogenic carbon. *Energy and Buildings*, *254*. https://doi.org/10.1016/j.enbuild.2021.111604

Jia Wen, T., Chin Siong, H., & Noor, Z. Z. (2015). Assessment of embodied energy and global warming potential of building construction using life cycle analysis approach: Case studies of residential buildings in Iskandar Malaysia. *Energy and Buildings*, *93*, 295–302. https://doi.org/10.1016/j.enbuild.2014.12.002

Mehdi, R., Daniel, D., Georgios, K. (2019). A method of uncertainty analysis for whole-life embodied carbon emissions (CO2-e) of building materials of a net-zero energy building in Australia. *Journal of Cleaner Production.* Elsevier Ltd. https://doi.org/10.1016/j.jclepro.2019.03.339

Pomponi, F., & Moncaster, A. (2016, October 1). Embodied carbon mitigation and reduction in the built environment – What does the evidence say? *Journal of Environmental Management*. Academic Press. https://doi.org/10.1016/j.jenvman.2016.08.036.

Cabeza, L. F., Barreneche, C., Miró, L., Morera, J. M., Bartolí, E., & Inés Fernández, A. (2013). Low carbon and low embodied energy materials in buildings: A review. *Renewable and Sustainable Energy Reviews*. https://doi.org/10.1016/j.rser.2013.03.017

Rasmussen, F. N., Birkved, M., & Birgisdóttir, H. (2020). Low- carbon design strategies for new residential buildings–lessons from architectural practice. *Architectural Engineering and Design Management*, *16*(5), 374–390. https://doi.org/10.1080/17452007.2020.1747385

Mackay, A. (2008). Climate Change 2007: Impacts, Adaptation and Vulnerability. Contribution of Working Group II to the Fourth Assessment Report of the Intergovernmental Panel on Climate Change. *Journal of Environmental Quality*, *37*(6), 2407–2407. https://doi.org/10.2134/jeq2008.0015br

European Parlıament. (2021). European Parliament resolution of 15 January 2020 on the European Green Deal (2019/2956(RSP)). *Official Journal of the European Union*, *C 270*(7.7.), 2–20.

Minunno, R., O'Grady, T., Morrison, G. M., & Gruner, R. L. (2021, June 1). Investigating the embodied energy and carbon of buildings: A systematic literature review and meta-analysis of life cycle assessments. *Renewable and Sustainable Energy Reviews*. Elsevier Ltd. https://doi.org/10.1016/j.rser.2021.110935

Lukić, I., Premrov, M., Passer, A., & Žegarac Leskovar, V. (2021). Embodied energy and GHG emissions of residential multi-storey timber buildings by height – A case with structural connectors and mechanical fasteners. *Energy and Buildings*, *252*.

https://doi.org/10.1016/j.enbuild.2021.111387

Takano, A., Pal, S. K., Kuittinen, M., Alanne, K., Hughes, M., & Winter, S. (2015). The effect of material selection on life cycle energy balance: A case study on a hypothetical building model in Finland. *Building and Environment*, *89*, 192–202. https://doi.org/10.1016/j.buildenv.2015.03.001

Hawkins, W., Cooper, S., Allen, S., Roynon, J., & Ibell, T. (2021). Embodied carbon assessment using a dynamic climate model: Case-study comparison of a concrete, steel and timber building structure. *Structures*, *33*, 90–98. https://doi.org/10.1016/j.istruc.2020.12.013

D'Amico, B., Pomponi, F., & Hart, J. (2021). Global potential for material substitution in building construction: The case of cross laminated timber. *Journal of Cleaner Production*, *279*. https://doi.org/10.1016/j.jclepro.2020.123487

Crawford, R. H., & Cadorel, X. (2017). A Framework for Assessing the Environmental Benefits of Mass Timber Construction. In *Procedia Engineering* (Vol. 196, pp. 838–846). Elsevier Ltd. https://doi.org/10.1016/j.proeng.2017.08.015

British Standards Institution. (2011). *Sustainability of construction works - Assessment of environmental performance of buildings - Calculation method*. *British Standards Institution* (p. 60).

Wijnants, L., Allacker, K., & De Troyer, F. (2019). Life-cycle assessment of timber frame constructions – The case of rooftop extensions. *Journal of Cleaner Production*, *216*, 333–345. https://doi.org/10.1016/j.jclepro.2018.12.278

Achenbach, H., Wenker, J. L., & Rüter, S. (2018). Life cycle assessment of product- and construction stage of prefabricated timber houses: a sector representative approach for Germany according to EN 15804, EN 15978 and EN 16485. *European Journal of Wood and Wood Products*, *76*(2), 711–729. https://doi.org/10.1007/s00107-017-1236-1

Hollberg, A., Genova, G., & Habert, G. (2020). Evaluation of BIM-based LCA results for building design. *Automation in Construction*, *109*. https://doi.org/10.1016/j.autcon.2019.102972

Hollberg, A., Lützkendorf, T., & Habert, G. (2019). Top-down or bottom-up? – How environmental benchmarks can support the design process. *Building and Environment*, *153*, 148–157. https://doi.org/10.1016/j.buildenv.2019.02.026

Basbagill, J., Flager, F., Lepech, M., & Fischer, M. (2013). Application of life-cycle assessment to early stage building design for reduced embodied environmental impacts. *Building and Environment*, *60*, 81–92. https://doi.org/10.1016/j.buildenv.2012.11.009

Soust-Verdaguer, B., Llatas, C., & Moya, L. (2020). Comparative BIM-based Life Cycle Assessment of Uruguayan timber and concrete-masonry single-family houses in design stage. *Journal of Cleaner Production*, *277*. https://doi.org/10.1016/j.jclepro.2020.121958

Pajchrowski, G., Noskowiak, A., Lewandowska, A., & Strykowski, W. (2014). Wood as a building material in the light of environmental assessment of full life cycle of four buildings. *Construction and Building Materials*, *52*, 428–436. https://doi.org/10.1016/j.conbuildmat.2013.11.066

Foraboschi, P., Mercanzin, M., & Trabucco, D. (2014). Sustainable structural design of tall buildings based on embodied energy. *Energy and Buildings*, *68*(PARTA), 254–269. https://doi.org/10.1016/j.enbuild.2013.09.003

Treloar, G. J., Fay, R., Ilozor, B., & Love, P. E. D. (2001). An analysis of the embodied energy of office buildings by height. *Facilities*, *19*, 204–214. https://doi.org/10.1108/02632770110387797

Lotteau, M., Loubet, P., & Sonnemann, G. (2017). An analysis to understand how the shape of a concrete residential building influences its embodied energy and embodied carbon. *Energy and Buildings*, *154*, 1–11. https://doi.org/10.1016/j.enbuild.2017.08.048

Serrano, A. Á. R., & Álvarez, S. P. (2016). Life cycle assessment in building: A case study on the energy and emissions impact related to the choice of housing typologies and construction process in Spain. *Sustainability (Switzerland)*, *8*(3). https://doi.org/10.3390/su8030287

Cuéllar-Franca, R. M., Azapagic, A. (2012). Environmental impacts of the UK residential sector: Life cycle assessment of houses. *Building and Environment, Volume 54, Pages 86-99, ISSN 0360-1323.* https://doi.org/10.1016/j.buildenv.2012.02.005

Takano, A., Pal, S. K., Kuittinen, M., & Alanne, K. (2015). Life cycle energy balance of residential buildings: A case study on hypothetical building models in Finland. *Energy and Buildings*, *105*, 154–164. https://doi.org/10.1016/j.enbuild.2015.07.060

Leskovar, V. Ž., Žigart, M., Premrov, M., & Lukman, R. K. (2019). Comparative assessment of shape related cross-laminated timber building typologies focusing on environmental performance. *Journal of Cleaner Production*, *216*, 482–494. https://doi.org/10.1016/j.jclepro.2018.12.140

Younis, A., & Dodoo, A. (2022, July 15). Cross-laminated timber for building construction: A life-cycle-assessment overview. *Journal of Building Engineering*. Elsevier Ltd. https://doi.org/10.1016/j.jobe.2022.104482

Žigart, M., Kovačič Lukman, R., Premrov, M., & Žegarac Leskovar, V. (2018). Environmental

impact assessment of building envelope components for low-rise buildings. *Energy*, *163*, 501–512. https://doi.org/10.1016/j.energy.2018.08.149

Zubizarreta, M., Cuadrado, J., Orbe, A., & García, H. (2019). Modeling the environmental sustainability of timber structures: A case study. *Environmental Impact Assessment Review*, *78*. https://doi.org/10.1016/j.eiar.2019.106286

Markström, E., Kitek Kuzman, M., Bystedt A., Sandberg, D., Fredriksson, M. (2018). Swedish architects view of engineered wood products in buildings. *Journal of Cleaner Production. 181, 33-41.*https://doi.org/10.1016/j.jclepro.2018.01.216

Ismailos, C., & Touchie, M. F. (2017). Achieving a low carbon housing stock: An analysis of low-rise residential carbon reduction measures for new construction in Ontario. *Building and Environment*, *126*, 176–183. https://doi.org/10.1016/j.buildenv.2017.09.034

Adekunle, T. O., & Nikolopoulou, M. (2016). Thermal comfort, summertime temperatures and overheating in prefabricated timber housing. *Building and Environment*, *103*, 21–35. https://doi.org/10.1016/j.buildenv.2016.04.001

Milwicz, R., & Nowotarski, P. (2015). Influence of Multiphase Flexible Timber Frame House Construction on Housing Affordability. In *Procedia Engineering* (Vol. 122, pp. 158–165). Elsevier Ltd. https://doi.org/10.1016/j.proeng.2015.10.020

Setter, L., Smoorenburg, E., Wijesuriya, S., & Tabares-Velasco, P. C. (2019). Energy and hygrothermal performance of cross laminated timber single-family homes subjected to constant and variable electric rates. *Journal of Building Engineering*, *25*. https://doi.org/10.1016/j.jobe.2019.100784

Nunes, G., de Melo Moura, J. D., Güths, S., Atem, C., & Giglio, T. (2020). Thermo-energetic performance of wooden dwellings: Benefits of cross-laminated timber in Brazilian climates. *Journal of Building Engineering*, *32*. https://doi.org/10.1016/j.jobe.2020.101468

Premrov, M., Žegarac Leskovar, V., & Mihalič, K. (2016). Influence of the building shape on the energy performance of timber-glass buildings in different climatic conditions. *Energy*, *108*, 201–211. https://doi.org/10.1016/j.energy.2015.05.027

Depecker, P., Menezo, C., Virgone, J., & Lepers, S. (2001). Design of buildings shape and energetic consumption. *Building and Environment*, *36*(5), 627–635. https://doi.org/10.1016/S0360-1323(00)00044-5

Persson, M.-L. (2006). Windows of Opportunities: The Glazed Area and its Impact on the Energy Balance of Buildings. *Australian Clinical Review / Australian Medical Association [and] the Australian Council on Hospital Standards*. Retrieved from

http://swepub.kb.se/bib/swepub:oai:DiVA.org:uu-6881?tab2=abs&language=en

Ratti, C., Baker, N., & Steemers, K. (2005). Energy consumption and urban texture. *Energy and Buildings*, *37*(7), 762–776. https://doi.org/10.1016/j.enbuild.2004.10.010

Danielski, I, Froling, M, Joelsson, A. (2012) The impact of the shape factor on final energy demand in residential buildings in nordic climates. *Conference world renewable energy forum, WREF 2012, including world renewable energy congress XII and Colorado renewable energy society (CRES) annual conference, vol. 6; 2012.*

Leskovar, V. Ž., & Premrov, M. (2011). An approach in architectural design of energy-efficient timber buildings with a focus on the optimal glazing size in the south-oriented façade. *Energy and Buildings*, *43*(12), 3410–3418. https://doi.org/10.1016/j.enbuild.2011.09.003

Mingfang, T. (2002). Solar control for buildings. *Building and Environment*, *37*(7), 659–664. https://doi.org/10.1016/S0360-1323(01)00063-4

Bouden, C. (2007). Influence of glass curtain walls on the building thermal energy consumption under Tunisian climatic conditions: The case of administrative buildings. *Renewable Energy*, *32*(1), 141–156. https://doi.org/10.1016/j.renene.2006.01.007

Hassouneh, K., Alshboul, A., & Al-Salaymeh, A. (2010). Influence of windows on the energy balance of apartment buildings in Amman. *Energy Conversion and Management*, *51*(8), 1583–1591. https://doi.org/10.1016/j.enconman.2009.08.037

AlAnzi, A., Seo, D., & Krarti, M. (2009). Impact of building shape on thermal performance of office buildings in Kuwait. *Energy Conversion and Management*, *50*(3), 822–828. https://doi.org/10.1016/j.enconman.2008.09.033

Jaber, S., & Ajib, S. (2011). Optimum, technical and energy efficiency design of residential building in Mediterranean region. *Energy and Buildings*, *43*(8), 1829–1834. https://doi.org/10.1016/j.enbuild.2011.03.024

Premrov, M., Žigart, M., & Žegarac Leskovar, V. (2018). Influence of the building shape on the energy performance of timber-glass buildings located in warm climatic regions. *Energy*, *149*, 496–504. https://doi.org/10.1016/j.energy.2018.02.074

Maučec, D., Premrov, M., & Leskovar, V. Ž. (2021). Use of sensitivity analysis for a determination of dominant design parameters affecting energy efficiency of timber buildings in different climates. *Energy for Sustainable Development*, *63*, 86–102. https://doi.org/10.1016/j.esd.2021.06.003

Lešnik, M., Kravanja, S., Premrov, M., & Žegarac Leskovar, V. (2020). Optimal design of timber-glass upgrade modules for vertical building extension from the viewpoints of energy efficiency and visual comfort. *Applied Energy*, *270*. https://doi.org/10.1016/j.apenergy.2020.115173

Dickson, M., Parker, D. (2014) Sustainable timber design. *Oxford: Taylor & Francis*

https://doi.org/10.4324/9781315774114

Ramage, M. H., Burridge, H., Busse-Wicher, M., Fereday, G., Reynolds, T., Shah, D. U., … Scherman, O. (2017, February 1). The wood from the trees: The use of timber in construction. *Renewable and Sustainable Energy Reviews*. Elsevier Ltd. https://doi.org/10.1016/j.rser.2016.09.107

Bukauskas, A., Mayencourt, P., Shepherd, P., Sharma, B., Mueller, C., Walker, P., & Bregulla, J. (2019, July 20). Whole timber construction: A state of the art review. *Construction and Building Materials*. Elsevier Ltd. https://doi.org/10.1016/j.conbuildmat.2019.03.043

Ayanleye, S., Udele, K., Nasir, V., Zhang, X., & Militz, H. (2022, April 1). Durability and protection of mass timber structures: A review. *Journal of Building Engineering*. Elsevier Ltd. https://doi.org/10.1016/j.jobe.2021.103731

Wang, Z., Gong, M., & Chui, Y. H. (2015). Mechanical properties of laminated strand lumber and hybrid cross-laminated timber. *Construction and Building Materials*, *101*, 622–627. https://doi.org/10.1016/j.conbuildmat.2015.10.035

BSI. BS EN 14081-1:2005+A1:2011 Timber Structures – Strength Graded Structural Timber With Rectangular Cross Section. 2005.

BSI. BS EN 338: (2009). Structural Timber. Strength Classes.

Pratt, G, H. (2010) The timber drying manual. *BRE*.

Gerasimov, Y., Seliverstov, A., & Syunev, V. (2012). Industrial round-wood damage and operational efficiency losses associated with the maintenance of a single-grip harvester head model: A case study in Russia. *Forests*, *3*(4), 864–880. https://doi.org/10.3390/f3040864

Hill, C. A. S. (2006). *Wood Modification: Chemical, Thermal and Other Processes*. *Wood Modification: Chemical, Thermal and Other Processes* (pp. 1–239). John Wiley and Sons. https://doi.org/10.1002/0470021748

Rowell, R. M. (2006). Chemical modification of wood: A short review. *Wood Material Science and Engineering*, *1*(1), 29–33. https://doi.org/10.1080/17480270600670923

Caniato, M., Marzi, A., Monteiro da Silva, S., & Gasparella, A. (2021, November 1). A review of the thermal and acoustic properties of materials for timber building construction. *Journal of Building Engineering*. Elsevier Ltd. https://doi.org/10.1016/j.jobe.2021.103066

Li, Y., Lattimer, B. Y., & Case, S. W. (2021). Measurement and modelling of thermal and physical properties of wood construction materials. *Construction and Building Materials*, *284*. https://doi.org/10.1016/j.conbuildmat.2021.122780

Lundgren, J. (2014). The Impact of Life Expectancy in LCA of Concrete and Massive Wood Structures - A Case Study of Strandparken in Sundbyberg. *Chalmers University of Technology, Department of Civil and Environmental Engineering. Gothenburg, Sweden*. Retrieved from https://hdl.handle.net/20.500.12380/215322

Barnaure, M., Ghita, A. M., Iftode, M., & SGEM. (2016). Life cycle analysis for the typical structural systems of Romanian houses. *Nano, bio and green - technologies for a sustainable future conference procedings, sgem 2016, vol ii*.

De Araujo, V. A., Cortez-Barbosa, J., Gava, M., Garcia, J. N., Souza, A. J., Savi, A. F., Morales, E. A. M., Molina, J. C., Vasconcelos, J. S., Christoforo, A. L., and Lahr, F. A. R. (2016). Classification of wooden housing building systems. *BioRes.* 11(3), 7889-7901

Gustafsson, A. (2019). *The CLT Handbook*. Swedish Wood. www.woodcampus.co.uk

Li, H., Wang, B. J., Wei, P., & Wang, L. (2019, February 1). Cross-laminated Timber (CLT) in China: A State-of-the-Art. *Journal of Bioresources and Bioproducts*. KeAi Communications Co. https://doi.org/10.21967/jbb.v4i1.190

Petruch, M., & Walcher, D. (2021). Timber for future? Attitudes towards timber construction by young millennials in Austria - Marketing implications from a representative study. *Journal of Cleaner Production*, *294*. https://doi.org/10.1016/j.jclepro.2021.126324

Markström, E., Kuzman, M. K., Bystedt, A., Sandberg, D., & Fredriksson, M. (2018). Swedish architects view of engineered wood products in buildings. *Journal of Cleaner Production*, *181*, 33–41. https://doi.org/10.1016/j.jclepro.2018.01.216

ISO, E. N. (2008). 13790: Energy performance of buildings–Calculation of energy use for space heating and cooling (EN ISO 13790: 2008). *European Committee for Standardization (CEN), Brussels*, *2006*(50).

Szokolay, S. V. (2008). *Introduction to architectural science: the basis of sustainable design*. *Journal of the American College of Radiology: JACR* (Vol. 8, pp. 259–64). Retrieved from

http://books.google.com/books?hl=en&lr=&id=VjwYnQ8q8I4C&oi=fnd&pg=PP2&dq=Introduction+to+Architectural+Science+the+basis+of+sustainable+design&ots=QJa9khbn7o&sig=ozEo4qjS0ICEY6z2OoDsbamwf50

Official Gazette RS, 52/ 2010. Rules on efficient use of energy in buildings. 2010.

ISO, ISO 14040, 2006 Environmental Management - Life Cycle Assessment - Principles and Framework, second ed., International Organization for Standardization, Geneva, Switzerland, 2006.

Anex, R., & Lifset, R. (2014). Life Cycle Assessment: Different Models for Different Purposes Anex and Lifset Different Models for Different Purposes. *Journal of Industrial Ecology*. Blackwell Publishing. https://doi.org/10.1111/jiec.12157

Sikkema, R., Styles, D., Jonsson, R., Tobin, B., & Byrne, K. A. (2023). A market inventory of construction wood for residential building in Europe – in the light of the Green Deal and new circular economy ambitions. *Sustainable Cities and Society*, *90*. https://doi.org/10.1016/j.scs.2022.104370

Climate-Data. (2022). Retrieved from https://en.climate-data.org/